DELFT UNIVERSITY OF TECHNOLOGY

SUSTAINABLE ENERGY TECHNOLOGY
MASTER THESIS PROJECT

Decarbonisation of district heating network and its interaction with electricity distribution network, a case study in South-Holland

Author: Motiejus Cicėnas
Student number: 6079075

Thesis Committee Members:
Chair: Dr. Ir. Milos Cvetkovic, IEPG, TU Delft
Core Member 2: Dr. Ir. Rudi Santbergen, PVMD, TU Delft
Advisor: MSc. Christian Doh Dinga, IEPG, TU Delft
First external supervisor: Arjan van Voorden, Stedin

June 27, 2025

To be defended in public on June 30, 2025

Acknowledgments

I would like to express thankfulness to Milos Cvetkovic and Christian Doh Dinga for their guidance and time spent providing valuable insights and feedback. In addition, Arjan van Voorden from Stedin for always being engaged in the project and sharing his professional expertise. Moreover, I thank Roald Arkesteijn from Eneco for his input on the heat model data and validation. The help of the supervisors proved crucial in acquiring the knowledge needed in energy systems modelling and optimisation, as well as understanding the operation of heat and electricity networks.

I am incredibly grateful to my family for the continuous and endless support, that provides me with the freedom to explore and learn. I hope that this work will be a good contribution to the scientific research community and will help to transition to more sustainable energy systems.

During the writing of this work ChatGPT 4 provided by OpenAI and Le Chat by Mistral were used to improve the structure of sentences, spelling and grammar. With the use of these services, the content was carefully reviewed and edited as required.

Motiejus Cicėnas
Delft, June 2025

Abstract

The decarbonisation of district heating networks (DHNs) is one of key ways in achieving the net-zero climate targets, especially in densely populated and energy consumption intensive regions like South-Holland in the Netherlands. As DHNs transition from fossil-based to renewable and electrified heat sources, the interactions with the electricity distribution network (EDN) becomes increasingly more critical. Nevertheless, current operational models and planning approaches often treat the development of heat and electricity networks separately, not considering their interactions and overlooking the operational and infrastructural challenges that arise from their growing interdependence.

This thesis addresses this gap by presenting an integrated modelling framework that combines an operational optimisation model of the South-Holland DHN, developed using PyPSA, with a time-series power flow analysis of the South-Holland EDN using pandapower. The South-Holland case study is carried out in which the implemented framework simulates hourly network operations across the future energy scenarios for the years 2030, 2040 and 2050. These scenarios are driven by real-world market data of electricity, natural gas and CO_2 prices, weather patterns, as well as future heat and electricity demand profiles. This master thesis is part of the TU Delft research project "DEMOSES" and is done in collaboration with Eneco and Stedin.

The results highlight that the large-scale introduction of electrified heat sources in the South-Holland DHN, such as heat pumps, electric boilers and geothermal energy plants, substantially reshapes the operation of the DHN and the loading patterns of the EDN. The operation of the DHN shifts from a more demand-responsive to a market-driven network, with a large reliance on the electricity market signals. This flexibility and responsiveness is largely driven by strategically placed thermal energy storage, especially near electrified production units. Moreover, the electrification of heat supply vastly reduces the reliance on gas and CHP units, resulting in geothermal energy, industrial waste heat and waste incineration becoming the key heat supply technologies. However, it also significantly increases the loading levels of key distribution network components, particularly on medium voltage transformers and lines, leading to critical network stress under future demand scenarios. Conversely, in future scenarios in times of high distributed energy generation, the addition of power-to-heat sources reduce the loading levels of the critical EDN components. It was identified that in times of high distributed energy generation, which results in net negative demand, the power-to-heat sources can consume power locally, lowering the amount of electrical power that needs to be transferred to the HV network, consequently reducing line and transformer loading. The reinforcement of physical assets and coordinated planning efforts between DHN and EDN operators are identified as key factors in mitigating these risks effectively.

Overall, this study provides a detailed description and analysis of the development of the integrated South-Holland heat and electricity model. In addition, the models are applied to perform multiple experiments in the case study, which allows to gain practical insights regarding the effect of large-scale electrification of the South-Holland DHN on the heat network itself and the EDN. The need for spatial-temporal coordination between heat and electricity network operators in the operational and network planning of integrated energy systems is highlighted. The proposed methodology serves as a practical tool for decision makers and policymakers seeking to balance the decarbonisation goals of the DHN with the EDN reliability.

List of Figures

List of Tables

Abbreviations

Abbreviation	Definition
AC	Alternating current
ATES	Aquifer Thermal Energy Storage
BTES	Borehole Thermal Energy Storage
CAPEX	Capital expenditure
CHP	Combined Heat and Power
CMIP	Coupled Model Intercomparison Project
CO_2	Carbon-dioxide
COP	Coefficient of Performance
DHN	District Heating Network
DSO	Distribution System Operator
EB	Electric Boiler
EDN	Electricity Distribution Network
EU	European Union
GHG	Greenhouse Emissions
GTE	Geothermal Heat Energy
HP	Heat Pump
HV	High-voltage
IEA	International Energy Agency
IWH	Industrial Waste Heat
KNMI	Royal Dutch Weather Institute
MV	Medium-voltage
P2H	Power-to-heat
PFA	Power-flow Analysis
PTES	Pit Thermal Energy Storage
PV	Photovoltaic
PyPSA	Python for Power Systems Analysis
RES	Renewable Energy Sources
SSP	Shared Socioeconomic Pathway
SOC	State-of-charge
STE	Solar Thermal Energy
SU	Start-up costs
TES	Thermal Energy Storage
TTES	Tank Thermal Energy Storage
TSO	Transmission System Operator
UC	Unit-commitment
WI	Waste Incineration

Nomenclature

List of indices

h Heat pipeline index

l Heat supply unit index (CHPs, gas boilers, geothermal, e-boilers, heat pumps, waste incineration)

n Bus index

g Generator index (Biomass and waste-heat recovery)

s Heat buffer index

j Fuel supply component index

t Time step index

List of variables

$o_{n,g}$ Marginal cost of dispatch of generator g at bus n, [€/MWh]

$o_{n,s}$ Marginal cost of dispatch of storage unit s at bus n, [€/MWh]

$o_{n,l}$ Marginal cost of dispatch of link l at bus n, [€/MWh]

$c_{price,t}$ Carbon price in the market at time t, [€/t]

$c_{CO2,l,t}$ Calculated costs of CO_2 for CHP or gas boiler l at time t, [€]

$p_{n,l,t}$ Dispatch of link l at bus n at time t, [MW]

$p^{nom}_{n,g,t}$ Dispatch of generator g at bus n at time t, [MW]

$p_{n,j,t}$ Dispatch of store j at bus n at time t, [MWh]

$e_{n,j,t}$ Energy level of store j at bus n at time t, [MWh]

$p^{th}_{n,l,t}$ Heat dispatch of link l at bus n at time t, [MW]

$p^{el}_{n,l,t}$ Electrical dispatch of link l at bus n at time t, [MW]

$p^{dispatch}_{n,s,t}$ Dispatch of storage unit s at bus n at time t, [MW]

$p^{uptake}_{n,s,t}$ Uptake of storage unit s at bus n at time t, [MW]

$soc_{n,s,t}$ State-of-charge of storage unit s at bus n at time t, [%]

$g_{n,l,t}$ Gas consumption of link l at bus n at time t, [MW]

$u_{n,l,t}$ Binary status value of link l at bus n at time t,

$h_{h,t}$ Heat transfer of link h at time t, [MW]

i_{ka} Line thermal current at time t, [kA]

$g^{min}_{n,g,t}$ Minimum output of generator g for each snapshot per unit of nominal power at time t, [pu]

$g^{max}_{n,g,t}$ Maximum output of generator g for each snapshot per unit of nominal power at time t, [pu]

$l^{min}_{n,l,t}$ Minimum output of link l for each snapshot per unit of nominal power at time t, [pu]

$l^{max}_{n,l,t}$ Maximum output of link l for each snapshot per unit of nominal power at time t, [pu]

$i_{hv,t}$ Current at the high voltage side of the transformer at time t, [kA]

$i_{lv,t}$ Current at the low voltage side of the transformer at time t, [kA]

$v_{hv,t}$ High voltage side of the transformer at time t, [kV]

$v_{lv,t}$ Low voltage side of the transformer at time t, [kV]

List of parameters

SU^{CHP} Fixed start-up cost if CHP unit is turned on at time t, [€]

$\eta_{l,th}$ Thermal efficiency of link l, [%]

$\eta_{l,el}$ Electrical efficiency of link l, [%]

$\eta_{n,s,+}$ Charge efficiency of heat buffer s, [%]

$\eta_{n,s,-}$ Discharge efficiency of heat buffer s, [%]

$\eta_{n,j,stand}$ Standing loss store s, [%]

$F_{CO2,l}$ CO_2 factor of link l, [t/MW]

$G_{n,g}$ Nominal power of generator g, [MW]

$L_{n,l}$ Nominal power of link l, [MW]

$H_{n,s}$ Nominal power of storage unit s, [MW]

$R_{n,s}$ Number of hours at nominal power that fill the state of charge, [h]

$G^{lb}_{n,g}$ Minimum power of generator if nominal power is extendable, [MW]

$G^{ub}_{n,g}$ Maximum power of generator if nominal power is extendable, [MW]

F_l Maximum absolute limit of link, [MW]

VM_{pu} Voltage magnitude, [pu]

VA_{degree} Voltage angle, [degree]

I^{max}_{ka} Maximum thermal current, [kA]

DF Derating factor, maximum current of line in relation to nominal current of line, [0 to 1]

$Parallel$ Number of parallel line systems, [No.]

SN_{mva} Rated apparent power of the transformer, [MW]

$Transformer_{loading}$ Load utilisation relative to rated power of transformer, [%]

$Line_{loading}$ Line loading, [%]

Contents

1 | Introduction

In the European Union (EU), half of the energy consumption is used by the heating and cooling sector, of which 75% comes from fossil fuels [1]. In the Netherlands, residential heating is heavily dependent on natural gas, covering 90% of demand [2]. However, the Dutch heating sector is dominated by individual boilers, which comprise 83.5% of total heating installations, while district heating networks (DHNs) hold only 6.6% of the share [3]. In the near future, a large portion of Dutch households and neighbourhoods will have to transition from natural gas to other sustainable alternatives for their heating needs. According to the Collective Heat System Act ("De Warmtewet 2"), 500,000 new district heating consumers will be connected to district heating until 2030, approximately doubling the number of connections compared to 2020 [4]. As a result, the Netherlands is emerging as a large market for district heating, offering opportunities to deploy advanced and novelty heating technologies on a large scale [5]. However, the effectiveness of the energy transition depends on how effectively the DHN operators can implement these carbon neutral technologies to supply heat sustainably and efficiently.

To achieve long-term sustainability of DHNs, multiple strategies can be selected for decarbonisation and reduction of greenhouse gas (GHG) emissions. These measures focus on reducing the carbon footprint by using combined heat and power systems (CHP) with biomass, adopting innovative technologies such as waste heat recovery systems, or lowering the temperatures of the heat supply by renovating buildings to enhance energy efficiency. In addition, electrified power to heat (P2H) heating solutions can be implemented, including heat pumps (HP) and electric boilers (EB) [6]. With the increasing capacity of variable renewable energy sources (RES), such as solar and wind, the potential to achieve the electrification of heat supply sources is greatly increased. For example, HPs can operate with a high coefficient of performance (COP) [7], which makes it more effective and environmentally friendly to implement them compared to traditional gas-fired systems. Moreover, the International Energy Agency (IEA) projects that almost half of total energy consumption will be met with electricity generation in 2050 [8], hence cross-sector integration is expected to develop and increase at a high rate in the upcoming decades.

As interactions between heat and electricity networks become more frequent, thorough examination of integrated heat and electricity networks becomes a necessity. Despite the need to investigate the interactions of heat and electricity networks, Liu et al. [9] argue that there is insufficient analysis conducted on how electrification of heat supply units affects the broader energy system. It is clear that large-scale electrification of DHNs will put additional pressure on electricity distribution networks (EDNs), while in the Netherlands, grid congestion in transmission and distribution networks is already a serious issue [10]. Therefore, incorporating additional electrified heat supply units must be done with a calculated and deliberate approach, as the electrical network is technically restricted by insufficient transformer or line capacity. Therefore, establishing robust methods to measure and determine the impact of heat and electricity sector integration is essential from a current perspective.

Historically, finding the optimal decarbonisation approach for a DHN could involve developing an independent optimisation tool, which is used to find the optimal operation and network planning strategies only for the DHN. Furthermore, the EDN could also be investigated separately based on the projected electricity demand scenarios, without considering the additional demand from the DHN. However, the separated network analysis approach would result in a limited representation of how electrification of heat supply units would affect the operation of integrated heat and electricity networks. Therefore, an integrated heat-electricity modelling approach is proposed to investigate DHN interactions with the EDN and to construct a modelling framework that is capable of supporting a wide range of network analysis, including optimal operation and network expansion planning. For heat and power network operators, it is necessary to understand the impact of heat supply electrification, which would allow a calculated and deliberate analysis of optimal energy network operation and development paths.

1.1 Thesis objectives

This master thesis is part of the "DEMOSES" (Designing and Modelling Future Systems of Energy Systems) research project at TU Delft, with the aim of developing "decision support models and tools for the redesign of the Dutch energy system by coupling heat, electricity, and gas distribution grids, with a focus on the interdependencies between them and the flexibilities that they provide" [11]. The objective of this thesis is to investigate the direct electrification of the future DHN and its interaction with the local distribution network. The research will focus on electrification of heat demand, through technologies like HP and EB, assessing their techno-economic impact on both the DHN and electricity distribution network. The intended outcome of the thesis is a developed a soft-linked heat-electricity model to investigate the pathways of electrifying the DHN and the impact of electrified heat sources on the electricity network. From the DHN side, the operation of the heat network is investigated, while on the distribution system operator (DSO) side, the operation and infrastructure reinforcement needs are examined. The resulting linked electricity and heat models of the thesis will allow Eneco, the DHN operator, and Stedin, the DSO, to understand the scenarios for a sustainable development of the DHN and the distribution grid and to determine their optimal operation and future outlook.

1.2 Scope

This thesis examines the physical DHN and electricity distribution network (EDN) infrastructures, which are operated by Eneco and Stedin, respectively. The DHN model is structured according to an actual network located in the South-Holland province, the Netherlands, which supplies heat to The Hague, Rotterdam and the Lansingerland region. In parallel, the corresponding EDN model is designed to represent the electricity network that supplies power to electrified heat sources within the same geographical boundaries. The case study is carried out to simulate the DHN and EDN operation in 2030, 2040 and 2050, to provide insight to decision makers in Eneco and Stedin regarding heat and electricity network operation and infrastructure reinforcement.

1.3 Research Questions

The primary research question of the thesis is as follows:

How does the decarbonisation of the DHN of South-Holland, facilitated by the electrification of the heat supply, affect the electricity distribution network?

The following sub-questions are formulated to answer the main research question:

1. What modelling aspects must be considered when designing an integrated heat-electricity system to investigate the DHN interactions with the distribution grid?
2. What are the different technology options for decarbonising heat demand (i.e. HP, EB, etc.), when combined into a DHN and what is the optimal mix from the perspective of the DHN?
3. How can operators of heat and electricity networks understand the impact of electrification of heat supply on their systems?

The first sub-question focuses on reviewing the existing modelling approaches and tools used for integrated electricity-heat network analysis. The aim is to identify state-of-the-art methods for modelling integrated energy systems and to explore how multiple tools can be effectively used to study the interactions between DHN and distribution networks. The second sub-question focuses on identifying the optimal technology mix of heat

supply and storage in a DHN. This includes evaluating the techno-economic feasibility of various heat energy technologies, such as power-to-heat (P2H), geothermal, combined heat and power (CHP), waste incineration (WI), IWH, biomass and gas heat boilers, and their role and operation in a large-scale DHN. Additionally, the importance of thermal energy storage (TES) in the DHN is analysed. The third and final sub-question builds on the previous analysis by evaluating how the optimal electrified heat technology mix would impact the networks of Eneco and Stedin. This involves comparing the current DHN with future scenarios and evaluating the cost and physical network expansion requirements. This will allow to test whether company-proposed scenarios align with the optimisation model solutions. The impact on the distribution network, conducted with power flow analysis (PFA), will be quantified by analysing the physical requirements of the network components, such as lines and transformers. The influence of heat supply electrification on the heat network will be determined from the costs analysis of the integrated heat-electricity models.

1.4 Outline

The remainder of this report is organised as follows. Chapter 2 introduces various concepts related to integrated energy systems (IES) and their components. In addition, various modelling approaches discussed in the literature are presented, focusing on the integration of district heating and distribution networks. Chapter 3 provides a detailed description of the current DHN model and the development and structure of the new DHN and EDN models. The new models are applied in the case study, discussed in Chapter 4, which also presents the experiment results. The interpretation of the results is presented in Chapter 5, while also the research questions are answered and the limitations of the methodology are discussed. Chapter 6 presents the final conclusions regarding the decarbonisation of the South-Holland district heating network and the constructed models, respectfully.

2 | Literature review

2.1 Energy networks

2.1.1 Heat networks

Space heating and hot water are key necessities in every household. In the Netherlands, more than 90% of homes use individual natural gas boilers for heating, while 6% of the residential sector is connected to district heating and 1% use fully electric or hybrid heating technologies [12]. The Dutch Climate Agreement has the goal of phasing out natural gas in the built environment by 2050, while a transitional goal states that 1.5 out of close to 8 million homes should use alternative heating sources by 2030 to meet the emission reduction targets [13]. The expansion of the district heating infrastructure is one of the measures that could lead to a sustainable and cost-effective heat supply in the domestic sector. DHNs supply centralised heat with a hot water pipeline network to consumers. Most Dutch DHNs supply heat at high temperatures (90°C), with natural gas, geothermal, biomass or RES-based heat supply units. Heat pipeline losses over distance increases substantially; thus, traditionally, DHNs have been developed on the municipal and neighbourhood level.

Most of the current operating Dutch DHNs are dominated by 3rd generation networks (3GDH) with high supply temperatures, as most networks are dependent on CHP or heat-only gas boilers. This creates a strict operating regime, which limits the use of renewable heat sources, which typically provide lower temperature heat [14]. The future DHN must rely on renewable, non-fossil fuel energy sources and align with smart thermal energy and smart grid principles. An especially compelling opportunity lies in the development of combined district heating and cooling networks; thus, a shift towards a new paradigm is appropriate. The next generation of DHN, 4th (4GDH), can supply heat at lower temperatures (30-70°C, see Figure 2.1) and is technically more suitable for more renewable heat sources, such as large-scale EB, HP, IWH and TES. However, the transition to 4GDH requires a highly developed infrastructure, primarily well-insulated buildings, efficient local heat exchangers, seasonal TES, highly insulated pipes and decentralised substations to meet the standards for space heating and warm water in buildings [15]. The transition calls for a complete overhaul of DHNs and simultaneous integration of heating, cooling, electricity and even transport sectors.

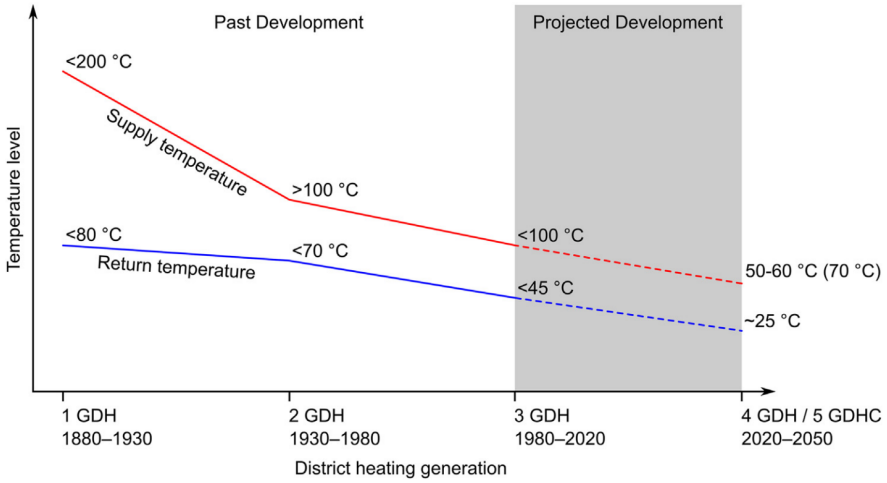

Figure 2.1: DHN development by generation [16].

2.1.2 Electricity networks

The four main pillars of an electrical power system are electricity generation, transmission, distribution and consumption. Generation units and consumers are distributed throughout the network at various voltage levels,

with conventional generators operating at the highest voltage and smaller generators with loads at the lowest voltage levels [17]. The power grid consists of three different voltage levels divided into high-voltage (HV), medium-voltage (MV) and low-voltage (LV). The Dutch transmission system operator (TSO) Tennet manages the HV transmission grid (110kV and above), while seven distribution system operators (DSO) manage everything below 110kV (voltage levels vary with DSO) [18]. In the Netherlands, around 16% of the total final energy consumption is covered by electricity [2]. However, the rapid expansion of distributed RES and electrification of demand have a direct effect on grid congestion, which occurs when technical limits of the equipment in the electricity network are reached. Figure 2.2 illustrates network congestion in the Netherlands. Accelerated installation of solar photovoltaic (PV), HPs and spreading use of electric mobility technologies are the main reasons why the Dutch low-voltage network experiences bottlenecks [10]. DSOs are tasked with managing the distribution network, but with shortages in manpower, capital investments, spatial planning challenges and long-lasting grid reinforcement projects, DSOs resources are stretched thin; thus, long waiting lists for new network connections are a consequence [19], [20].

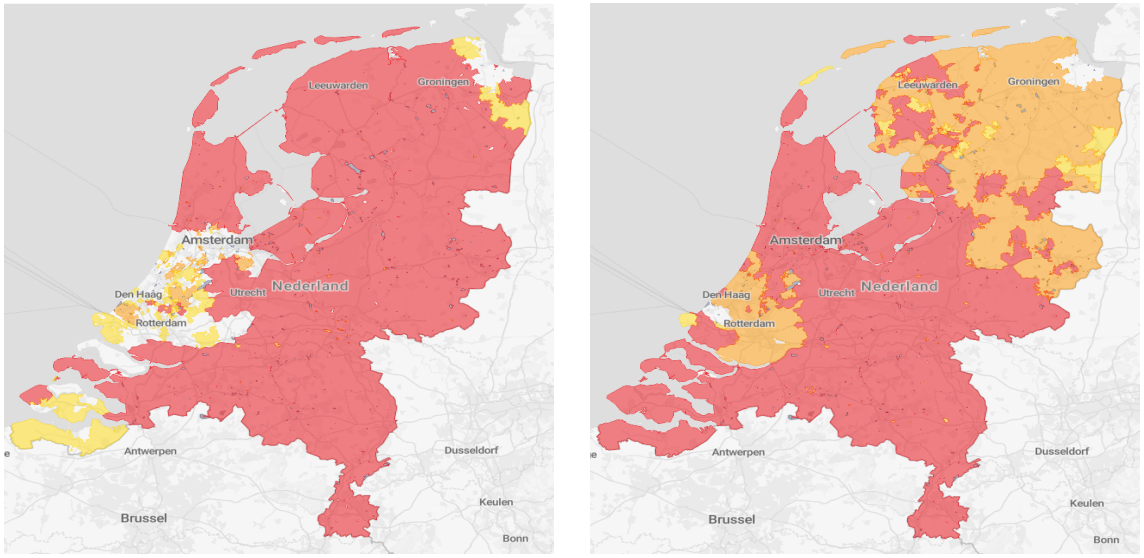

(a) Network congestion of electricity supply

(b) Network congestion of electricity demand

Figure 2.2: Netherlands electricity network congestion (April 2025) Red areas - existing waiting list with no available transmission capacity. Orange areas - existing waiting list, being evaluated for available capacity. Yellow areas - limited capacity. White areas - have available capacity [21].

Grid congestion is not unsolvable; as necessity is the mother of invention, DSOs have multiple solutions to tackle it. The primary solution is physical network reinforcement, by upgrading the existing infrastructure or expanding it. For example, creating new connection points in the network, increasing transformer capacity, installing supporting equipment for voltage and frequency regulation. Nevertheless, these solutions require high initial capital expenditure. An alternative to expansion of the grid is to take leverage of the flexibility of the network by shifting loads from congested areas. This approach is called congestion management, which involves active participants in the market, both producers and consumers, to prevent peak loads [22]. Currently, congestion management comes with its drawbacks, as most devices cannot be controlled smartly and are therefore dependent on consumer behaviour. As stated in [22], implementation of curtailment algorithms by DSOs may unevenly favour consumers located closer to the integral infrastructure, such as transformers. As a result, electricity network operators must carefully plan the expansion of the network and implementation of load management techniques, taking into account a tremendous number of variables to ensure optimal and reliable operation.

2.2 Energy storage

The rapid increase in intermittent energy generation has made the need for excess energy storage more critical than ever, while also presenting significant challenges in its implementation. RES are relying on natural

resources, such as solar irradiation, wind speed and geothermal energy potential, which are hardly predictable. The implementation of RES in energy networks creates inconsistent dynamics, where sometimes more or less energy is produced than is demanded. To reduce these irregularities, energy storage can be used to allow energy networks to operate in a predictable and controlled way. Energy storage is categorised into electrical, thermal, chemical, electrochemical and mechanical systems and, depending on the type, plays a different role in heat and electricity networks.

2.2.1 Storage in heat networks

As indicated in [23], there are three main gaps between the supply and demand of thermal energy in DHNs: first, the time difference between generation and consumption; second, the difference between the peak and off-peak thermal energy costs (seasonal); third, the separation between the place of production and consumption. If thermal energy is not consumed, it is depleted in the environment; hence, TES prevents the wastage of excess heat until it is demanded in the network. Heat demand in DHNs follows an inherently seasonal pattern, as more heat is demanded in the colder winter months. Energy prices are also higher in the winter, thus depending on the scale of TES, it can not only be beneficial on a daily or weekly timescale, but it could also be applied as seasonal storage. The three types of thermal energy storage are sensible, latent and thermochemical [24]. Sensible heat storage is most commonly used in DHNs, as water is the main transport medium. Figure 2.3 indicates the types of TES in large-scale district heating applications. The pit, borehole and aquifer thermal energy storage (PTES, BTES and ATES, respectively) are used for long-term heat storage. The illustrated long-term storage units typically range in 50-1000 MWh storage capacities; however, come with large space requirements and significant energy losses. In contrast, short-term storage is usually supplied by tank thermal energy storage (TTES) with storage capacities of 10-50 MWh, which requires less space, results in better efficiency and can be applied as a supplementary asset in the electricity market, if combined with P2H technologies [25].

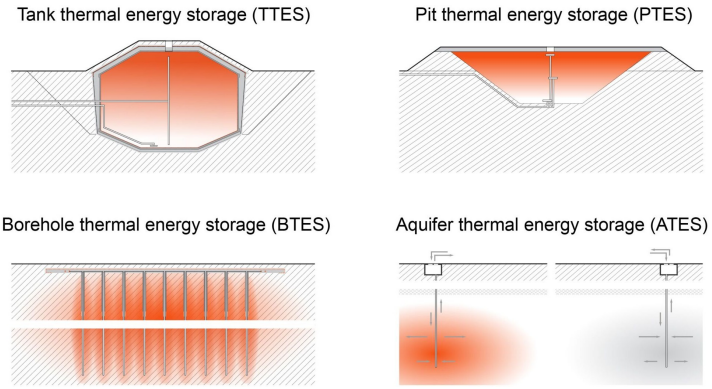

Figure 2.3: Large-scale TES applications [26].

2.2.2 Storage in electricity networks

Local distribution networks are experiencing a transition period, where integration of renewables brings not only benefits, such as grid decarbonisation and reductions in greenhouse gas emissions, but also challenges, including grid congestion and concerns about reliability. Figure 2.4 illustrates how energy storage systems (ESS) can be categorised. Most of ESS applications come in the form of lithium-ion (Li-ion) batteries, other methods such as flow batteries, flywheels and super-capacitors are also implementable. In the Netherlands, 410 MWh of new storage capacity came from battery energy storage systems (BESS) in 2023, while 98% of installations were less than 20 kWh [27]. Given the continuous increase in solar PV installations and their compatibility with BESS, the trend of more BESS installations is likely to continue. BESS can provide a supporting role for distributed RES by improving power quality, providing voltage and frequency regulation support, allowing load management services (load shifting, peak shaving, load levelling) and allowing smooth network operation and ensuring security of supply. Nevertheless, incorrect application of ESS can negatively affect the distribution network, degrading the power quality, affecting the voltage and frequency, thus the optimal placement, sizing and operation of ESS is critical [28], [29].

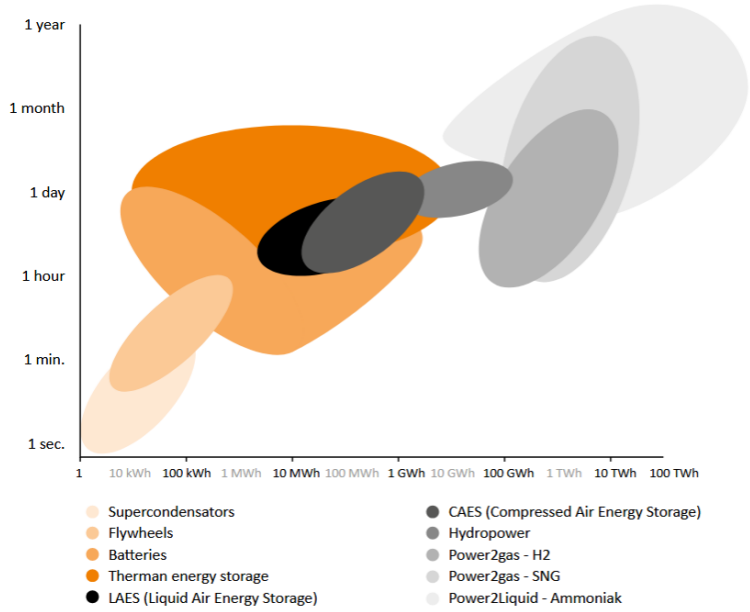

Figure 2.4: Energy storage categories [30].

2.3 Modelling Integrated Energy Systems

2.3.1 Energy system integration

Integrated energy systems (IES) are defined as interacting renewable energy systems that operate in a coordinated and interdependent manner, allowing organised production, delivery and consumption of energy. The primary objective of IES is to allow an efficient and flexible supply of energy carriers, such as electricity, thermal and cooling energy [31]. This is a modern approach for optimizing energy systems, which allows to lower primary energy consumption, increase RES utilisation, reduce capital expenditure, increase productivity, flexibility and reliability [32]. In literature, IES can also be named as sector-coupled, multi-energy or smart-energy systems [33], [34].

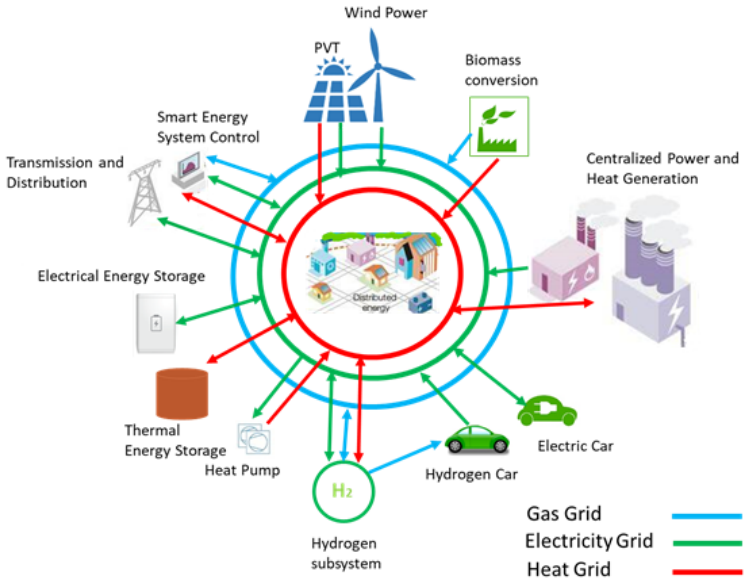

Figure 2.5: Schematic of IES [35].

Traditional energy systems are managed individually by their respective operator; however, in IES a distributed or decentralised control solution is preferred, as it improves the independence of network participants and in-

creases computational efficiency [36]. Another key aspect of IES is the bidirectional flow of energy, which enables the integration of prosumers who consume and supply energy to the networks. Figure 2.5 illustrates the interconnection between the heat, electricity and gas grids. Although cooling networks are not included in the diagram, they could be incorporated as well. Electricity and heat networks interact through P2H technologies, solar PV thermal applications and hydrogen systems. Electricity, heat and gas networks have traditionally been integrated with CHP. In Figure 2.5, thermal and electrical storage is shown to operate on a single grid; however, pairing P2H technologies with ESS is becoming a general practice, so sector integration can also benefit from ESS.

The main focus of this thesis is the integration of heat and electricity networks, mainly the integration of the DHN and the low-voltage distribution network. The main coupling link of the two networks is P2H technologies, such as HP, EB and waste heat recovery systems; also integration of heat storage technologies is considered. As indicated in [37], HPs can supply around 25% of energy in DHN. HPs are able to extract low-grade heat from air, ground, various industrial applications, or data centres, and supply hot water to the network. Another key functionality of HP is their ability to provide balancing services to the electricity network, enable the use of low-temperature heat networks, and contribute to the decarbonisation of district heating systems. The key difference between EBs is that they use electricity to generate heat, operating at a lower coefficient-of-performance (COP) compared to HP, but can supply heat at higher temperatures. They also provide peak shaving and backup generation capabilities. TTES is commonly applied together with HP and EB, which results in increased demand management flexibility, better efficiency, grid balancing opportunities and cost-effectiveness.

2.3.2 Network operation and planning

In an IES, network operation refers to the management energy flows across the interconnected energy infrastructures, ensuring reliable and efficient delivery of electricity, heat and other energy carriers. It involves continuously balancing the dispatch of the generation and storage units, all of which are responding to fluctuations in the markets and the required demand. On the other hand, network design deals with the long-term planning of the network structure and evaluating the possible development of new infrastructure. With network planning, calculated decision can be made regarding the new implementation of generation, transmission and distribution systems, while considering the projected growth in future energy demand. By employing both conditions, an operational strategy with a long-term holistic view of the energy system can be achieved, thus capital investments can be allocated in a coordinated and optimal manner for the networks to operate as intended.

Traditionally, energy network operation and planning was done by constructing operational dispatch models and possible future demand and supply scenarios, allowing to determine the optimal network performance and to allocate the required funds for investments [17]. However, when applied to IES this approach faces a key obstacle of critical data sharing between the stakeholders. Due to privacy concerns, energy network operators often rely solely on their own datasets, which excludes information from other market participants. This situation limits the ability of the models or future scenarios to have an accurate representation of the integrated networks, limiting their analysis. With the projected increase in the energy system integration, the need to establish robust and accurate communication between network operators and modelling techniques with respect to future network operation and development is paramount.

2.3.3 Modelling applications

The modelling of IES has become one of the essential techniques to plan and optimise the expansion of the future energy network infrastructure. These models help energy companies and policy makers determine the locations and capacity of new assets, while also help to find optimal operational settings of network components. In particular, IESs of heat and electricity have been the subject of academic research, with various modelling tools and approaches being applied. It is rare that independent development of separate network models will produce meaningful results, as combined operation of multi-energy systems must be addressed. Hence, the literature presented covers the attempts of academia in developing coupled heat and electricity network models.

The physical interactions of separate networks were modelled by Pan et al. [38], using integrated quasi-steady multi-energy flow with Matpower. The findings emphasised the existence of physical interactions between heating and electricity systems, where a disruption in one network affects the other, thus requiring the examination of coupled networks in future energy system modelling. To further explore the physical interactions of sector coupling with Matpower, Liu et al. [39] developed two calculation methods based on quasi-steady hydraulic-thermal and electrical power flow models, called decomposed and integrated. The decomposed method included the sequential solving of the hydraulic, thermal, and electrical power flow equations, while the integrated method combined the equations and solved at the same time. The integrated method demonstrated greater computational efficiency, requiring fewer iterations, whereas the number of iterations in the decomposed method increased proportionally with the size of the networks.

On the other hand, Kavvadias et al. [40] utilised an open-source unit commitment and dispatch Dispa-SET model to study the European power network under electrified heat production scenarios. The study demonstrated that HP, electric heaters and air conditioners can increase electricity demand by 20-70%, and in some countries lead to instances of load shedding. Moreover, Magni et al. [41] applied the Dispa-SET model to analyze DHN where heat is supplied via power-to-heat (P2H) and CHP units. The analysis found that DHN coupled with P2H and TES provides greater flexibility in operation with the power network by maximising the penetration of RES. Moreover, the inclusion of CHP units was associated with a lower integration of renewables and higher carbon emissions. Furthermore, Brown et al. [42] used the PyPSA Europe model to evaluate sector coupling strategies. The results indicate that in high-density areas DHN with TES can substantially reduce the costs, while the best cost-saving option for the future European energy system includes increased cross-border transmission capacity.

The national-level energy planning approach was adopted by Sørknaes [7], who applied the EnergyPLAN tool to holistically analyse the effects of direct electrification (with HP and EB) on DHNs in Austria and Denmark. Based on electrification scenarios, the respective impacts of technology mixes on network performance were highlighted. The EBs were found to enable greater integration of variable RES because of their lower efficiency and operational flexibility, making them less constrained by heat demand. However, HPs showed greater potential to reduce biomass consumption, particularly by eliminating biomass-fired CHP boilers. Focusing on a regional scale, Liu W. et al. [9] investigated the development of the DHN in Utrecht, the Netherlands. The findings obtained by modelling future network scenarios with the EnergyPLAN model showed that a mix between district and individual heating at the neighbourhood level results in the highest energy savings and the lowest costs.

Javansir N. et al. [43] applied EnergyPro to simulate the operation of DHN to evaluate the pairing of P2H and TES technologies to provide balancing services for the electricity network in Finland. The findings concluded that HPs are well suited for automatic frequency restoration reserve (aFRR) due to their longer activation times, while EBs, with their faster response capabilities, are more suitable for containment reserve (FCR) and fast frequency reserve (FFR). Friedrich et al. [44] implemented mixed-integer linear and non-linear programming models (MILP and MINLP, accordingly) in Python, using Pyomo, to focus on optimizing DHN operation by coupling HP and CHP technologies. From a modelling perspective, the study examined whether the additional development time required for a more complex MINLP model is justified compared to the results achieved using a simpler MILP model. The non-linear modelling can reduce DHN operational costs by up to 16%, however, cost savings highly depend on network structure. Lastly, non-linear models improve planning accuracy, but were shown to lead to unstable oscillations in network operation, displaying the need for further research on non-linear model stability conditions.

These studies collectively highlight applied modelling tools to capture the complexity of coupled heat and electricity networks. As seen, some researchers focus on simulating physical flows in network interactions, some concentrate on the planning aspect of the future coupled energy networks, while others simulate optimal operation of coupled networks to help reach better operational and optimal decisions. Each emphasises a

tailored modelling method based on the scope of the network and various research goals. The selection criteria for the preferred modelling tools for this thesis are discussed in the following section 2.3.4.

2.3.4 Modelling tool overview

Numerous models and modelling tools have been developed for analysing energy networks, with new methods and approaches being released on a regular basis. Based on the modellers needs, the modelling software differs in its accessibility (open-source or commercial), temporal resolution, technical complexity, spatial coverage, analytical objectives and the employed optimisation methodologies. As indicated by Brown et al. [45], many of the tools used for network modelling were created before sector coupling was a necessity. For this thesis, it is essential to use tools that can accurately represent the interaction between heat and electricity networks, encompassing everything from long-term planning and system-wide optimisation to detailed operational analysis and power-flow modelling. The main criteria for selecting the modelling tool for this thesis are:

1. Functionality to design coupled network topology;
2. Ability to easily adjust model parameters (objective function, constraints and variables);
3. Functionality to run network optimisation and optimal dispatch;
4. Functionality to run power-flow analysis (PFA);
5. Hourly time resolution and yearly time scale;
6. Free and open-source software, preferably Python based.

The software tool selected for the modelling in this paper must meet the essential criteria listed above. First, it should be capable of modelling a coupled energy network, which involves heat, electricity, and gas networks, to accurately reflect their interactions. Second, the tool must be flexible to construct and modify network components, also allowing the modeller to define custom optimisation models with adaptable objective function, constraints, and variables. Furthermore, the tool should enable operational optimisation and optimal dispatch of generation and storage technologies across one calendar year, using hourly resolution. In addition, it must offer PFA capabilities to model the electrical network. Lastly, to comply with the university and DEMOSES research project guidelines, free and open-source software is preferred.

Table 2.1 shows the selected modelling tools to compare their strengths and weaknesses. Tools such as Matpower and pandapower offer robust electrical network modelling and PFA, however, lack long-term planning and sector coupling capabilities. Moreover, EnergyPLAN and EnergyPRO tools are applicable for scenario-based simulations that rely on having a heuristic approach but offer flexibility for system-wide optimisation. Dispa-SET focuses on dispatch and unit-commitment (UC), but is insufficient for physical network modelling. In contrast, PyPSA provides a powerful open-source Python-based platform for co-optimizing electricity, heat and gas sectors over long time horizons, in addition with support for investment planning, storage and sector-coupling through LP or MILP approaches. A drawback of PyPSA is that it cannot do state estimations and short-circuit calculations. Therefore, once optimal dispatch and infrastructure layouts are derived from PyPSA, pandapower can be employed for more detailed PFA, capturing voltage variations, line and transformer loading. This integrated modelling approach takes advantage of the network-level optimisation strengths with PyPSA and accurate electricity network operation with pandapower.

Tool	Time scale	Resolution	Optimisation	Primary scope	Network modelling
Matpower	Snapshot	Snapshot	LP, PFA, OPF	Operation	Yes
Dispa-SET	Annual	Hourly	MILP	Operation	No
PyPSA	Lifetime	User-defined	LP, MILP	Planning	Yes
pandapower	Snapshot	User-defined	AC/DC PFA	Operation	Yes
EnergyPLAN	Lifetime	Hourly	Heuristic, rule-based	Planning	No
EnergyPRO	Lifetime	User-defined	Simulation-based	Operation	No

Table 2.1: Comparison of energy system modelling tools

2.3.5 PyPSA and pandapower overview

Python for Power System Analysis, or PyPSA, is an open-source Python-based tool, designed to model and optimise energy systems [45]. PyPSA provides a platform for modelling and optimizing the operation and planning of energy systems. PyPSA leverages several well-established Python libraries, such as *Linopy* for network optimisation, *pandas* for data handling and *NumPy* for numerical computations. Additionally, PyPSA supports various optimisation techniques, including UC, economic dispatch and multi-objective optimisation, which can be applied to centralised and decentralised energy networks. In general, PyPSA is capable of performing large-scale and long-period simulations, making it suitable for both operational analysis and long-term planning [46]. It is a particularly useful tool for analysing RES technologies in sector-coupled scenarios, including heat and electricity, which allows to examine synergies across the sectors.

The components used to represent the energy systems are presented in Table 2.2. Each object, static or time-dependent, is stored within the *network* container, which also has executable functions. *Buses* are the fundamental nodes to which every component must attach. They enforce the law of energy conservation, meaning that the energy flowing in is equal to the energy flowing out. The *carrier* component is used to describe energy carriers; for electricity networks AC and DC, while for other energy systems arbitrary energy carriers can be described, such as heat, natural gas or biomass. *Loads* are components used to model energy consumption, while *generators* represent energy production units. Furthermore, *links* represent a controllable connection between two buses and are used to model energy conversion between different energy carriers or energy transfer. These elements are highly flexible and are applied to simulate heat transfer in pipelines, CHP systems or P2H applications. Unlike *generators*, *links* in PyPSA are defined with specific efficiencies and can accurately model the directionality of energy flows. Moreover, a *store* component functions as energy storage and is used to model the optimal energy storage capacity independently of the storage power capacity. Lastly, *storage units* are used to model storage systems with coupled energy and power capacity constraints, allowing for time-dependent charge and discharge behaviour.

Component	Description
Network	Represents the overall structure that contains all network elements
Bus	A fundamental node, serving as a connection point to other components
Carrier	Energy carrier (e.g., wind, solar, gas, etc.)
Load	Consumer of energy
Generator	Supplies energy to the network
Store	A component responsible for storing energy without charging and discharging constraints
Storage Unit	A storage unit with fixed nominal-energy-to-nominal-power ratio.
Link	A controllable connection between two buses, often used to model heat pipes, CHP systems or EBs

Table 2.2: PyPSA network components [45].

Pandapower is another open-source, Python-based tool that focuses specifically on the analysis and optimisation of power networks [47]. This tool utilises *pandas* library for data analysis and integrates PYPOWER as its underlying power flow solver. The network models in pandapower are based on electrical elements, such as lines, transformers or circuit breakers. This allows performing power flow (PF), optimal power flow (OPF), state estimation, and short-circuit calculations. Pandapower is particularly suitable for the detailed modelling of distribution and transmission systems, making it valuable for the operational analysis of electricity networks.

The components used for power network modelling in pandapower are presented in Table 2.3. All network components are organised within the *empty network*, which stores network topology data used for simulations. *Buses* serve as essential nodes connecting all network elements. An *external grid* is used to model a higher-level power network, acting as a constant voltage source with unlimited capacity. *Loads* represent power consumption, while *generators* represent power production units. Lines are used to model overhead or underground transmission and distribution lines that enable power transfer across the network. Transformers link buses operating at different voltage levels, enabling connection between high-voltage transmission and lower-voltage distribution systems.

Component	Description
Empty network	Represents the overall structure that contains all network elements
Bus	A fundamental node, serving as a connection point to other components
External Grid	Represent the connection to the higher-level power grid
Load	Consumer of power
Generator	Supplies power to the network
Line	Represents transmission or distribution lines that transfer power across the network
Transformer	A branch that connects two buses of different voltages

Table 2.3: Pandapower network components.

3 | Modelling and optimisation

In this chapter, three models are discussed: the old DHN model, its new version and the newly developed electricity distribution network (EDN) model. Initially, a brief analysis is done on the old DHN model structure. This is followed by a detailed description of the new DHN and new EDN model architectures, including the modelling approach and configurations. The description involves all essential aspects required for model development: network structure, input data, mathematical formulation, key assumptions, model validation and verification, and the generation of outputs.

3.1 Old district heating network model

The old model was developed with the objective of accurately representing the South-Holland DHN to perform operational optimisation of the heat network. Users can run scenarios related to network expansion and demand or price changes, for the years 2018-2022. Table 3.1 lists the available scenarios, respectively. The original version of the South-Holland DHN model was developed by Eneco using the Linny-R graphical specification language, however, the second (old) version of the model was implemented using Pyomo and NetworkX [48].

Network expansion scenarios	Demand scenarios	Price scenarios
Base case	Base case	Base case
Case 1 - Additional sources	10% demand increase	25% demand increase
Case 2 - Additional storage	15% demand increase	50% demand increase
Case 3 - Additional sources and storage	-	-

Table 3.1: Old DHN model scenario choices.

3.1.1 Scope

The old model represents the South-Holland DHN, which supplies heat to customers in Rotterdam, The Hague, and the Lansingerland regions. Figure 3.1 illustrates the geographical boundaries of the South-Holland DHN. The heat distribution network connects industrial and domestic buildings with heat generation and storage sources such as waste incineration, biomass, combined heat and power (CHP), geothermal, gas boiler and waste heat recovery plants. The main purpose of the South-Holland DHN is to continuously meet end-user heat demand while maintaining network stability. Heat demand within the DHN is divided into three main components, space heating, hot water supply and thermal losses in the heat distribution network. Among the listed, space heating holds the largest share, which is highly sensitive to weather conditions.

At the moment of writing the thesis (2025), the "Vlaardingen-Den Haag" pipe called "Warmtelinq" (WLQ) is under construction [49]; however, in the old model the WLQ connection was modelled as operational. The WLQ connection acts as the main linkage, allowing the heat networks of The Hague and Rotterdam to be connected into one. In Rotterdam, the Rozenburg waste incineration plant is connected to the city through two main pipelines: the northern "Leiding over Noord" (LoN) and the southern "Botlek/Pernis" pipes [50], [51]. The LoN pipeline passes through the municipalities of Vlaardingen and Schiedam before reaching the city of Rotterdam. From there, the "Boszoom" pipeline extends further east, connecting the eastern part of Rotterdam. Moreover, the greenhouses in Berkel en Rodenrijs, Bleiswijk, and Bergschenhoek (named "Tuinders") are connected via a pipeline that extends south and connects to the eastern part of Rotterdam. In the Hague direction, the Uniper "City Power Plant" with CHP units acts as the main heat supply and is connected to the Hague by one pipeline called "CR Plein", while smaller geothermal heat supply units are connected via other pipelines. When the real-world equivalent of the WLQ pipeline is complete, the main connection point will be located at the Uniper CHP plant, connecting the heat networks of Rotterdam and The Hague [52].

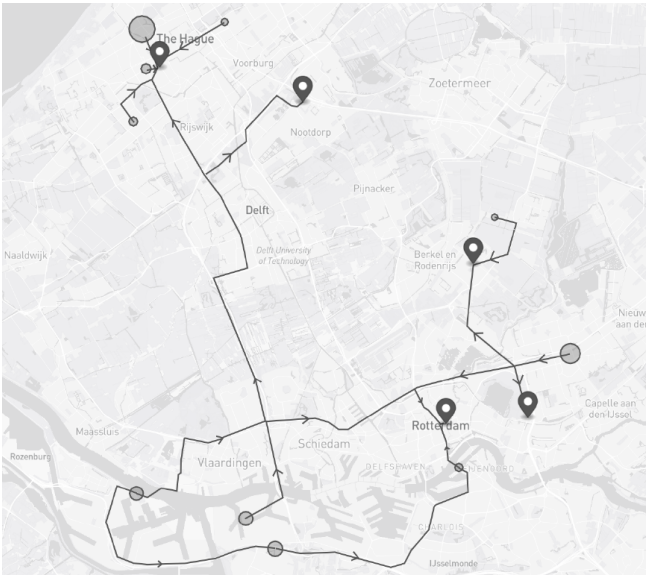

Figure 3.1: Representation of South-Holland heat network, [48].

3.1.2 Model inputs

The main inputs of the old DHN model include the network topology, hourly heat demand and price data for CO_2 gas and electricity, as shown in Figure 4.2. The network structure consists of heat distribution pipelines, demand nodes, supply units and buffer points. Table 12 in Appendix C provides an overview of the heat sources included in the DHN model of the base network scenario. The main heat supply units in the base network case are the waste incineration (WI) plant, two industrial waste heat (IWH) recovery plants, five CHP units (two in The Hague and three in Rotterdam), one biomass plant, seven heat only gas boilers and one geothermal plant. In addition, four TES units are connected near the four demand nodes in the Hague, Rotterdam, and Tuinders. The heat sources and storage are connected via heat pipelines to supply the heat to the demand nodes. In Case 3, which has an expanded network configuration, additional heat and storage sources are incorporated: two HPs, one EB, five geothermal sources and three additional TES units. Based on the desired scenario and research objectives, the user prepares the corresponding Excel-based input data for use in the simulation.

3.1.3 Model formulation

The Python programming language was chosen to develop the old DHN model, with NetworkX and Pyomo serving as the primary packages for network formulation and optimisation. NetworkX package was used to study the dynamics and functions of complex networks [53]. The main components of NetworkX are edges and nodes, symbolizing connection points and point objects, accordingly. Compared to the physical system, the edges represent pipelines for transferring heat and all other component connections, while the nodes indicate heat supply, demand and storage points. A graphical representation of the base DHN, plotted using NetworkX, is shown in Figure 3.2. For the formulation and solving of the mathematical model the Pyomo library was used, which is another open-source package used to define and solve optimisation problems [54].

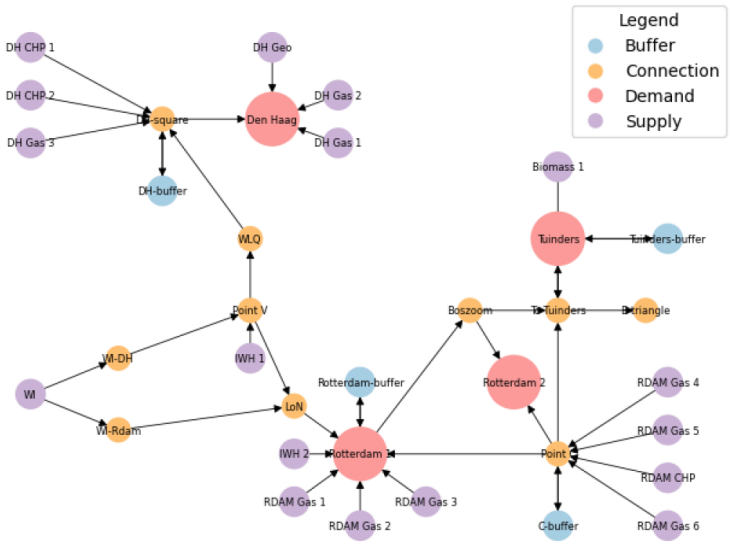

Figure 3.2: NetworkX representation of the old model, [48].

The old model was formulated as a multi-period unit-commitment (UC) problem using MILP. The optimisation framework consists of decision variables (both continuous and integer), an objective function and a set of constraints. In general, the primary objective is to minimise operational costs and maximise revenue from CHP electricity production. As shown in 3.1, the objective function is the sum of all the node and edge-related costs. The operating costs of the nodes (3.2) include variable CO_2, natural gas and electricity costs. Additionally, start-up (SU) and variable costs are applied specifically to CHP units, which implies that all other heat production and storage units can run continuously with zero SU and variable costs attached. Edge costs are represented as transportation costs (3.3), which account for connection costs per edge and the corresponding heat flow through each edge. However, only one heat pipeline, connecting the WI plant with The Hague, has assigned seasonal transportation costs; all other pipelines were modelled with zero transportation costs.

$$\min C_{\text{total}} = \sum_{t=1}^{T} \sum_{n=1}^{N} \sum_{e=1}^{E} C_{n,t}^{\text{nodes}} + C_{e,t}^{\text{edges}} \tag{3.1}$$

$$C_{n,t}^{\text{nodes}} = C_{n,t}^{\text{gas}} + C_{n,t}^{\text{CO2}} + C_{n,t}^{\text{elec}} + C_{n,t}^{\text{SU}} + C_{n,t}^{\text{var}}, \quad \forall n \in N, \forall t \in T \tag{3.2}$$

$$C_{e,t}^{\text{edges}} = C_{e,t}^{\text{edge}} * flow_e, \quad \forall e \in E, \forall t \in T \tag{3.3}$$

**full description of given formula provided in [48].*

3.1.4 Model settings

The old model operates with an hourly temporal resolution, aligning with the day-ahead market structure, where prices are determined for each hour for the following day at noon. This resolution ensures consistency with the heat demand and price data provided by Eneco, which is also in hourly time steps. As a result, the old DHN model can accurately reflect market conditions and operational realities, capturing the major fluctuations in price and demand. In addition, the model utilises a look-ahead period, enabling the solver to anticipate the future implications of present decisions during the optimisation process. The look-ahead period of the optimisation model is 12 hours, ensuring that the storage state-of-charge (SOC) is not zero at the end of each optimisation period, maintaining operational flexibility. The old model also uses a rolling time horizon strategy, meaning that it optimises over a 36-hour window, stepping forward each day while overlapping with the period that passed. The overlap with the previous period ensures continuity in variables such as the storage level of buffers and the unit commitment status of the supply units. The model is optimised over one year for each hour, that is, 8760 time steps. Using a commercial *Gurobi* solver, the run-time of the old DHN model is around 20

minutes for a full optimisation period with the rolling time horizon.

3.1.5 Model assumptions

The old DHN model is based on a set of assumptions and constraints, which shape the structure and final the output of the model. The parameters of production and storage units used in the old model are described in Tables 12 and 13, in Appendix C. These are the core data that describe the base network topology case of the DHN and its operation. Furthermore, drawing from the supporting description of the old DHN model [48] and the input files of the network, additional parameters and constraints are used in the model, which are summarised in Table 3.2:

Scope	**Assumption**
Seasonality	Seasonal flow limits set to imitate IWH1 yearly production constraint
Heat production	Annual contracted heat production of IWH1 unit
Heat production	Minimum generation constraints, $p_{min,pu}$ (applied to certain units)
Heat production	Constant COP of EB, HP and geothermal units
Heat production	Perfect efficiency of heat production units (biomass, IWH, WI)
Heat production	Biomass unit turned of during August
Heat storage	Perfect efficiency of all heat storage
Heat transport	Heat losses in distribution pipes (applied to 4 out 15 pipes)
Costs	SU and variable costs applied to CHPs only (all other units zero costs)
Costs	Zero costs of heat storage
Costs	Seasonal pricing of WI heat distribution to The Hague
Merit order	RDAM CHP3 can operate when WI at max capacity

Table 3.2: Old model assumptions and constraints

The seasonal flow restrictions for IWH1 are enforced to simulate the annual contracted heat constraint, set at 170,833.33 MWh. The model enforces production limits on IWH1 unit based on the season: 39.18 MWh in winter, 15 MWh in autumn and spring and 7 MWh in summer. Moreover, minimum generation constraints ($p_{min,pu}$) are imposed for geothermal units, EB, HPs, WI, RDAM CHP1–3 and IWH2. For geothermal units, $p_{min,pu}^{\text{geothermal}} = 1$, which results in continuous operation at maximum heat output each hour. The EB operates with $p_{min,pu}^{\text{EB}} = 0.5$, while the HPs have a minimum generation of $p_{min,pu}^{\text{HP}} = 0.3$. For WI, the constraint is set to $p_{min,pu}^{\text{WI}} = 0.375$. RDAM CHP1 and CHP2 have a minimum generation level of $p_{min,pu}^{\text{RDAM CHP1-2}} = 0.6$, while RDAM CHP3 operates with a lower threshold of $p_{min,pu}^{\text{RDAM CHP3}} = 0.45$. Finally, IWH2 is subject to a $p_{min,pu}^{\text{IWH2}} = 0.2$ minimum generation constraint. In addition, the COP values for geothermal, EB and HPs are fixed: $COP_{EB} = 0.95$, $COP_{HP} = 3$ and $COP_{geothermal} = 1$. Next, the heat production efficiency is set at 100% for WI, biomass, IWH1 and IWH2 units, while also the heat storage units are assumed to be perfectly efficient. The old DHN model only includes heat distribution losses in 4 out of 15 pipelines, while other pipes do not have associated heat losses. With regard to costs, SU and variable costs are only applicable to CHP units, while all other units operate cost-free and are only exposed to market prices. Furthermore, heat storage and dispatch incur zero costs. The distribution cost of heat produced by WI and transferred to The Hague varies seasonally: 0.773 €/MWh in summer and 2.442 €/MWh in winter. Additionally, the biomass unit is turned off during August due to planned maintenance. Lastly, RDAM CHP3 is only allowed to operate when the WI is running at maximum capacity. All of these constraints are part of the old DHN model. Although some have been retained in the new DHN model, others have been discontinued, as discussed in Section 3.2.6.

3.1.6 Model outputs

The old DHN model optimises the operation of the DHN by minimising total costs and maximising electricity revenues, hence the fundamental output data is the total heat dispatch costs of the network per optimisation pe-

riod. The old model calculates the values of key variables for all time steps, such as heat supply unit production levels, SU states, heat storage content, CO_2 emissions and heat flow in distribution pipes. These variables are used to calculate the operational costs, including those related to the operation of heat production units and their start-ups, electricity revenue, CO_2 costs, natural gas consumption costs. The output data are stored in Excel *.csv* file format, which allow to easily extract the data and visualise the outputs. In the end, comparative analyses can be performed across different years (e.g., from 2018 until 2022) and various network configurations based on the selected simulation scenarios.

3.2 New district heating and electricity distribution network models

The new representation of the South-Holland DHN was developed with the aim of creating a more user-friendly model with improved computational performance, suitable both for operational and long-term planning. To enable the modelling of integrated heat and electricity networks a new EDN model was also designed. The third version of the DHN model leverages a well-structured and robust Python-based library, such as PyPSA, which provides a comprehensive and structured toolbox for detailed modelling analysis of coupled energy systems. The new EDN model applies the pandapower package to model the medium-voltage distribution network that is connected to DHN heat sources. The development of the new models is carefully described, including the description of the network structure, assumptions and methods applied. The results and various decarbonisation scenarios can be found in Chapter 4, focusing on the case study of the South-Holland DHN and its interaction with the EDN.

3.2.1 Conceptualisation

The previous version of the DHN model was developed to optimise the operation of the South-Holland heat network. It provided an overview of heat supply distribution and analysed how various demand and price scenarios affected the flexibility and long-term sustainability of the heat network. The model delivered valuable findings regarding the heat network, but the addition of the electrified heat sources did not include an investigation on how these heat sources integrated and affect the EDN that acts as the main linkage for power supply. In this thesis, a new DHN model is implemented to more accurately model the operation of the South-Holland heat network using a well-established open-source PyPSA library. Similarly to the previous version, the main focus of the DHN model is still on the optimal operation of the heat network; however, the electrified heat supply demand and CHP unit power production is considered as the main output of the DHN model. To address the growing importance of modelling integrated energy networks, a separate EDN model was developed, allowing a detailed analysis of the interactions between the DHN and the EDN. The addition of the EDN model allows this study to analyse the integrated operation between heat and electricity networks. Overall, the new models must provide a platform, which would allow multiple network simulations for operational optimisation and long-term network planning. This would allow the strategical guidance of the decision makers towards decarbonised and flexible network operation with the required network reinforcements.

The South-Holland DHN is operated by Eneco, which supplies heat to its customers, while Stedin manages the EDN, ensuring the distribution of electricity at the medium voltage level. Based on data provided by both companies, the interactions points between the two networks were established, enabling a comprehensive analysis of their integration and interdependencies. As illustrated in Figure 3.3, the primary network integration technologies include geothermal systems, P2H and CHP units. Geothermal and P2H systems require electricity to produce heat for the DHN, while CHPs use natural gas to simultaneously generate heat and electricity for both networks. Additional heat sources include gas and biomass boilers, waste incineration, waste heat recovery and thermal storage. Although waste heat recovery often involves the use of HPs, in this study it is not considered a sector-integrated option. In general, the new DHN and EDN models must be developed to represent the South-Holland heat network and the accompanying local distribution network with the highest possible level of detail, resulting in accurate operational optimisation of the DHN and PFA of the EDN.

Capturing the structural and operational complexity of real-world heat and electricity networks is desired; however, for models to serve as a practical and flexible analytical tool, they must be constructed to include the capabilities of scenario-based simulations. This includes the ability to simulate different network topologies, modify input parameters, such as heat and electricity demand, market prices and temperature profiles, all depending on the selected simulation year. The model must allow simulations to be run for both historical years (2018–2022) and projected future years (2030, 2040 and 2050). This enables to compare the simulation scenarios, helping to capture the impact of dynamic fuel and electricity prices, and growing heat and electricity demand over daily and seasonal cycles. Moreover, the modelling tool must take advantage of open-source libraries, to model the DHN and the EDN, accordingly. These Python libraries provide robust functionality, making them ideal for modelling and optimizing large scale integrated energy networks. In addition, the tool must be user-friendly, while the development process must be thoroughly described. Ultimately, the modelling framework should function as a decision support tool for network operators, helping to identify the cost-effective and technically feasible pathways for electrification and decarbonisation of the DHN and the development of the distribution network. Hence, scenario-based modelling of coupled networks is instrumental in facilitating a smooth and realistic transition towards sustainable energy networks.

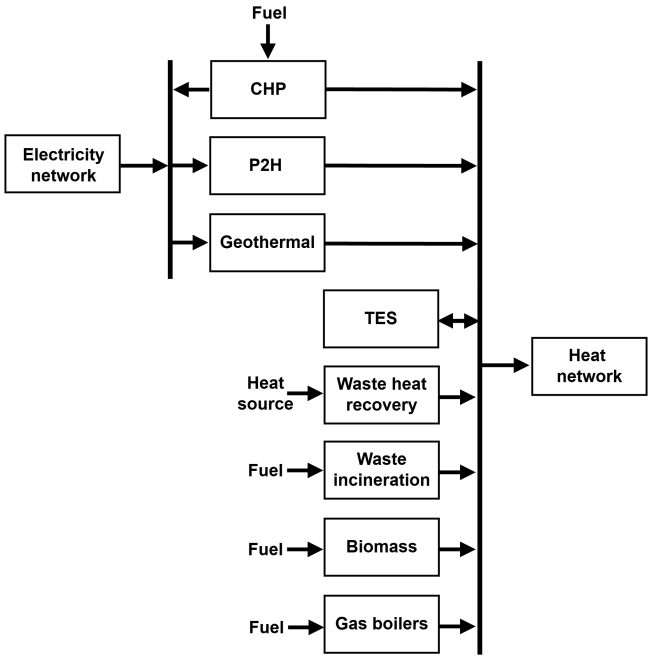

Figure 3.3: Heat and electricity network interaction in South-Holland

In summary, the main requirements for the integrated heat and electricity models are as follows:

- To perform operational optimisation of the South-Holland DHN, taking into account the heat network topology and input data (prices, heat demand and temperature);
- To perform PFA of the EDN, taking into account the distribution network topology and input data (electricity demand and supply from DHN and Stedin load profiles);
- To have the ability to simulate multiple scenarios by adjusting heat and electricity network topology and input data (demand and supply, prices, temperature) depending on the selected year;
- To leverage the functionality of PyPSA and pandapower libraries, i.e. to create a model that would allow the user to freely expand or simplify the network topology, making it possible to simulate the operation and plan the future network investments, according to the selected research questions;
- To be well described, have distinct outputs and to ensure coherent structure;

- To have the ability to precisely determine the impact of DHN electrification on the EDN to determine the possible decarbonisation pathways.

3.2.2 Modelling approach

The modelling approach consists of three sections depicted in Figure 3.4. The first step is the development and execution of the DHN model. Firstly, the DHN topology is created using the PyPSA library, which includes defining all the network architecture and component parameters. Then the relevant input data can be assigned to the network components and applied to the calculations necessary for the heat network optimisation. For example, the hourly heat demand is assigned to the demand buses, air and ground temperature data is imported to calculate the COP of HP and geothermal units, while natural gas, CO_2 and electricity price data (provided by Eneco) are assigned to production units. With additional constraints and functionality (discussed in Section 3.2.6) added to the heat network, the yearly operation of the DHN based on the selected year can be optimised. The main output of the DHN operational optimisation is the time series data of electricity consumption and production, which is then used as load and generation data in the EDN model.

The second step involves developing and modelling the EDN by accurately identifying and representing the points of interaction between the heat and electricity network. The following interaction points are obtained from expert knowledge from Eneco and Stedin side, allowing to construct only the part of the EDN topology that feeds or receives power from the DHN sources. The EDN is constructed using the pandapower library. Having the output profiles from the DHN optimisation, the substation load demand data (provided by Stedin) and the distribution network topology, the time series PFA of the EDN can be performed for the entire year. The third and last step involves the analysis of the results, meaning a visual and numerical comparison between scenarios and analysis of the heat and electricity network component operation. Overall, the integrated network models are produced to represent the real-life physical systems as closely as possible. Each assumption is made with the help of industry expert knowledge, applied from the previous version of the DHN model or based on open-source data and literature.

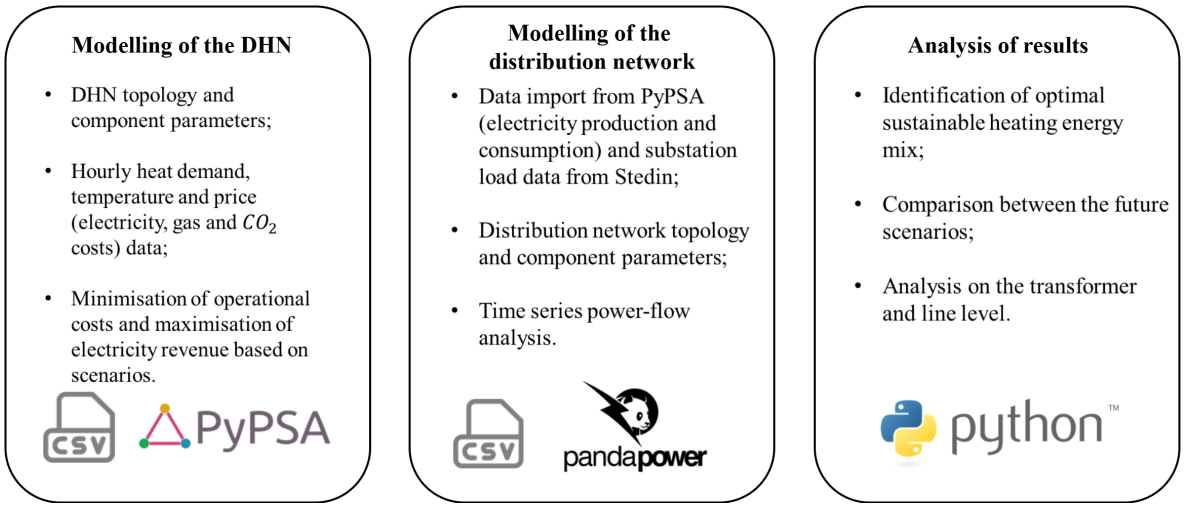

Figure 3.4: Summary of the intended modelling approach

3.2.3 Model Inputs

This section outlines the main input data utilised in the new South-Holland DHN and EDN models. First, the input data of the DHN model is discussed, followed by the EDN input data discussion. At each step, the key modifications made compared to the old DHN model are highlighted.

3.2.3.1 DHN model

Initially, the heat network topology is created by importing the network files, with each network component defined in a separate Excel *.csv* file. These files contain static parameters for elements such as buses, carriers, generators, links, loads, storage units and stores. The full and base heat network topologies with all components are presented in Appendix G. Moreover, Tables 3.3 and 3.4 summarise the key parameters of all the components used in the DHN model. As shown, the same supply and storage units have been retained to ensure consistency between the old and new models. In addition, due to PyPSA functionality, each network component file includes dedicated columns for every applicable attribute, as defined in the PyPSA documentation [55]. This structure provides a high level of flexibility that allows the modeller to easily include or exclude optional component attributes. As a result, the model can be modified to represent fewer or greater detail, depending on the specific objectives and the selected constraints. Although between the old and new DHN models the same supply and storage units have been used, some parameters were changed to have a more real-world representation of the heat production and storage units. The main numerical changes made in the new DHN model are discussed in Section 3.2.6.

Compared to the old DHN model, the input data for heat demand and prices remain unchanged, as provided by Eneco, the heat network operator. Before running the DHN optimisation model, the user can select the historical simulation data for five calendar years, ranging from 2018 to 2022. In addition, the new DHN model introduces year-specific weather data, including air and ground temperatures. Furthermore, the demand and price data are adjusted to reflect projected scenarios for years 2030, 2040 and 2050, which offers flexibility in conducting future and past scenario analysis based on the provided baseline data. In general, the input of the DHN model is composed of multiple Excel *.csv* files, which collectively form the basis for the modelling, optimisation and analysis of the DHN operation and planning. In the DHN model, the input data serve the following purposes:

1. Defines the heat network topology (heat production plants, heat buffers, heat pipes and demand points);
2. Specifies technical and economic parameters for each component;
3. Provides time-series data of hourly prices (CO_2 natural gas and electricity), weather data (ground and air temperature) and heat demand profiles;
4. Includes scenario-specific parameters used to assess various decarbonisation pathways and network configurations.

Storage	Type	Buffer Capacity (MWh)	Rated Capacity (MW)	Max SOC (Hours)	Store eff.	Dispatch eff.	Marginal costs (€/MWh)
DH Storage1	TTES	347	40	8.675	0.98	0.98	1.656
DH Storage2	TTES	500	50	10	0.98	0.98	1.656
RDAM1 Storage1	TTES	700	700	1	0.98	0.98	1.656
RDAM1 Storage2	TTES	500	50	10	0.98	0.98	1.656
RDAM2 Storage	TTES	53.3	53.3	1	0.98	0.98	1.656
B-triangle Storage	TTES	500	50	10	0.98	0.98	1.656
Tuinders Storage	TTES	750	750	1	0.98	0.98	1.656

Table 3.3: PyPSA network heat storage

Production unit	Heat. Eff.	El. Eff.	Min. prod. (MW)	Max. prod. (MW)	Gas con. (MW)	CO_2 factor (ton/MW)	El. prod. (MW)	SU cost (€)	Marginal costs (€/MWh)
Rotterdam									
WI	0.8	-	60	200	-	0	-	0	scenario based
IWH1	1	-	0	39.17	-	0	-	0	scenario based
IWH2	1	-	4	20	-	0	-	0	scenario based
RDAM Gas1	0.789	-	0	120	152	0.2325	-	0	var[2]
RDAM Gas2	0.801	-	0	25	31.2	0.2280	-	0	var[2]
RDAM Gas3	0.788	-	0	43.89	55.7	0.235	-	0	var[2]
RDAM Gas4	0.791	-	0	140	177	0.2329	-	0	var[2]
RDAM CHP1	0.487	0.214	34.17	56.94	117	0.2265	25	1652	var[2]
RDAM CHP2	0.487	0.214	34.17	56.94	117	0.2265	25	1652	var[2]
RDAM CHP3	0.4	0.38	90	200	500	0.4600	190	13500	var[2]
RDAM Geo	var[1]	-	0	4	-	0	-	0	var[3]
RDAM HP	var[1]	-	0	30	-	0	-	0	var[3]
Den Haag									
DH CHP1	0.389	0.414	0	40	102.7	0.4725	42.5	5000	var[2]
DH CHP2	0.389	0.414	0	40	102.7	0.4725	42.5	5000	var[2]
DH Gas1	0.797	-	0	110	138	0.2300	-	0	var[2]
DH Gas2	0.791	-	0	25	31.6	0.2280	-	0	var[2]
DH Gas3	0.808	-	0	45	55.7	0.2267	-	0	var[2]
DH Geo1	var[1]	-	0	3.33	-	0	-	0	var[3]
DH Geo2	var[1]	-	0	4	-	0	-	0	var[3]
DH Geo3	var[1]	-	0	4	-	0	-	0	var[3]
DH Geo4	var[1]	-	0	4	-	0	-	0	var[3]
DH HP	var[1]	-	0	30	-	0	-	0	var[3]
DH EB	var[1]	-	0	20	-	0	-	0	var[3]
Tuinders									
Biomass	0.8	-	0	43.22	-	0	-	0	scenario based
Tuinders Geo	var[1]	-	0	4	-	0	-	0	var[3]

var[1] – variable on air/ground temperature
var[2] – variable gas and CO_2 market price
var[3] – variable electricity market price

Table 3.4: DHN sources and their parameters

3.2.3.2 EDN model

The input data for the EDN model in pandapower is taken from two main sources: the operational optimisation results of the DHN model and substation data provided by Stedin. From the DHN optimisation, the EDN model receives the hourly active power consumption and production profiles for P2H, geothermal systems and CHP units, while Stedin provides the active power demand data of the 10 kV and 25 kV substations. The distribution network topology is defined with the help of professionals from Eneco and Stedin, since the heat operator identified the locations of the planned heat sources, allowing the DSO to determine the possible substation connection points. The EDN topology is defined using a single Excel *.csv* file, containing static parameters for all network components, including buses, lines, transformers, loads and generators. The single Excel *.csv* file adheres to the pandapower data format, allowing users to easily add and remove components while also changing the specific component parameters. The distribution network structure is presented in Appendix H. Despite the network topology illustrations for Rotterdam and The Hague being separate, both locations are modelled within a single unified model, as they are connected to the same external grid component. Additionally, pandapower requires to define physical parameters of lines and transformers or use standard types from the pandapower library. Since the standard pandapower component types are not applicable for the South-Holland distribution network, new line and transformer types are defined with the help of Stedin. The new standard line and transformer types are defined in Appendix B. Regarding the line connections, the model utilises HV, MV and LV lines, with specific line lengths obtained from open-source data in the *HoogspanningsNet Netkaart V6.5* [56]. The input data in EDN model serves the following purposes:

1. Defines the distribution network topology (lines, transformers, loads, buses and generation);
2. Specifies technical parameters for each component;
3. Provides time-series data of hourly active power demand and generation to specific components.

3.2.4 Model formulation

This section provides an overview on the structure of the underlying optimisation model of the DHN and the time series PFA of the EDN. For script implementation, high-level Python programming is applied using the PyPSA and pandapower libraries. The fundamental mathematical formulation and optimisation techniques of

the PyPSA model are discussed in detail, highlighting how the optimisation problem is changed according to varying DHN conditions. For the EDN model, the focus is placed on the pandapower time series PFA method, which is used to assess the performance of the network under dynamic load conditions introduced by the electrification of the heat supply.

3.2.4.1 DHN model

The DHN network optimisation problem is defined mathematically and consists of an objective function, decision variables (binary and continuous) and constraints. Equation 3.4 is used to represent the objective function, as the main constituents are the operational cost of heat generation and transport of heat, plus the start-up costs of the heat supply units. Additionally, the PyPSA library adds the capital costs term to the objective; however, in this thesis, capital investment costs are not considered, since only operational dispatch optimisation is performed. Furthermore, the objective function can be expanded further into 3.5, where the cost components are expanded to represent the minimisation of the operational costs of the heat production units (by links and generators) and transmission, the maximisation of the revenue from electricity production and the minimisation of the start-up of the CHP units. With the given objective, the optimisation is formed as a MILP problem, since binary values determine the operation of the CHP units. Operational cost minimisation preferentially dispatches those units with the lowest marginal costs, while also utilises heat pipes with the lowest distribution costs. Additionally, the revenue maximisation element ensures that in preferable periods the CHP units are operational to produce electricity for maximum profit. Overall, this is a well-ordered approach for solving a complex DHN network structure, which optimises the network from several layers, resulting in a closer representation to the real-life DHN operation.

$$C_{\text{total}}(x) = \text{Operational Costs}(x) + \text{SU Costs}(x) \tag{3.4}$$

The mathematical representation of the objective function can be further expanded to Equation 3.5:

$$\begin{aligned} C_{\text{total}}(x) = \sum_t w_t \Bigg[& \sum_{n,g} C_{\text{generator}} + \sum_{n,s} C_{\text{storage}} + \sum_{n,l} C_{\text{link}}^{\text{CHP}} \\ & + \sum_{n,l} C_{\text{link}}^{\text{gas boiler}} + \sum_{n,l} C_{\text{link}} + \sum_{n,l} C_{\text{transport}} \Bigg] + \sum_t C_{\text{SU}}^{\text{CHP}} \end{aligned} \tag{3.5}$$

where:
$C_{\text{generator}}$ = Generator operational costs, [€]
C_{storage} = Storage operational costs, [€]
$C_{\text{link}}^{\text{CHP}}$ = CHP operational costs, [€]
$C_{\text{link}}^{\text{gas boiler}}$ = Gas boiler operational costs, [€]
C_{link} = Link operational costs, [€]
$C_{\text{transport}}$ = Heat pipe transfer costs, [€]
$C_{\text{SU}}^{\text{CHP}}$ = CHP start-up costs, [€]

Equation 3.5 depicting the complete mathematical representation of the objective function can be expanded further to 3.6 - 3.15. In the DHN model, the generator component in PyPSA is used to represent biomass, external grid and waste heat recovery units, while the link component is used to model CHP units, gas boilers, waste incineration, geothermal, P2H (HP and EB) and heat distribution pipelines. The generator costs in 3.6 are calculated as a product of the marginal costs of fuel $O_{n,g}$ and the nominal power of the heat production unit $P_{n,g,t}$. For biomass and waste heat recovery units, the costs of fuel are static, while the external grid has attached market costs of electricity based on the selected simulation year. Equation 3.7 defines heat buffer costs, which is a product of storage marginal costs $O_{n,s}$ and heat dispatch $P_{n,s,t}$. For links, the costs of fuel vary by technology, waste incineration plant has a static fuel price, CHP and gas boilers operate according to market

prices of natural gas, while P2H with geothermal units take on the electricity market prices, since they are attached to the eternal grid, and heat distribution pipes operate with zero costs except WLQ pipe connection the waste incineration plant to The Hague. However, gas boilers and CHP units have predetermined CO_2factors, in addition, CHP units must consider the revenue from electricity. As a result, the costs of the CHP and gas boiler units are separated from the rest of the link components and are represented with their own formulation. CHP costs are defined as the sum of heat production costs $O_{n,l}P^{\text{th}}_{n,l,t}$, minus the revenue from the produced electricity $O_{n,l}P^{\text{el}}_{n,l,t}$, plus CO_2 costs $C_{CO2,l,t}$, as in 3.8. Similarly, gas boiler costs follow the same logic, only the electricity revenue term is not applicable, see 3.9. Natural gas costs are attached to a store component in PyPSA, however, they are still defined as $O_{n,l}$, since link components are attached to the store component (which act as fuel supply) take on the marginal costs of the store (linked to market price of natural gas) as their marginal costs. However, the costs of waste incineration, geothermal and P2H units are determined by 3.10. The costs of heat distribution (3.11) are calculated as a result of the marginal cost of transport $O_{n,l}$ (since heat pipes are modelled as links) and heat flow through the pipe $H_{l,t}$. Lastly, binary variables $u_{n,l,t}$ are included to describe the on and off status of CHP units and are used to include the fixed start-up costs SU^{CHP} in the objective function, as in 3.12. In general, all operational costs in this simulation are based on the marginal cost of fuel (dynamic or static) and exclude other variable costs, such as operation and maintenance (O&M). The exact assignment of fuel prices is discussed in the South-Holland case study in Chapter 4.

$$C_{\text{generator}} = o_{n,g} \cdot p^{nom}_{n,g,t} \tag{3.6}$$
$$C_{\text{storage}} = o_{n,s} \cdot p^{dispatch}_{n,s,t} \tag{3.7}$$
$$C^{\text{CHP}}_{\text{link}} = o_{n,l} \cdot p^{\text{th}}_{n,l,t} - o_{n,l} \cdot p^{\text{el}}_{n,l,t} + c_{CO2,l,t} \tag{3.8}$$
$$C^{\text{gas boiler}}_{\text{link}} = o_{n,l} \cdot p^{\text{th}}_{n,l,t} + c_{CO2,l,t} \tag{3.9}$$
$$C_{\text{link}} = o_{n,l} \cdot p^{\text{nom}}_{n,l,t} \cdot \eta_{l,\text{th}} \tag{3.10}$$
$$C_{\text{transport}} = o_{n,l} \cdot h_{h,t} \tag{3.11}$$
$$C^{\text{CHP}}_{\text{SU}} = SU^{CHP} \cdot u_{n,l,t} \tag{3.12}$$
$$C_{CO2,l,t} = c_{price,t} \cdot g_{n,l,t} \cdot F_{CO2,l} \tag{3.13}$$
$$p^{\text{th}}_{n,l,t} = g_{n,l,t} \cdot \eta_{l,\text{th}} \tag{3.14}$$
$$p^{\text{el}}_{n,l,t} = g_{n,l,t} \cdot \eta_{l,\text{el}} \tag{3.15}$$

Overall, the objective function and constraints are defined as:

$$\min C_{\text{total}}(x) = \text{Operational Costs}(x) + \text{SU Costs}(x) \tag{3.16}$$
subject to (3.17)
$$g^{min}_{n,g,t} \cdot G_{n,g} \leq p^{nom}_{n,g,t} \leq g^{max}_{n,g,t} \cdot G_{n,g} \tag{3.18}$$
$$G^{lb}_{n,g} \leq G_{n,g} \leq G^{ub}_{n,g} \tag{3.19}$$
$$0 \leq p^{dispatch}_{n,s,t} \leq H_{n,s} \tag{3.20}$$
$$0 \leq p^{uptake}_{n,s,t} \leq H_{n,s} \tag{3.21}$$
$$0 \leq soc_{n,s,t} \leq R_{n,s} \cdot H_{n,s} \tag{3.22}$$
$$soc_{n,s,t} = soc_{n,s,t-1} + \eta_{n,s,+} p^{uptake}_{n,s,t} - \eta_{n,s,-} p^{dispatch}_{n,s,t} \tag{3.23}$$
$$-\infty \leq p_{n,j,t} \leq +\infty \tag{3.24}$$
$$e_{n,j,t} = \eta_{n,j,stand} e_{n,j,t-1} - p_{n,j,t} \tag{3.25}$$
$$| h_{h,t} | \leq F_l \tag{3.26}$$
$$u_{n,l,t} \cdot l^{min}_{n,l,t} \cdot L_{n,l} \leq p_{n,l,t} \leq u_{n,l,t} \cdot l^{max}_{n,l,t} \cdot L_{n,l} \tag{3.27}$$

**Formulas adopted from PyPSA documentation [45].*

3.2.4.2 EDN model

PFA, also known as load flow analysis, is used to determine the steady-state operation of an electrical power networks. In this thesis, it is assumed that the three network phases are balanced, allowing the network to be represented as a single-phase equivalent circuit. The EDN model utilises the pandapower time series module, which is specifically designed to execute time-dependent electrical networks behaviour. This function enables the simulation of multiple time steps by running sequential full AC power flow calculations (referred to as snapshots in pandapower) [47]. Each snapshot models the EDN statically at a given time step, accounting for variations in load demand and power generation. Therefore, the EDN model involves solving the non-linear AC power flow equations over a full year with varying substation data from Stedin, demand from electrified heat sources and production from the CHP units.

In pandapower, the PFA model is based on the full AC formulation, which follows the formulas based on Kirchhoff's laws. At each bus i, the key variables are net active power injection P_i, net reactive power injection Q_i, voltage magnitude $|V_i|$ and relative voltage angle θ_i [57]. The power balance at each bus is governed by the following complex power Equation 3.28:

$$S_i = V_i I_i^* = V_i \sum_{j=1}^{n} Y_{ij}^* V_j^* \tag{3.28}$$

This can be expanded into real and reactive power components:

$$P_i = \sum_{j=1}^{n} |V_i||V_j||Y_{jk}|cos(\theta_i - \theta_j - \delta_{ij}) \tag{3.29}$$

$$Q_i = \sum_{j=1}^{n} |V_i||V_j|sin(\theta_i - \theta_j - \delta_{ij}) \tag{3.30}$$

Where:

- $S_i = P_i + jQ_i$ is the apparent power injected at bus i and is a complex sum of real and reactive power,
- $V_i = |V_i|e^{j\delta_i}$ is the complex voltage at bus i,
- $Y_{ij}^* = |Y_{ij}|e^{j\delta_{ij}} = G_{jk} + jB_{ij}$ is the complex admittance between buses i and j, which consists of conductance G ans acceptance B,
- V_j^* is the complex conjugate of the voltage at bus j,
- n is the total number of buses.

The output of the DHN model is the active power demand and production of electrified heat supply units and CHPs. Stedin load profile data of the substations also contains only active power data, while reactive power is estimated internally by the pandapower model. All input data are stored external pandas *DataFrame* structures. These input values are indexed by time and linked to the corresponding network elements via controllers. The controllers are used to update the network parameters at each time step before executing the PFA. The simulation is essentially performed in a loop, where at each snapshot, the network values are updated and full AC power flow is solved. The results are logged by *OutputWriter* object in pandapower, which stores the selected output variables by the user. The main selected outputs of the EDN model include bus voltage magnitudes, voltage angles, line loading and transformer loading. The EDN model setup enables to capture both short and long term variations of the network, in particular the load variations added by the P2H and geothermal technologies. With this approach, the impact of heat supply source electrification can be analysed under various scenarios. The key output data used to assess the network performance are defined by 3.31 and 3.32:

$$Line_{loading} = \left(\frac{i_{ka}}{I_{ka}^{max} \cdot DF \cdot Parallel} \right) \cdot 100 \tag{3.31}$$

$$Transformer_{loading} = \max\left(\frac{i_{hv,t} \cdot v_{hv,t}}{SN_{mva}}, \frac{i_{lv,t} \cdot v_{lv,t}}{SN_{mva}}\right) \cdot 100 \tag{3.32}$$

$$VM_{pu} = |V_{bus}| \tag{3.33}$$

$$VA_{degree} = \angle V_{bus} \tag{3.34}$$

Equation 3.31 computes the line loading percentage used to reflect the utilisation of a line relative to the rated current capacity. Line loading in pandapower is based on current loading compared to the maximum allowable current (or ampacity) of the line. For this thesis, the maximum safe line loading conditions are assumed to occur at 80% of the maximum allowable current. Temporary loading levels of 100-120% allowed to occur, but only for very short time period (1-2hours), hence, all lines above this limit require reinforcement. Moreover, 3.32 calculates the transformer loading percentage by comparing the apparent power flow on the HV and LV sides compared to the transformer nominal rating. Monitoring these outputs is crucial for identifying bottlenecks and planning EDN reinforcement measures. According to the industry, [58] and [59], under normal operation a 20% safety buffer is recommended for transformers, thus the transformer should not exceed 80% of its maximum load capacity under normal loading conditions. Similar to lines, temporary loading levels of 100-120% are allowed to occur for very short periods. In addition, the voltage magnitude per unit (p.u.) and the voltage angle at each bus are captured using Equations 3.33 and 3.34, respectively.

3.2.5 Model settings

With PyPSA the heat network is translated into an optimisation model. The PyPSA library internally relies on linopy as its optimisation framework, which defines the required objective function, decision variables and constraints. Both commercial and open-source solvers can be used to solve the resulting Pyomo model, such as Gurobi, CPLEX, HiGHS, GLPK or CBC. However, in this simulation, the commercial Gurobi solver was utilised under an academic license because of its superior computational efficiency. On average, the full-year simulation of the DHN model is completed in approximately 2.5 minutes, representing a significant improvement compared to the previous model, which required approximately 20 minutes per scenario when solved on a rolling horizon based manner.

With pandapower, the distribution network is structured to run the PFA. Nevertheless, the pandapower library is primarily designed to perform static PFA for a single snapshot of the network. However, the modelling approach in this case requires to study the distribution network over a time period of a year. For this reason, a time series simulation method is applied in the pandapower script, which performs a static PFA, solving the power network equations for a given number of input data steps. The simulation tracks the critical elements of the network over time, such as bus voltage magnitudes, line, and transformer loading, which are the main output of the model. The time series simulation is set up to run with *continue on divergence* input set to *True*, which results in time series calculation continuing even when the power flow analysis does not converge. Upon experiencing a convergence error the given output of bus voltage is set to zero, while line and transformer loading is calculated. With this input in the run time series function the network behaviour can be studied and the points of failure clearly identified. The average solving time of the EDN model for 8760 time steps is approximately 2.5 minutes, thus the full results of integrated heat and electricity models can be obtained in around 5 minutes.

The solving time of the models are influenced by three key factors: temporal resolution, network simulation period and the mixed-integer programming (MIP) gap (applicable only to the DHN model). The temporal resolution determines the length of a single time step used in the model. Although a smaller time step will increase the accuracy of the model and enable exploring new network dynamics (for grid balancing services, etc.), it will also significantly increase the computational time. In this study, hourly time-steps are applied to both DHN and EDN models to maintain compatibility with the available input data and to ensure consistency with the previous DHN model version. Hourly resolution allows for a realistic representation of network component dynamics, that captures the intra-day and seasonal fluctuations in correlation with electricity, fuel and CO_2 prices, heat and electricity demand, as well as differences in air and ground temperatures.

For both models, the chosen optimisation period is 8760 hours, representing a full year. Nevertheless, the models are flexible and support smaller time scales. This can be useful for focusing on component operation, such as evaluating network performance during the coldest and warmest weeks of the year. Naturally, opting for a reduced time horizon will result in faster computation. Lastly, the MIP gap parameter is used to control the relative tolerance between the upper and lower bounds of the objective function. Essentially, this parameter enforces an accuracy constraint on the solver, as it has to find the optimal solution within the specified gap. The MIP gap is kept at 0.02 to balance computational efficiency and accuracy. However, for users with higher computational capacity, the default MIP gap value of 0.001 is recommended for increased precision. The computer which was used for running both models has the following specifications: AMD Ryzen 3750H CPU, 2.4 GHz.

3.2.6 Model assumptions

This section focuses primarily on outlining the constraints and new functionalities integrated into the DHN model. In addition, the key assumptions for creating the EDN model as discussed.

3.2.6.1 DHN Model

The primary objective of introducing a new range of capabilities is to align the model's operation more closely with real-world behaviour. In addition to introducing new capabilities, several assumptions from the previous model have been removed or altered to better reflect the dynamics and operation of the network.Table 3.5 lists the key assumptions made in the new DHN model:

Scope	Assumption
Heat production	Annual contracted heat production of IWH1 unit
Heat production	Minimum generation constraints, p_{pu}^{min} (applied to certain units).
Heat production	Variable COP of HP and geothermal units, constant EB efficiency
Heat production	Applied efficiency parameter to heat production units (biomass, IWH, WI)
Heat production	Biomass unit turned of during August
Heat storage	Applied efficiency parameter to heat storage
Heat transport	Applied heat losses in distribution pipes
Costs	SU costs applied to CHPs only (all other units zero costs)
Costs	Applied costs of heat storage
Costs	Seasonal pricing of WI unit heat distribution to The Hague

Table 3.5: Current model assumptions and constraints

Regarding the production of waste heat units, the annual production limit of 170,833.33 MWh per year is maintained for the IWH1 unit. Instead of setting a seasonal heat output constraint, the PyPSA library allows setting the maximum total energy produced (e_{sum}^{max}) during the optimisation horizon. The efficiency of IWH1 and IWH2 is still set to 100%, while IWH2 unit has an assigned $p_{pu}^{\min}$ value equal to 0.2. It has been decided to retain some similarity to the old model and to model the waste heat supply as the base heat supply that does not fluctuate with the market prices. Moreover, the efficiency of the biomass and WI units is set to 80% to simulate the production of heat with the losses that occur. The shutdown of the biomass plant during August is kept to simulate the planned maintenance period. The shutdown time-steps are adjusted to for the month of August. The constraint that links the production of RDAM CHP3 and WI is removed, to model independent operation of the units. Furthermore, a 2% storage and dispatch loss is introduced as heat losses cannot be avoided. With respect to heat distribution pipes, heat losses are now assigned to all pipes, while the seasonal distribution costs for the WLQ pipeline remain. Additionally, pipe 10 and pipe 11 have been made bidirectional to utilise the available storage not only to store heat but also to dispatch it. The SU costs are applied to CHP units only as the previous version of the model did not include SU costs for other heat production units. Hence, the operation of the CHPs are linked to SU and market prices of natural gas.

The previous DHN model assumed that the COP values for HPs and geothermal heat sources were constant. Specifically, HPs were assigned a COP of 3, while geothermal sources were stated to operate with a COP of 8, however, in practice, a value of 1 was used. In the new model, hourly COP values for both geothermal and HPs are calculated and applied. These values are based on the hourly ground and air temperature data, as well as the sink temperature level, and are determined by applying 3.35 and 3.36. These COP formulations are based on the methodology of the PyPSA-Eur model [60] and were used to model air-source heat pumps (ASHPs) and ground-source heat pumps (GSHPs).

$$\mathrm{COP}_{\mathrm{ASHP}}(T_{\mathrm{source}}, T_{\mathrm{sink}}) = 6.81 - 0.121\Delta T + 0.000630\Delta T^2 \tag{3.35}$$

$$\mathrm{COP}_{\mathrm{GSHP}}(T_{\mathrm{source}}, T_{\mathrm{sink}}) = 8.77 - 0.150\Delta T + 0.000734\Delta T^2 \tag{3.36}$$

,where $\Delta T = T_{\mathrm{sink}} - T_{\mathrm{source}}$ is the temperature difference between the sink and the source [46], [60].

Figure 3.5 shows the hourly COP curves for HPs and geothermal heat sources based on air and ground temperature data from 2022. For air-source HPs, the COP is assumed to vary between 1.2 and 3.7, while for geothermal systems, it ranges from 4.1 to 5.2 depending on the season. These numbers are a result of the chosen sink temperature, which is 65°C for HPs and 45°C for geothermal systems. A higher sink temperature for HPs and for geothermal systems leads to a reduced COP.

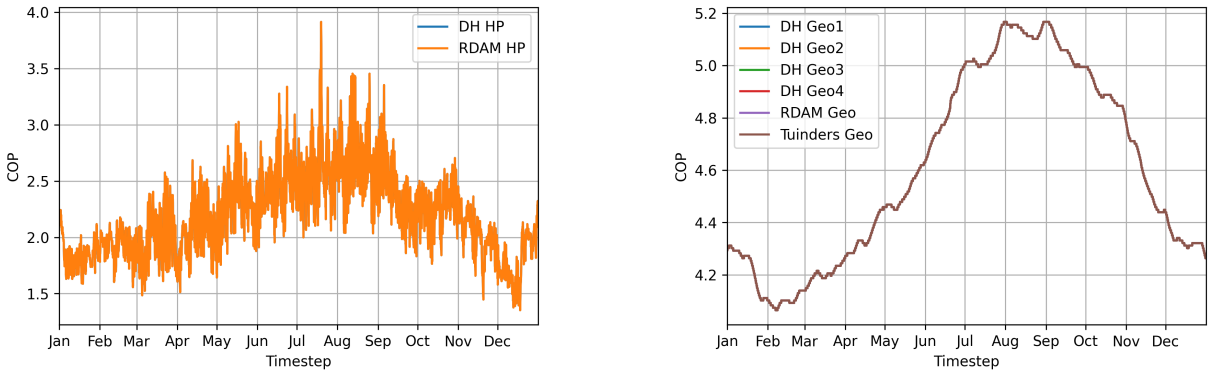

(a) Heat pump COP

(b) Geothermal COP

Figure 3.5: COP values of HPs and geothermal heat sources in 2022

The old DHN model imposed a minimum heat production constraint on all geothermal units, EB, HPs, WI, Rotterdam CHPs and IWH2. In contrast, the new DHN model links the operation of geothermal units, EBs and HPs directly to electricity prices. This approach offers a more realistic representation of the operation, as these units typically respond to market indicators, such as electricity price, to adjust their heat output. This change allows for more flexible and economically driven heat dispatch behaviour, improving the ability of the model to determine the required load to power these units. On the other hand, the minimum heat production constraint was maintained for the WI, IWH2 and Rotterdam CHPs. However, this caused issues in the PyPSA model during periods of low heat demand, as the enforced minimum heat output exceeded the heat requirement. Because PyPSA does not allow heat dumping, such an oversupply of heat resulted in a failed simulation.

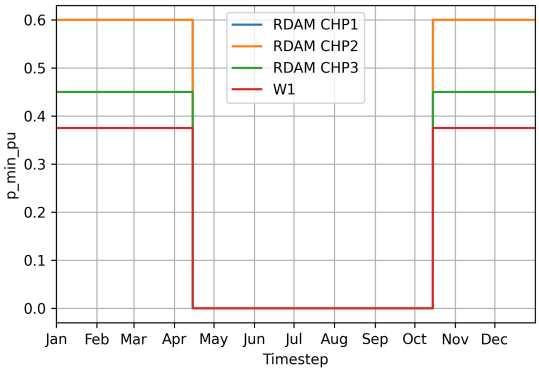

Figure 3.6: Seasonality constraints

Two solutions were implemented to resolve this: first, adjustments were made in the modelling area in how the components supply heat to the network; second, the model was assigned to operate seasonally, thus periods of oversupply of heat could be managed or avoided. In Appendix G, the full representation of the DHN model is presented. As seen, the units with minimal generation constraints have heat sinks for heat dumping. The heat sink was modelled as a store component with 100% standing loss, thus the heat can be dumped instantaneously (on the hourly basis) without the need for calculating the optimal size of the heat sink. A link component was added to connect the bus (where both the heat sink and supply units are attached) to the heat distribution network. This ensures that any heat not directed to the sink is routed into the heat network. For CHPs, the AC sink is used to illustrate the power transferred to the power network. Regarding the heating seasonality, it is assumed that the heating season starts at 15th of October and ends at 15th of April. During the warm season the *p_min_pu* are set to zero, allowing the system to optimise the heat supply based on costs.

3.2.6.2 EDN Model

The key assumptions regarding the EDN model primarily concern the network topology. To accurately simulate the operation of the electricity distribution network, it is required to include the higher level network as well. In this thesis, both DSO and TSO network components are included, however, the analysis is done only for the DSO part. Given that the South-Holland DHN covers a large geographical area, with electrified heat sources and CHP units distributed across multiple locations, the EDN model adopts a focused approach by including only those network components that either supply power to electrified heat sources or receive power from CHP units. With this approach specific substation and line operations can be targeted and analysed. The EDN topology has been validated and confirmed in collaboration with DSO Stedin, ensuring that the network representation is both realistic and aligned with actual network structure. No other parameters or constraints are implemented with regard to the EDN model, as standard line and transformer types are utilised, which are also validated by Stedin. The operation of the EDN is directly linked to what constraints and scenarios are chosen to be applicable in the DHN model.

3.2.7 Model validation

Model validation was performed to assess whether the old Pyomo model is comparable to the new PyPSA model. For model validation, the base network scenario was taken, which does not have additional heat sources and storage units, however, uses base heat demand and base price (gas, CO_2 and electricity) data for 2022. The new model configuration is shown in Appendix C, which replicates the architecture of the old base model. Tables 12 and 13 in Appendix C show the parameters of heat sources and storage that were used to achieve similarity between models.

As depicted in Figure 3.7, the old model is compared with two cases of the new model: first, without variable costs assigned to the CHP units and second, with variable costs assigned to the CHP units. During model test

runs, it was noticed that by replicating the exact parameters of the Pyomo model, the output of the PyPSA model is different (represented by Fig. 3.7c). Only by removing the fixed variable cost parameters from the CHP units do the two models show similarity (seen in Fig. 3.7b). Since variable and SU costs are only applicable to CHPs, while all other heat generation units have zero variable and SU costs, the PyPSA model sees CHP generators as too expensive to operate. Instead, a waste-incineration plant is used in combination with cheaper heat-only gas boilers and heat storage to cover demand. Hence, the base and future models of the South-Holland DHN network in PyPSA do not have variable costs assigned to the CHP generators. In contrast to the old model, the CHPs operate based on CO_2 and gas price of the market. Hence, the new PyPSA model is validated with the settings described above.

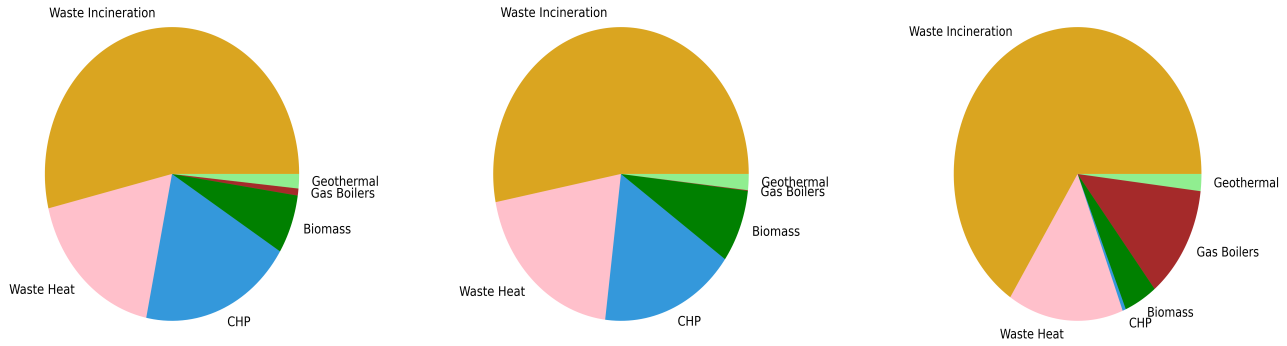

(a) Pyomo model, base case *(b) PyPSA model, base case* *(c) PyPSA model, with variable costs*

Figure 3.7: Base model production per category in 2022

In 2022, the real-world South-Holland DHN had a different network structure compared to the base cases modelled in Pyomo and PyPSA. The main difference is the lack of the WLQ connection between the Hague and Rotterdam. Therefore, the real DHN consisted of two separate heating networks at the time. In addition, the IWH2 industrial waste heat plant did not supply heat to the network at the time, therefore, it is also excluded from the model compared to the real-world data. Figure 3.8 illustrates the difference in total heat supply by category, while Table 14 in Appendix C provides a comparison of the numerical data. The heat supply of DH Gas3 is added to the sum of the CHP supply in the real DHN data, hence, the same is done in the PyPSA model. Moreover, there is uncertainty about the real-world industrial waste heat, biomass and geothermal data, while RDAM Gas2 units data is missing. Therefore, precise comparison is not reachable, however, the main operational trends are comparable as seen in Figure 3.8.

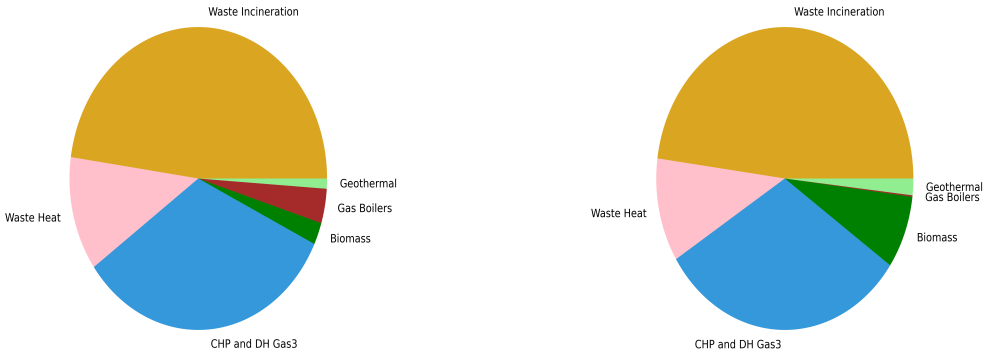

(a) Real-world *(b) PyPSA model*

Figure 3.8: Total heat supply per category in 2022 (without WLQ connection and IWH2).

3.2.8 Model verification

Model verification was completed to evaluate the precision of the DHN and EDN models. Regarding the DHN model, the examination was conducted by modifying the objective function and investigating whether the optimisation outputs logically align with the conceptual model. The EDN model was verified by altering the structure of the distribution network by means of adding or removing network components and by running the model with altered electricity demand profiles. Overall, verification of both models is essential in not only measuring the accuracy of the models, but also understanding their dynamic operation.

3.2.8.1 DHN model

To ensure accurate verification of the DHN model, the same base network scenario used in the model validation section was tested. This includes the base heat demand and prices (gas, CO_2 and electricity) data for 2022, and the network without additional heat sources and storage. Multiple test runs were conducted, during which a specific parameter was removed or added, resulting in a modified objective function. The following verification scenarios are listed in Table 3.6, while the visual and numerical results of each run are listed in Appendix D.

No.	
1	Base model
2	No electricity revenue expression
3	No CO_2 price (zero)
4	No TES units
5	No CHP start-up costs
6	No UC constraints (committable=FALSE)
7	No natural gas price (zero)
8	Added fixed marginal costs of production for CHP

Table 3.6: DHN model verification scenarios

To compare verification scenarios, the total production per time step per category was plotted for the first 15 days of January in 2022 (see Fig. 1 in Appendix D). For the first run, the expression of electricity revenue was removed from the objective function. The results in Figure 1b indicate that the CHPs are not operating, while the gas boilers cover the peak demand. This behaviour is expected, since gas boilers have zero SU costs and can supply heat with higher heat efficiency. Moreover, the peak demand is also covered more by TES, which is charged during off-peak periods. With zero CO_2 price, the generation trend is similar to the base model, seen in Figure 1c. However, CHPs tend to operate longer during peak demand times, which also coincides with a high electricity price (shown in Fig. 3.9). This means that the revenue from electricity production is maximised without the penalty of additional CO_2 price. With removed TES, the heat production matches the demand, which is the expected model performance, since for every time step the DHN must meet the required heat demand and account for the losses in the network (illustrated in Fig. 1d).

Moreover, the lack of SU costs results in the CHPs being turned off and on more frequently (Fig. 1e), allowing the CHPs to match their operation more favourably to electricity prices to maximise revenue from electricity production. The consequences of removing the unit-commitment (UC) constraints from the PyPSA model are that the SU costs are ignored and the model transitions from a MILP problem to LP problem (Fig. 1f). This results in all generators running continuously and makes the model computationally simpler. With zero natural gas price assigned to gas supply, the model maximises revenue from electricity production as indicated in Figure 1g showing high usage of CHP. Lastly, with fixed marginal costs of production added to CHP units, it results in no CHP operation, while peak demand for heat is covered by the gas boilers (as in Fig. 1h). The fixed variable cost of production data was taken from the previous version of the DHN model developed with Pyomo [48]. The combination of SU, fixed marginal cost of production and CO_2 price for CHP is too high. Even with the variation in electricity prices, the revenues cannot cover high operating costs.

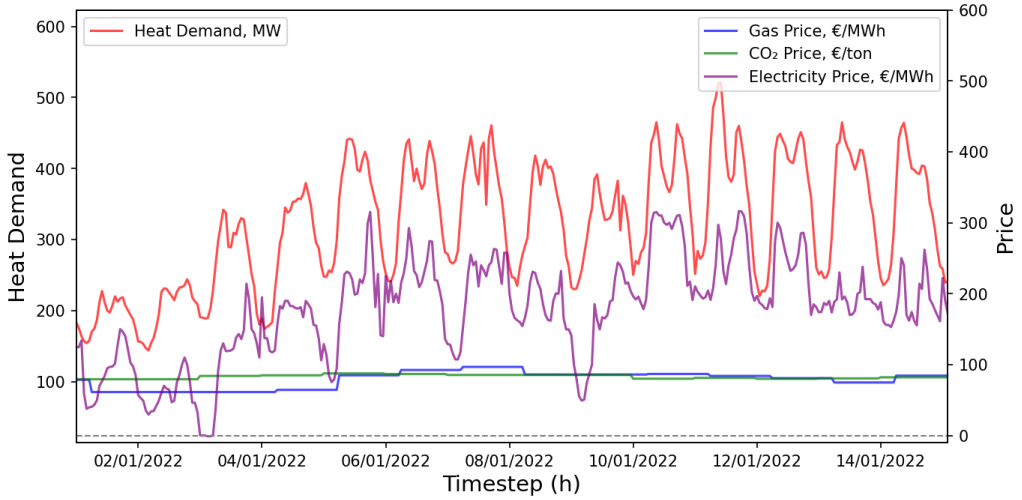

Figure 3.9: Heat demand and price data per timestep, 1st–15th of January 2022.

3.2.8.2 EDN model

Verification of the EDN model was performed to measure its accuracy and to analyze if the model behaves as expected when certain conditions are set. The selected EDN model structure is linked to the base DHN network expansion scenario in 2030, which implies that no additional heat and storage sources are added to the DHN. Thus, the corresponding EDN model does not reflect the infrastructure connections to additional heat sources, such as geothermal and P2H technologies, and uses the base network expansion case. The electrical network structure used for the verification of the model is illustrated in Figures 7 and 9 in the Appendix H. Table 3.7 shows the experiments that were conducted to verify the correct operation of the EDN model.

No.	
1	Run pandapower.diagnostic function
2	Remove critical components
3	Add network reinforcement components
4	Increase all loads by 20%
5	Reduce all loads by 20%

Table 3.7: EDN model verification experiments

The first step in verifying the model involved running the in-built *pandapower.diagnostic* function, which detects common problems that cause simulation errors. This includes check for invalid values (negative indices), voltage mismatches, disconnected elements, inconsistent or zero line impedance, missing external grid component and checking whether multiple generators are connected on a single bus. In general, this function ensures model consistency by finding any parameter mismatches. For the base EDN model under the 2030 scenario, no errors were found. To further test the model behaviour, a critical 380/150 kV Waterningen transformer, which feeds all substations in The Hague, was removed. As expected, this disrupted the power supply to The Hague, while the PFA only converged for the Rotterdam region. The results of this test are presented in the Appendix E, Tables 19 and 20, which represent loading levels of transformers and lines only for the Rotterdam branch.

In experiment No. 3, the base EDN case was simulated without any reinforcement, to receive the primary outlook of the network operation. These base case results guided the addition of critical components to confirm whether the reinforcements can solve overloading issues. Figure 2 in Appendix E depicts the medium voltage transformer loading with the unenforced and enforced base network in 2030. The numerical results of both cases are summarised in Tables 19 and 20 in Appendix E, indicating the minimum and maximum line and transformer loading throughout the simulation year of 2030. The corresponding tables indicate that for

the unenforced base case all transformers and lines failed to converge at certain time steps (shown as 0% loading). In other time steps, lines and transformers reached extremely high loading, which is operationally unsafe. For example, the Voorburg 150/25 kV transformer in one time step reached 433.61% loading, while nominal transformer and line operation occurs between 80-90%, with temporary levels of 100-120% allowed to occur. Therefore, all high and medium voltage transformers for which loading levels exceed nominal loading were reinforced with an additional transformer, by adjusting the *parallel* parameter to 2 in the pandapower network file. After reinforcement, transformer loadings returned to nominal levels and line reinforcements were no longer necessary due to current redistribution.

The No. 4 & 5 experiments were carried out to assess the model response to increasing and decreasing load demand of 20%. For the simulations the enforced base EDN network with additional transformers was used. Figure 3 in Appendix E illustrates the medium voltage transformer loading levels for increased and decreased demand. Again, the numerical results are summarised in Tables 19 and 20. The results indicate that the model responds as expected, as a higher demand results in increased loading and a lower demand reduces the loading levels. All of the experiments performed confirm that the EDN model behaves as expected under varied conditions.

3.2.9 Model outputs

The key output of the DHN model is the dispatch of heat by heat production and storage units, the electricity demand of the P2H and geothermal units and electricity production of the CHP units. The output data of the DHN model is structured in Excel *.csv* file format, while the simulation results are saved in *.nc*. Hence, the network results can be investigated without the need to execute the simulation again. The data stored in Excel can be applied to calculate operational costs, such as production costs or electricity production revenues. The main output of the EDN is hourly bus, line and transformer data, which is stored in Excel *.csv* files. Before running the PFA, the modeller can choose which component-specific data to extract by using the output writer in pandapower (indicated in the *dtypes* sheet in the distribution network file). Overall, the output data for both models is easily extractable and allows quick data investigation and visualisation of the outputs. Comparative analyses can be performed for past and future years.

4 | South-Holland case study

As described in Chapter 3, the primary goal of this thesis to develop integrated heat and electricity models was achieved. These models can be applied in a variety of ways for the future research in the operational and network planning of the real-world networks. To gain valuable answers to the research questions of this thesis, a real-world case study of the South-Holland district heat and electricity distribution networks was performed. This chapter describes how both heat and electricity models were applied to perform the analysis, based on deterministic future scenarios approach for 2030, 2040 an 2050. At first, the construction of the future scenario simulations is discussed, followed by the description of the scaling of the input data and the detailed analysis of the simulation results.

4.1 South-Holland networks

Based on the economic, social and industrial policies adopted in the region, each DHN has evolved differently, resulting specific operational patterns of the network. However, one attribute that all heat networks share is their significant dependence on energy market prices, weather patterns and consumer demand. Fuel prices are one of the primary variables in heat networks influencing their operational dynamics. Historically, the heat network operators have aimed to hedge the fluctuations in fuel prices by signing long-term bilateral contracts for fuel supply; therefore, not exposing the consumers to market fluctuations. Typical feedstock fuels for DHN heat sources include natural gas, coal, biomass (peat or wood products), waste, oil or other alternative fuels, all of which have established markets, linked to the operation of the heat networks.

However, due to sustainable energy transition goals the decarbonisation of heat supply sources in DHNs is required. This creates a new environment where the heat network operators must look for alternative heat production sources to meet the necessary heat demand. As outlined in Chapter 2, the decarbonisation of DHNs will result in the large-scale integration of electrified heat sources, such as P2H, waste heat recovery and geothermal technologies. Hence, the use of electricity as a primary energy source for the generation of heat will increase. The link between heat and electricity networks will tighten, creating a new system in which heat network operators must rely on the distribution network operators for the required supply of power to meet the heat demand. Thus, for heat network operators it essential to understand both the effect of the electrified heat sources on the operation of the heat network and whether the infrastructure requirements can be met from the DSO side for the integration of new heat production units.

Likewise, the state of the distribution networks depend on regional factors and by the established policies of the DSO operating the network. The available infrastructure of substations, connection cables and supporting equipment form the basis of each EDN. However, with the increasing decentralised generation and consumer demand, the physical network components experience excessive loading, forcing the network operators to physically expand or reinforce the network. In addition to the physical expansion, the DSOs must apply sophisticated algorithms to balance the operation of the network in real-time, often relying on market signals and flexibility services to maintain operational stability. In addition to the already present challenges, the decarbonisation of DHNs will require additional distribution network capacity and operational flexibility as more large-scale heat sources must be connected to the network. Therefore, for the distribution network operators it is necessary to understand the impact of the electrified heat sources on the operation and the physical infrastructure requirements on the distribution network.

Given the need to assess the impact of DHN decarbonisation on heat and electricity networks, a real-world case-study of the South-Holland region in the Netherlands was conducted. Based on the constructed DHN and EDN models described in detail in Chapter 3, the operation of the DHN was evaluated based on various network expansion, price, demand and weather scenarios. Resulting from that, the operation and physical infrastructure requirements of the EDN are assessed. The application of linked heat and electricity models is aimed at

analysing the operation of future networks and their investment strategies for 2030, 2040 and 2050.

4.2 Building of scenarios

To evaluate the impact of the electrification of heat supply, future scenarios for 2030, 2040 and 2050 were constructed. The construction of simulations for each year is based on the heat network expansion and heat demand projections. The following section describes the distinction between the network expansion and heat demand scenarios and how were they applied in each year of the future scenarios.

4.2.1 Heat demand scenarios

With regard to the simulations based on the future heat demand projections, two schools of thought emerge. On one side, heat demand is expected to drop due to the rising global temperatures, an increase in the built-environment heat isolation quality and the implementation of of 4GDH networks with lower heat production temperatures. Jansen [61] argues that the demand for space heating of Dutch DHNs is expected to decrease by 0.8% annually. The primary reasons being improved insulation of buildings, reduced losses in the heat distribution network due to pipe reconstruction and rising global temperatures. However, the situation in the South-Holland DHN may prove to be divergent, as the large-scale Warmtelinq project to connect Rotterdam with the Hague [49] is being completed and the Collective Heat System Act ("De Warmtewet 2") proposes to transition to sustainable heat sources via heat networks. Therefore, the operational optimisation of the South-Holland DHN was conducted based on low and high heat demand scenarios. For 2030, 2040 and 2050 low and high heat demand scenarios are investigated. Section 4.2.8 describes the how the input data was scaled accordingly.

4.2.2 Network expansion scenarios

Regarding the network expansion, two cases are considered called *base* and *full*. The *base* network configuration represents the current structure of the South-Holland DHN, while the *full* network includes all additional heat source and storage units planned for the future implementation by Eneco. Accordingly, two corresponding electricity networks were constructed to match each network expansion scenario of the DHN. It is important to note that the base DHN structure used for network validation, illustrated in Appendix F by Figure 4, is not used in this case study. A revised version of the base network case was developed, depicted in Appendix G by Figure 5. In the revised case, the operation of the geothermal unit is linked to the electrical power network feeding the source, while the WI unit is modelled as a link component in PyPSA. This way the energy conversion of waste as a fuel source is modelled, while also allowing the WI unit to operate with a defined efficiency, which the generator unit lacks as a feature.

Furthermore, the full DHN expansion case is shown in the Appendix G by Figure 6. The two structures of the EDN are depicted in Appendix H: base configuration by Figures 7 and 9, while the full configuration by Figures 8 and 10. Under the base network expansion case, the EDN supplies power to only one geothermal source, while the full expansion case includes a total of nine electrified heat sources. In both cases, the CHPs feed power into the network, except for the RDAM CHP3 unit, which is connected to the HV grid on the Tennet side and does not fall under the scope of this research. Note, that base and full network structures are split into The Hague and Rotterdam branches. Both The Hague and Rotterdam branches are linked to the same external grid component, indicating the 380kV Tennet transmission grid. The branches were split for the ease of illustration.

Having established the base and full DHN and EDN configurations, the PFA of the EDN is performed under three distinct cases: unenforced, reinforced and no P2H. The "unenforced" case represents the default EDN configuration aligned with each DHN setup, using a single transformer per substation and a fixed number of lines, without any reinforcement. The "reinforced" case reflects the manually adjusted EDN configuration, where the amount of transformers and lines are adjusted in locations with high loading levels to ensure stable network operation. The "no P2H" case uses the same network setup as the reinforced case but excludes all

electrified heat sources (HPs, EB and geothermal units) to isolate their impact. Figure 4.1 outlines experiment workflow of the case study. The first choice is the scenario year followed by the heat demand case. Next, with low and high heat demands both network expansion scenarios can be simulated. Based on the two previous selections the DHN operational optimisation can be conducted, which is then followed by the corresponding EDN analysis, which again is split into three PFA simulations: "unenforced", "enforced" and "no P2H".

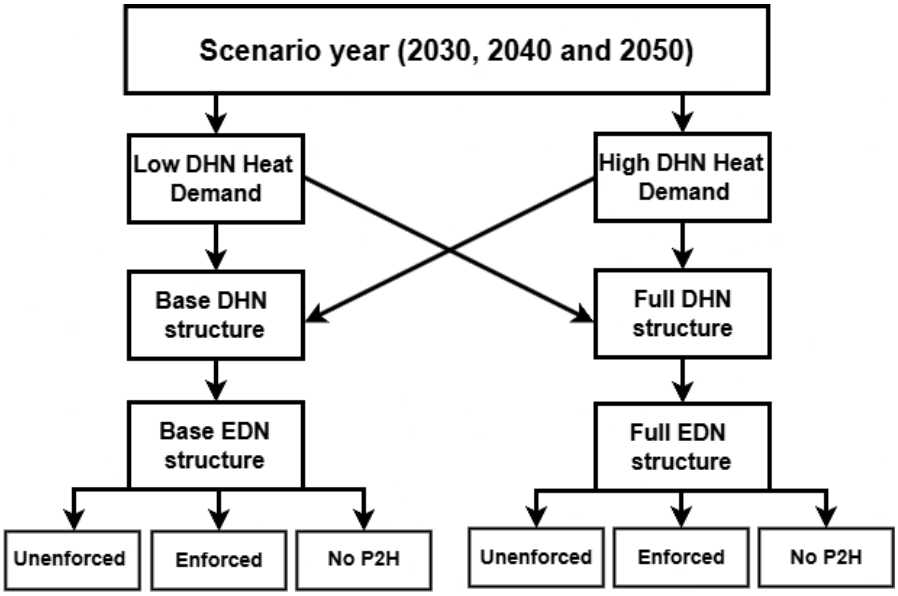

Figure 4.1: Network expansion scenarios

4.2.3 Scenario overview

Table 4.1 summarises the case-study experiments that were performed for each scenario year. The experiments with the DHN model were conducted based on low heat demand (referred as "Low") and high heat demand (referred as "High") projections, as well as base and full (with additional heat and storage sources) network expansion configurations. In all scenarios, the operational optimisation of the future DHN with low and high heat projections was performed. However, only the DHN of 2030 with low and high heat demand was simulated with base and full network expansion scenarios. It is assumed that in 2040 and 2050 all of the planned electrified heat sources and storage units will be operational.

Heat demand scenario	Full network expansion	Base network expansion
2030 Low	✓	✓
2040 Low	✓	–
2050 Low	✓	–
2030 High	✓	✓
2040 High	✓	–
2050 High	✓	–

Table 4.1: Overview of DHN experiments

Table 4.2 summarises the PFA simulations that were conducted with the EDN model based on network expansion and heat demand scenarios. The base network expansion case was simulated only with the 2030 low heat demand scenario. The reason behind this choice is that the base network only has one electrified heat source (DH Geo1), thus even with high heat demand the effects of one geothermal source on the operation of the DHN and EDN remain similar. Moreover, the 2030, 2040 and 2050 full network expansion cases with high heat demand did not include the "no P2H" simulations. Since the main variable in low and high heat demand cases

is the electrified heat source demand, with all electrified heat sources removed the simulations will yield equal results.

Heat demand scenario	Base network expansion			Full network expansion		
	Unenforced	Enforced	No P2H	Unenforced	Enforced	No P2H
2030 Low	✓	✓	✓	✓	✓	✓
2040 Low	–	–	–	✓	✓	✓
2050 Low	–	–	–	✓	✓	✓
2030 High	–	–	–	✓	✓	–
2040 High	–	–	–	✓	✓	–
2050 High	–	–	–	✓	✓	–

Table 4.2: Overview of EDN experiments

4.2.4 EDN Reinforcement methodology

The EDN infrastructure reinforcement was performed using a manual and iterative simulation approach. Since transformers and lines can be damaged during short periods, maximum loading levels were used as key indicators for identifying components that exceeded the nominal operational limits. The general procedure followed in each scenario is presented below:

- Run the unenforced EDN simulation to determine the overloaded substations and lines;
- Add one component at the selected overloaded location;
- Re-run the yearly PFA simulation with the added unit and analyse the results;
- If overloading persists, add an additional unit at the same location. Otherwise, consider reinforcement at a neighbouring location;
- Repeat the process until all components operate within their nominal limits.

Initially, the addition of reinforcements started from the MV network. However, the repeated simulations showed that the addition of MV transformers and lines in the overloaded areas had a minimal impact. Overloading persisted even after multiple added units at the MV level. As a result, reinforcements were done on the HV side, which proved significantly more effective, bringing down the loading levels of both transformers and lines at the upstream and downstream level. The additional HV components were added one by one, starting from the 380/150 kV transformers and followed by the 150/25 kV transformers, each time re-running the PFA with an added unit to clarify the effect of the reinforcement. Only when upstream network reinforcement were in place, the MV network was reinforced.

The greater effect of the HV network reinforcement compared to MV reinforcement is due to the external grid component being modelled as the only voltage-regulating element. With such a model configuration, the reinforced MV substations have limited ability to improve voltage profiles or reduce upstream congestion, as voltage stability and power balance are primarily controlled at the HV level by the external grid component. The reinforcement of the HV transformers effectively increases the capacity of the network to draw power from the external grid and distribute it downstream, thus improving the overall performance of the network and alleviating overloaded substations.

4.2.5 EDN Scenario analysis

During the analysis of the EDN scenario results, particular attention was paid to line and transformer loading levels to assess the infrastructure requirements of the future EDN. For each network expansion case, three PFA simulations were conducted: an "unenforced" case, representing the minimum medium-voltage (MV) network

infrastructure, an "enforced" case, which includes additional network reinforcements with which nominal loading levels are achieved, and a "no P2H" case where the electrified heat production units (geothermal and P2H) are removed, but the reinforced distribution network structure remains. In the "unenforced" case, the operation of the minimum EDN structure (with one transformer at each substation and a fixed number of lines) is evaluated under the electricity load profiles. Next, the "enforced" case is used to determine the requirements for network infrastructure reinforcement, specifically identifying the number of additional lines and transformers needed for nominal network operation. Lastly, the "no P2H" uses the reinforced network structure, but with removed electrified heat sources. As a result, the direct impact of DHN decarbonisation and the large-scale implementation of electrified heat sources can be measured on the EDN infrastructure.

The main physical components of the EDN that connects to the South-Holland DHN are MV lines and transformers. This case study specifically analyses the operation of 25 kV, 23 kV and 10 kV lines, as well as 25/23 kV, 23/10 kV and 25/10 kV transformer types. However, to conduct an accurate simulation of the EDN using pandapower, it is necessary to include the high-voltage (HV) levels of the power system, specifically the 150 kV and 380 kV transmission networks that supply power from the upstream external grid component. In several instances (with base and full networks in unenforced cases), it was observed that insufficient transformer capacity at these HV level transformers led to non-convergent PFA. To ensure the stability of the model, this paper also includes the expansion needs of the HV network layers. The expansion of the higher-level network is the direct consequence of the loading levels applied and experienced by the MV network.

4.2.6 Input data

To conduct the real-world simulation of the South-Holland networks, genuine input data must be used in the models. Since the selected case study approach is deterministic, i.e., choosing one or several heat demand, price and network expansion cases, the results of the case study are highly dependent on what input data is fed into the models. As highlighted in Chapter 3, the main inputs of the DHN model are the historical hourly price profiles of electricity, CO_2 and natural gas and heat demand, provided by Eneco. On the other hand, the input of the EDN model comes from the operational optimisation of the DHN and the future scenario electricity demand profiles of the substations provided by Stedin. Figure 4.2 indicates the hourly price data of electricity, CO_2 and natural gas from 2018 to 2022. For the future scenarios, this data was applied for scaling according to the projected price scenarios of the future.

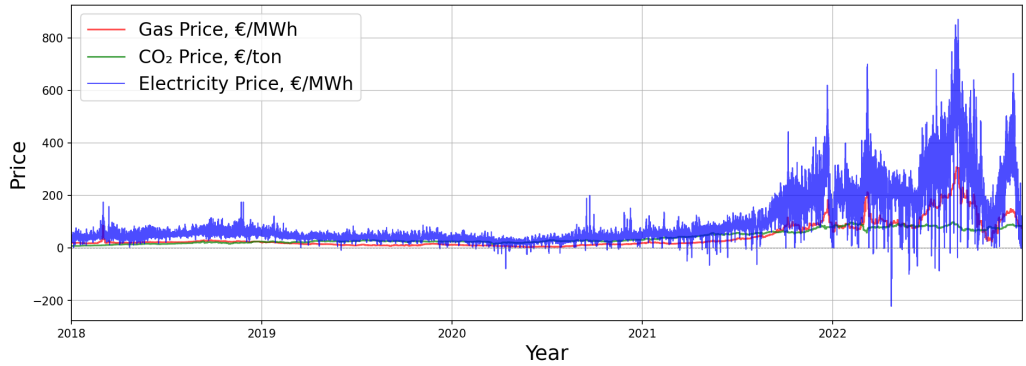

Figure 4.2: Hourly price data of natural gas, CO_2 and electricity prices, 2018-2022.

As depicted in Figure 4.2, from 2018 until the beginning of 2021 the price profiles are stable and without large fluctuations, however, from the middle of 2021 to the end of 2022 prices exhibit large variations due to an energy crisis in Europe. Natural gas and electricity prices are dynamic, therefore, for the scaling of dynamic price profiles the data from the 2020 was used. In addition to electricity and natural gas, the DHN of the South-Holland region uses biomass, waste heat and municipal waste the primary energy sources for heat production. These fuel source have assigned static price profiles applied, as the fuel prices for these units historically exhibit little variation. Additionally, the DHN model applies hourly air and ground temperature profiles to calculate the variable COP values of HPs and geothermal sources. The static fuel prices and the temperature in the future

scenarios were determined after an extensive literature review.
Historical weather data for 2018-2022 (shown in Fig. 4.3) were obtained from the Royal Netherlands Meteorological Institute (KNMI). Specifically, air temperature measurements at an altitude of 1.50 meters were taken from weather station No. 344, located near Rotterdam airport [62]. Ground temperature data, measured at a depth of -1 meter, were sourced from weather station No. 260 in De Bilt [63]. These hourly temperature data sets are used to calculate the COP of the HP and geothermal systems, allowing the DHN model to reflect how seasonal and daily temperature variations affect the heat network.

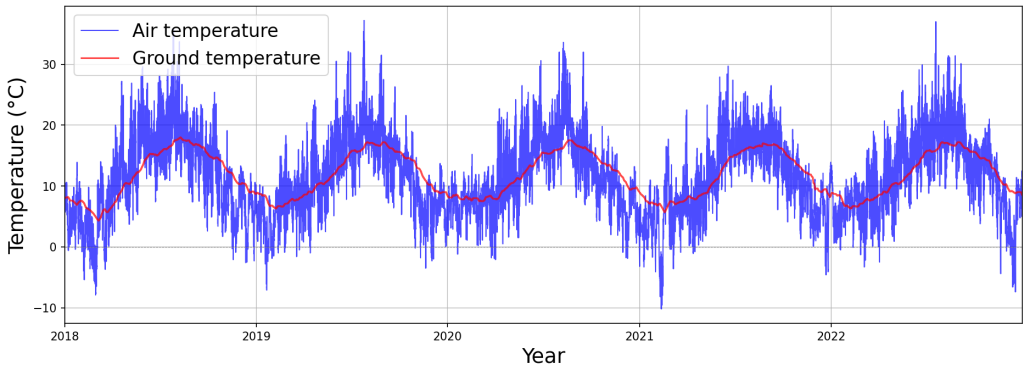

Figure 4.3: Hourly air and ground temperature, 2018-2022.

4.2.7 Price scenarios

The following section covers the construction of future price, demand and weather profiles based on the historical data from Eneco and literature. The described input data are applied in the operational optimisation of the South-Holland DHN. This case study applies is a deterministic approach for setting prices, future heat demand and temperatures, meaning that all input parameters are predefined and fixed for each scenario year. The deterministic approach assumes perfect foresight and no deviation from the specified input values (unlike stochastic or probabilistic models, which incorporate uncertainty and variability), enabling direct comparison between different network configurations and expansion planning strategies. It is important to consider that actual price developments may vary significantly due to unforeseen events, such as technological breakthroughs or shifts in policy frameworks.

4.2.7.1 Dynamic Prices

In the PyPSA library, heat supply units can be modelled as links or generators, depending on their characteristics. Links represent controllable energy conversion units between buses and include directional efficiency. They are used to model technologies that convert one energy carrier to another, such as P2H, gas boilers and CHP systems. Conversely, generators are used to represent direct heat supply units, they lack an efficiency parameter and function as fixed-output sources supplying heat to the DHN. In the DHN model configuration, the CHPs, gas-boilers, geothermal and P2H systems are modelled as link components and are assumed to operate with dynamic fuel prices. The operation CHP and gas boilers are linked to the prices of natural gas and CO_2 while the external grid component, which supplies power to the geothermal and P2H systems, is linked to variable electricity market prices for the respective simulation year.

As previously depicted in Figure 4.2, 2021 and 2022 represent extreme cases of price variability due to the energy crisis, with extreme fluctuations in both the electricity and natural gas markets. Moreover, even the CO_2market price, which historically is very stable, experienced increased variability. For that reason, the future scenario price data of 2030, 2040 and 2050 are scaled according to 2020 data, which exhibits a more stable variability pattern. As a result, with the scaling of 2020 price data the future scenarios maintain a realistic market variability and avoid modelling worst-case scenarios. The scaling of the hourly data set is performed by

using a normalised factor, which is calculated by dividing the average annual price of each future scenario by the average annual price of 2020. Formula 4.1 depicts the scaling factor calculation:

$$\text{Scaling factor} = \frac{\text{Average annual price}_{scenario}}{\text{Average annual price}_{2020}} \tag{4.1}$$

Table 4.3 presents the mean annual prices for electricity, CO_2 and natural gas in both past and future scenario years. The mean future scenario prices were derived from the EU Reference Scenario 2020 and the EU Energy Outlook 2050 reports [64], [65]. These sources provide official projections for energy markets, aligning with the EU climate and energy policies. Future electricity prices are projected to be largely shaped by increasing CO_2 costs and the expansion of RES. The higher availability of solar and wind will lower the effect of high CO_2 prices, as negative power prices will become increasingly more frequent. However, the increased network tariffs caused by electrical network expansion and reinforcement projects, will result in a marginal increase in electricity prices, from approximately 69 €/MWh in 2030 to 78 €/MWh in 2050. Looking at the natural gas projections, from 2027 onward, the EU market will gradually stop russian gas imports and shift towards the global market of liquefied natural gas (LNG). This transition is expected to bring the prices levels to 22 €/MWh by 2030 and rise to around 31 €/MWh by 2050. The carbon emission prices are a central policy tool used by the EU to incentivise decarbonisation and internalise the environmental cost of emissions. The carbon price is expected to increase from 110 EUR/MWh in 2030 to 165 EUR/MWh in 2050, placing more pressure each year to transition to low-carbon technologies.

Year	Mean electricity price, €/MWh	Mean gas price, €/MWh	Mean CO_2 price, €/MWh
2020	32.19	9.31	24.72
2030[1]	69.00	22.13	110.00
2040[1]	72.00	28.47	140.00
2050[1]	78.00	31.28	165.00

[1] Based on [64] and [65].

Table 4.3: Average electricity, natural gas and CO_2 prices.

4.2.7.2 Static Prices

Biomass and IWH are modelled as generators, while the WI unit is represented as a link component. All three are assumed to operate with static fuel prices, as these fuel sources exhibit limited price variability. For the biomass unit, it is assumed that wood chips are used as fuel with a fixed marginal cost of 22.32 €/MWh in 2020, consistent with the value used by Sifnaios et al. [66]. The Baltpool international biomass exchange reports that wood chip prices fluctuate between 19.35 and 29.35 €/MWh (based on 2024-2025 data) [67]; however, the fluctuations a minimal and biomass costs are treated as static. For industrial waste heat, a fixed cost of 8.4 €/MWh is applied, as this value is derived by Van der Roest et al. [68], based on heat recovery from an electrolyser. Although industrial waste heat can be dynamically modelled using a HP linked to electricity prices, the heat recovery process is assumed to be continuous due to the stable waste heat supply temperature; thus, a constant marginal cost parameter is appropriate. According to [69], the estimated lower heating value (LHV) of the WI (AVR) plant is 9.2 GJ/tonne in 2018. According to the report published by the European Commission [70], the treatment cost of waste for incineration is around 77 €/tonne, thus with these two values a conservative cost of waste fuel for 2020 reference year is set to 30 €/MWh.

Year	Wood chips[1], €/MWh	Waste heat[2], €/MWh	Waste[3], €/MWh
2020	22.32	8.40	30.00
2030	25.56	7.50	26.00
2040	27.36	7.00	24.00
2050	29.52	6.50	22.00

[1] Based on [66], [67] and [71]
[2] Based on [68] and [72]
[3] Based on [69] and [70]

Table 4.4: Static fuel prices.

The price of biomass depends on local resource availability of the resource, transportation costs and specific grade of fuel used at the plant. Many other variables are in play, as price trends vary by region. According to the medium CIF (Cost, Insurance, and Freight) Danish port wood chip price projection in [71], biomass prices are expected to increase slightly, reaching 29.52 €/MWh by 2050. According to [72], the rising demand for energy efficient solutions and increasing fossil fuel costs are expected to bolster the wider adoption of IWH in district heating applications. As a result of these market dynamics, it is assumed that the cost of IWH will decline, reaching 6.50 €/MWh by 2050. In [69], the key trends of waste incineration include improved waste processing and a greater emphasis on recycling, hence a limited drop in price is expected to occur, dropping to 22.00 €/MWh by 2050.

4.2.7.3 Heat storage

In this thesis, thermal heat storage is assumed to be TTES systems, characterised by a high round-trip efficiency of 0.96% for both charging and discharging. By design TES systems do not generate heat, instead these units are used to store surplus thermal energy from other production sources. Thus, the minimal operational energy requirement comes from operating the electric pump needed to transfer heat into or out of storage. The actual cost of using TES largely depends on the characteristics and marginal costs of the heat sources used to charge it. However, PyPSA does not currently support the calculation of dynamic input source dependent costs of storage units. Therefore, within the model a fixed marginal cost must be assigned to storage unit components. Based on the findings of Jongsma et al. [73], the variable cost of charging TTES systems with residual heat is estimated at 1.656 €/MWh. This value reflects the lowest cost scenario and is adopted in all modelled cases of the case study as the marginal cost of storage. This is a reasonable approximation for all scenarios in which WI and IWH and other low cost and emission sources are used to fill the TTES systems.

Year	Type	Marginal costs (€/MWh)
2030, 2040 and 2050[1]	TTES	1.656

[1]Based on [74].

Table 4.5: Thermal heat storage costs

4.2.8 Demand scenarios

The heat demand scenarios are structured to represent both cases of annual decrease and increase in heat demand by 0.8%. Table 4.6 shows the average annual heat demand values in the four demand nodes in the DHN. For the scaling of high and low demand scenarios 2022 heat demand data from Eneco was used. Equation 4.2 is applied to calculate the future values of the heat demand by applying a annual compound reduction and increase formula, where *"n"* is the number of years after 2022:

$$\text{Scaling factor} = (1 \pm 0.008)^n \tag{4.2}$$

Year	Den Haag, MWh	Rotterdam, MWh	Rotterdam RoCa, MWh	Tuinders, MWh
2022[1]	37.28	75.62	42.27	18.96
2030 Low[2]	34.96	70.91	39.64	17.78
2040 Low[2]	32.27	65.44	36.58	16.41
2050 Low[2]	29.77	60.39	33.76	15.14
2030 High[3]	39.74	80.59	45.06	20.21
2040 High[3]	43.04	87.28	48.80	21.89
2050 High[3]	46.60	94.52	52.84	23.70

[1] Reference year applied for scaling
[2] Based on [61] with 0.8% annual decrease
[3] With 0.8% annual increase

Table 4.6: Average heat demand by year

Using the low heat demand scenario, from 2022 the heat demand will decrease by -6.2% in 2030, -13.46% in 2040 and -20.14% in 2050. With the high demand scenario, from 2022, the projected increase of 6.58%, 15.4% and 24.99% in 2030, 2040 and 2050 is calculated, accordingly.

4.2.9 Temperature scenarios

The temperature scenarios for 2030, 2040 and 2050 are derived from the Shared Socioeconomic Pathway 2–4.5 (SSP2-4.5), also known as the "middle of the road" scenario, developed as part of the Coupled Model Intercomparison Project (CMIP) [74]. SSP2-4.5 states that by following moderate climate policy and socioeconomic tendencies, a global average temperature increase of approximately +2°C is projected by 2050 relative to pre-industrial levels. Based on this trajectory, the projected average temperature increases used in this study are +0.1°C for 2030, +0.4°C for 2040 and +0.9°C for 2050, since the IPCC Sixth Assessment Report (AR6) states that at 2020 the global temperature already increased by +1.1°C. To generate future temperature profiles, the 2020 hourly temperature data set is used as a reference. Following the method used to adjust the energy price data, the future temperature scenarios are scaled according to the projected average annual temperature increases. Table 4.7 presents the average annual air and ground temperatures for both past and future scenarios.

Year	Mean air temperature, °C	Mean ground temperature, °C
2020[1]	11.97	12.02
2030[2]	12.07	12.12
2040[2]	12.37	12.42
2050[2]	12.87	12.92

[1] Based on [62] and [63].
[2] Based on [74].

Table 4.7: Average air and ground temperature

4.3 DHN Scenario results

This section describes the results of the South-Holland DHN operation. At first the 2030 vs. 2050 with high heat demand case is discussed. Next, the 2030 scenario with low heat demand is described to highlight the differences base and full network expansion cases and the effect of the addition of the electrified heat sources. The results comparing all cases of the DHN are summarised in Section 4.5, while results of all DHN cases are presented in Appendix I.

4.3.1 DHN 2030 vs. 2050 with High heat demand

4.3.1.1 Hourly production

The variation in total heat production per category of supply at each time step throughout 2030 and 2050 with full network expansion and high heat demand are illustrated in Figure 4.4, where sub-figure 4.4a refers to 2030 case, while sub-figure 4.4b depicts the 2050 case. Both scenarios have the same network, structures, while only the change in heat demand separates the operation of the networks. The main observables differences are the utilisation of the biomass plant, which operates more continuously in 2050 during the winter, while also, larger production of HPs and gas boilers are observed during the same period. Operational dynamics in the summer remain largely unchanged.

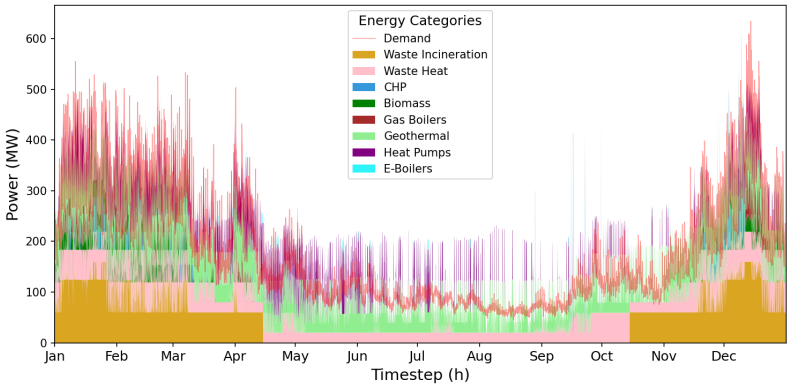

(a) 2030

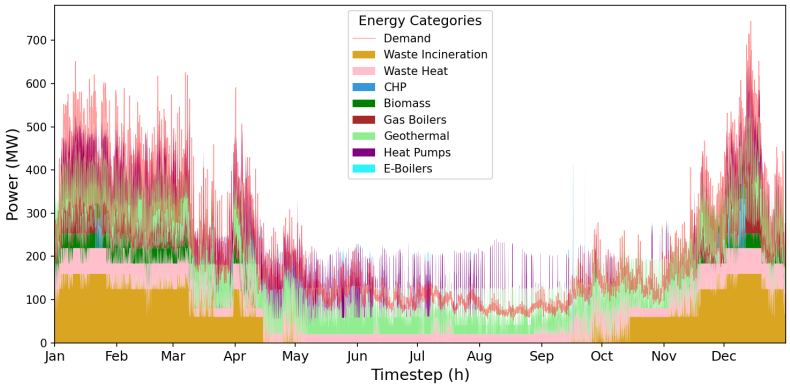

(b) 2050

Figure 4.4: Heat production per time step in 2030 and 2050 (high heat demand)

4.3.1.2 Total production per category

The annual heat supply per category is illustrated by Figure 4.5. In the 2030 scenario, the majority of heat was produced by geothermal energy sources, resulting in 35% of total heat production. IWH and WI plants produced 23% and 21%, respectively. The remaining parts were split between HPs (13%), biomass and gas boilers (both with 3%) and CHPs with only 2% of the total. In contrast, in 2050, the rise in heat demand

resulted in higher share of the total production for gas boilers, biomass and WI plants. WI produced 27%, gas boilers 6%, while the biomass 4%. In 2050, the heat production of gas boilers reached 110,671 MWh, which is 59,360 MWh more than in 2030. In both scenarios, the gas boilers in The Hague remained inactive. However, in the Rotterdam RoCa heat and power production plant, RDAM Gas4 became the primary unit to meet the local peak heat demand, producing 96% of all heat production from gas boilers. In addition, the RDAM Gas2 unit produced 4,513 MWh, which represents just 4% of the total gas boiler output.

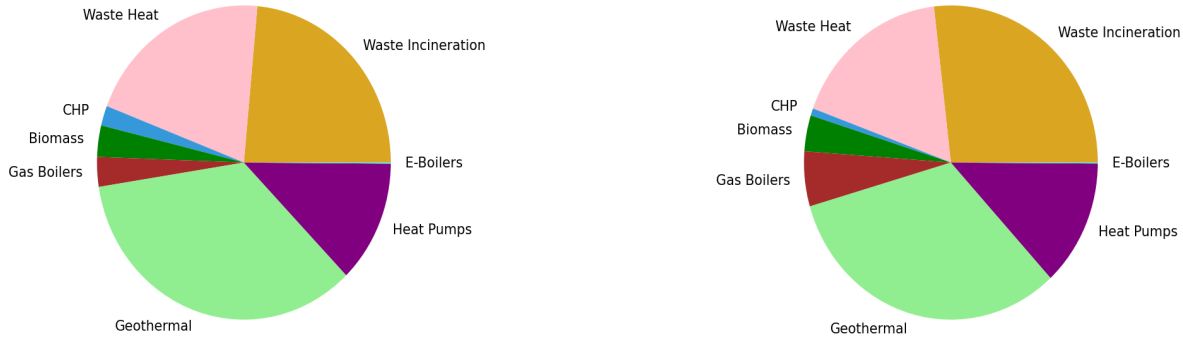

(a) 2030 *(b) 2050*

Figure 4.5: Total heat supply per category in 2030 and 2050 (high heat demand)

4.3.1.3 Load duration curves

The load duration curves depicted in Figure 4.6 highlight the operational behaviour and supply dynamics of the DHN under two network expansion scenarios in 2030 with the low heat demand case. The curves indicate the relationship between heat production capacity and its utilisation. The production data is not ordered chronologically, but rather in a descending order of total heat production. Thus, the height of each production category measures the dispatched heat capacity, while the width indicates the capacity factor of the production category. In general, the load duration curves can depict how the optimisation model dispatches the heat production units and can indirectly reflect the actual heat demand. However, due to TES and market-based CHP dispatch, the shape of heat demand can only be approximated.

Again, the difference between two cases are reflected by the utilisation rate of gas boilers, biomass and WI plants. The Rotterdam RoCa demand node has no heat sources that are directly connected to it, meaning that all heat supply has to come via the heat distribution network from the Rotterdam node and the RoCa power plant. The maximum heat capacity that can be transferred from Rotterdam is 60 MW (via Pipe8 and Pipe12), meaning that in times when heat demand in Rotterdam RoCa exceeds 60 MW additional heat supply must be generated locally from the RoCa power plant. However, since its three CHP units are dispatched based on revenue maximisation and have start-up costs, they cannot offer continuous heat output. Therefore, the RDAM Gas4 unit becomes the source of heat with the lowest dispatch costs. The same applies for the biomass plant, as it acts as the primary peak demand suppler for the Tuinders demand node.

This outcome suggests that gas boilers remain critical in high-demand conditions, particularly in areas lacking local heat generation options or sufficient distribution capacity. To reduce dependence on natural-gas powered gas boilers, the expansion of Pipe8 and Pipe12 capacities could enable WI and RDAM HP units to supply heat to Rotterdam RoCa during peak heat demand hours. Furthermore, adding an additional electrified heat production plant closer to the Rotterdam RoCa node or enabling the multidirectional flows in the DHN, could significantly reduce the reliance on fossil-fuel based heat generation backup.

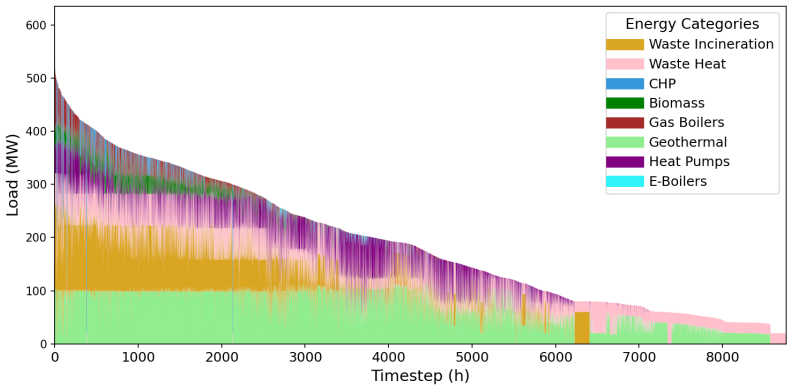

(a) 2030

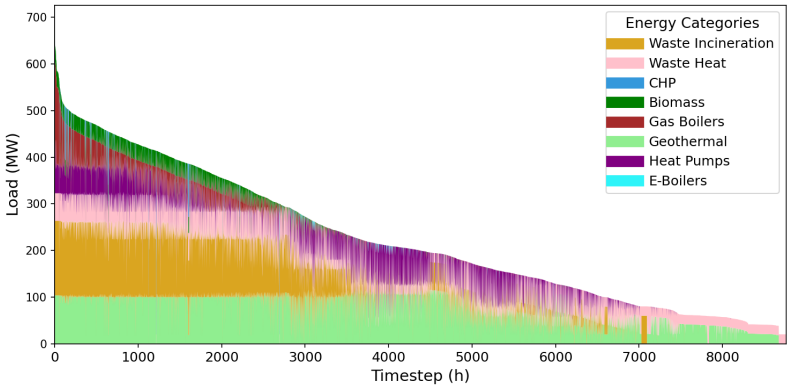

(b) 2050

Figure 4.6: Load duration curves in 2030 and 2050 (high heat demand)

4.3.1.4 DHN model output

As stated above, the main output of the DHN model is the production of electrical energy from the CHPs and the consumption from P2H and geothermal units. In the EDN model, this output data of the DHN is referred to as electricity demand and generation. Figure 4.7 presents the aggregated data of the electricity demand and generation to be used as input in the EDN analysis. It should be noted that the electricity production of the RDAM CHP3 unit is not included in both cases. The RDAM CHP3 unit has a 190 MW electrical power production capacity and such a large system is assumed to supply power directly to the TSO network, which falls outside the scope of the EDN analysis. In theory, electrified heat production should be considerably higher in the 2050 scenario with the increased heat demand.

Nevertheless, as indicated in Figure 4.7, the load demand profiles of electrified heat sources remain similar. The main differences can be observed in the month of January, where in the 2050 scenario, electrified heat sources draw power in a more stable manner, while in 2030 more variation is observed. Overall, comparing the two cases, in 2050 only 28 GWh additional electricity demand will be required annually, increasing from 229 GWh to 257 GWh (see Table 21 in Appendix I). This indicates that the utilisation rate of the electrified heat sources is restricted by the capacity and directionality of the heat distribution network. Four out of six geothermal units, as well as one HP and EB supply The Hague, which creates a highly competitive environment, as heat cannot be transferred to Rotterdam. Thus, the largest change in the electricity demand is observed in RDAM HP, which requires 18 GWh of electricity more in 2050.

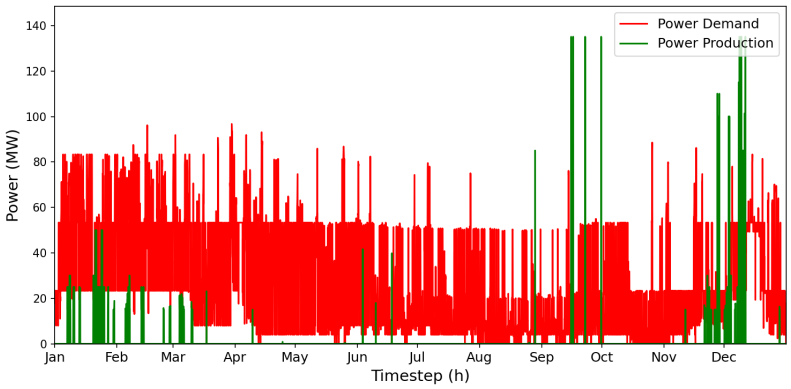

(a) 2030

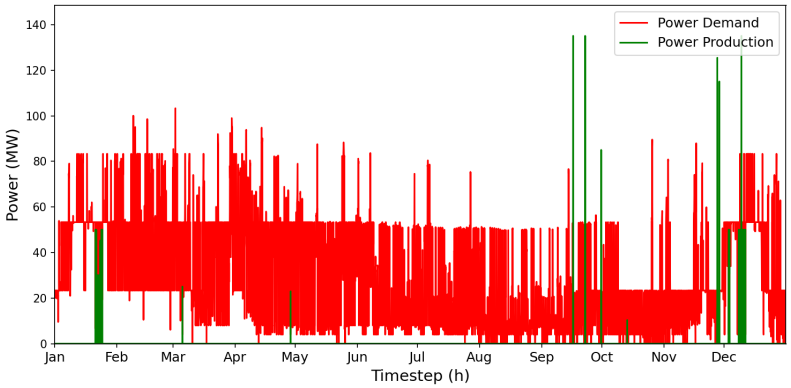

(b) 2050

Figure 4.7: Electricity demand and production in 2030 and 2050 from heat supply units (high heat demand)

4.3.2 DHN 2030 Base vs. Full network expansion

4.3.2.1 Hourly production

The variation in total heat production per category of supply at each time step throughout 2030 is illustrated in Figure 4.8, where sub-figure 4.8a refers to the base DHN expansion case, while sub-figure 4.8b depicts the network operation under full DHN expansion with additional heat production and storage sources. In the base case, the WI plant in Rotterdam operates as the primary base load unit, frequently producing at its maximum capacity during the winter months. In contrast, during the summer months with low heat demand the minimum operation constraint is not binding; thus, the WI plant is dispatched based on its cost competitiveness relative to the biomass and IWH units. The 99% of the WI heat production is supplied to the Rotterdam direction, as a result of Pipe4 that connects the WI plant to The Hague being the only heat distribution pipe with assigned marginal costs. Consequently, the heat demand in The Hague is primarily met with local heat sources, with some support provided by the WI and IWH1 heat sources.

Moreover, both IWH and biomass plants demonstrate similar production patterns to WI, operating continuously at full capacity during winter. The IWH2 unit connected to Rotterdam operates at maximum capacity annually. In addition, the IWH1 plant is capable of supplying even more heat to the network but is limited by a fixed contractual agreement for annual supply of 170,833 MWh per year. The biomass plant is the main supplier for Tuinders demand node, shutting down in August for planned maintenance. CHPs and gas boilers are primarily utilised to meet the peak heat demand. In addition, during periods of elevated electricity prices (observed in the month of September), the CHP units are utilised in combination with TES systems to maximise revenue from electricity sales while storing the surplus heat for later use. Furthermore, the single geothermal unit DH Geo1 is a key heat supplier in The Hague with a very high CF of 0.92. Despite being temporarily shut down during periods of high electricity prices, it operates almost continuously throughout the year.

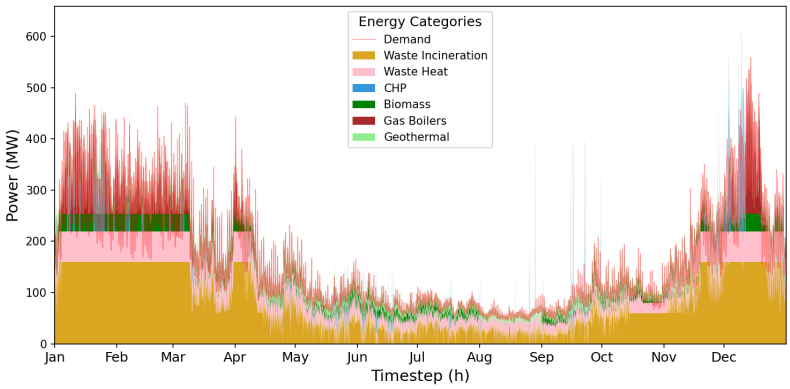

(a) Base network

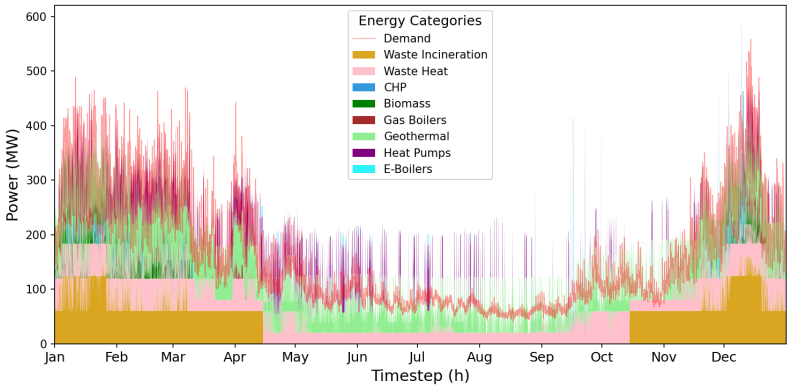

(b) Full network

Figure 4.8: Heat production per time step in 2030

In the full network case, integration of additional heat production and storage sources significantly alters the operation of the DHN. The implementation of the heating season constraint is evident with the WI plant starting and stopping the operation on October 15th and April 15th, respectively. The role of WI as the primary base load supplier is reduced, as periods of maximum output rarely occur even during the heating season. Instead, the distributed geothermal heat sources become the primary base load source. With a total installed capacity of 23.33 MW and COP ranging between 4.2 and 5.2, geothermal units are capable of dispatching over 120 MW of thermal energy, representing a substantial contribution to the overall heat supply. In addition, HPs play a key role: in winter, they supply heat directly to demand nodes, while in summer they operate in tandem with TES, storing heat during periods of low electricity prices. In contrast, the EB in The Hague operates exclusively during low electricity price periods, supplying heat solely for storage. Due to superior COP, geothermal units and HPs are prioritised for filling storage over the EB.

Moreover, the role of IWH units remains unchanged compared to the base case with both IWH units producing the same total amount of heat. The role of the biomass plant in the Tuinders region shifted to serving as a peak load unit due to the implementation of Tuinders Geo geothermal plant which operates with a high CF of 0.69. Gas boilers continue to function as peak load units. but with lower utilisation rate, while CHP units are dispatched only when revenue from electricity production is higher than marginal production costs. Throughout the summer, the electrified heat sources produce more heat than is demanded. The integrated operation with TES enables the overproduction and storage of heat during low electricity price periods and the dispatch of storage during peak price intervals. In the absence of TES, this operational flexibility would considerably reduce as heat demand would have to be met directly and heat could not be stored during summer.

4.3.2.2 Total production per category

The annual heat supply per category is illustrated by Figure 4.9. In the base network scenario, nearly half of the total heat was produced by the WI plant, which accounted for approximately 49% of total production. IWH

systems contributed 23%, while the remaining part was distributed among the biomass plant (10%), geothermal plant (8%), gas boilers (6%) and by CHP (4%).

In contrast, the full DHN network expansion scenario demonstrates a significant shift in the heat generation mix, reflecting the impact of additionally integrated electrified heat sources. Geothermal heat sources supplied the majority of heat demand, resulting in 36% of the total annual production. The shares of heat produced by the WI and IWH units were almost equal, accounting for 24% and 23%, respectively. Moreover, HPs contributed to 10% of produced heat, an outcome coming from the flexible operation with coupled heat storage, which optimises the production during low electricity price periods. Due to low efficiency of the EB (98%) unit compared to geothermal and HPs in The Hague, the optimisation model limited its use, contributing to only 0.00124% of total heat production. Furthermore, the contributions from CHP units, biomass and gas boilers declined in the full network case. CHP amounted to only 2% of the produced annual heat. Due to high carbon price and high penetration of electrified heat units the number of favourable dispatch hours dropped significantly. The total heat production of the biomass plant dropped by 7% due to the additional geothermal plant built to supply the heat demand of Tuinders. The usage of gas boilers fell to 2%, keeping their role as peak heat demand suppliers.

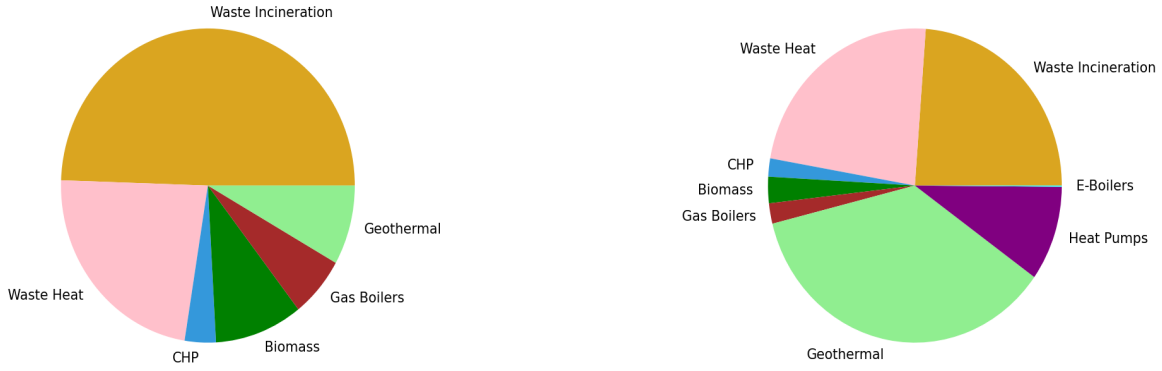

(a) Base network *(b) Full network*

Figure 4.9: Total heat supply per category in 2030

4.3.2.3 Load duration curves

The load duration curve of the base DHN expansion case in 2030 is illustrated by sub-figure 4.10a. During high heat production periods the WI plant supplies the majority of heat, followed by the IWH, biomass and geothermal units, all of which operate near their maximum capacity and provide a continuous heat output. The primary peak-shaving units are gas boilers, seen from the parabolic shape of the load curve. The CHP units are dispatched throughout the year in combination with TES to take advantage of electricity price peaks, thus CHP utilisation is irregular and occurs selectively during periods when with high electricity prices revenue can be generated. During periods of low heat production, the WI, IWH, biomass and geothermal units are the main heat suppliers, following a similar pattern with WI producing the majority of heat. Overall, the base network expansion case displays relatively low operational variability, as most units are not price sensitive (such as units with static prices: WI, IWH and biomass), with only the geothermal and CHP heat sources responding to fluctuations in the electricity market. Still, due to high COP the DH Geo1 holds a very high capacity factor acting as an almost constant source of heat. Consequently, it can be argued that the behaviour of the DHN without electrified heat sources is more driven by heat demand rather than by market conditions. The use of TES and market-responsive CHPs introduced some variability and distortions, still, the parabolic decline in the load duration curve reflects a production profile that closely follows the heat demand patterns.

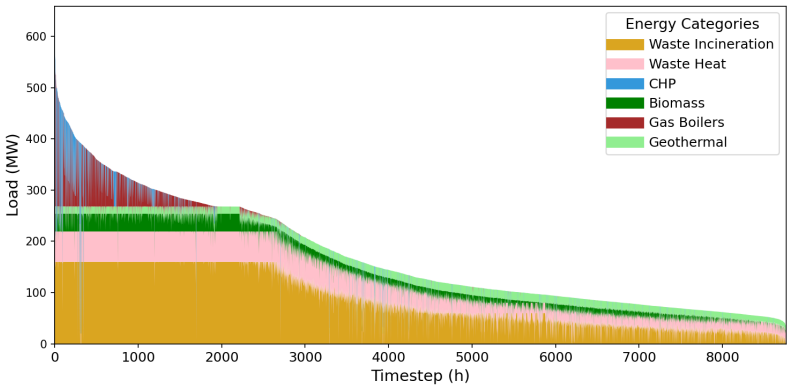

(a) Base network

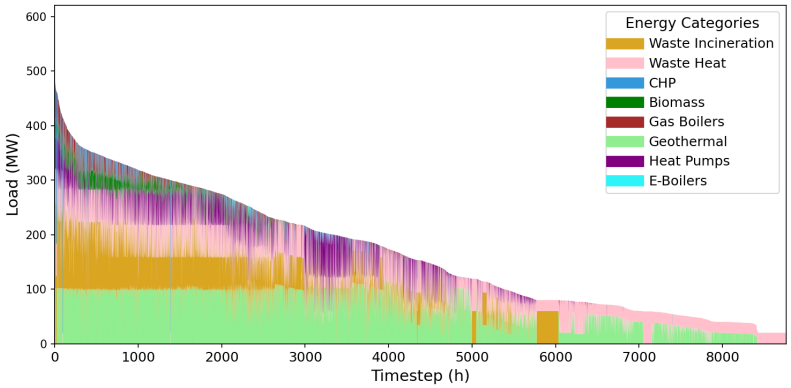

(b) Full network

Figure 4.10: Load duration curves in 2030

In the full network expansion case, depicted in sub-figure 4.10b, the production structure becomes significantly more dynamic, due to the addition of electrified heat sources that are driven by market prices and variable efficiencies. The expansion in the geothermal energy capacity, shifts the geothermal units into the role of primary base load production units, supported by the WI and IWH plants. In addition, in times of low electricity prices, HPs contribute significantly, lowering the utilisation rate of the WI. The role of the biomass plant also changes significantly - i.e., from a continuos heat production source to primarily serving as a peak-shaving unit together with gas boilers during high heat demand. As in the base network case, the CHPs are operational when electricity market conditions are favourable for dispatch. In general, the implementation of P2H and geothermal technologies with inherent variable efficiencies and market-driven behaviour, results in a more dynamic and responsive heat production structure. The DHN with additional electrified heat sources and storage is therefore highly market-driven, as heat sources are dispatched to fill the heat buffers when the price and calculated efficiency factors are satisfactory. This shift is reflected in the lack of the parabolic declines in the load duration curve. When the market conditions are unfavourable, the heat sources with static price parameters and TES can temporarily assume the role of the main heat providers, for example, in low heat demand periods (close to 6000th hour in sub-fig. 4.10b) the WI and IWH plants with TES are covering the heat demand.

4.3.2.4 Thermal heat storage

The differences in the utilisation of TES in both network expansion cases are observable in Figure 4.11, indicating the state-of-charge (SOC) of the heat storage systems. During the high heat demand periods both network cases illustrate similar TES usage profiles, with storage units being often charged and discharged. However, the charge and discharge of heat buffers is more rare in the base network case, especially in the summer season, when heat demand is met directly from the heat sources (done to avoid both heat distribution and storage losses). With additional electrified heat production and storage units the TES is utilised more and on a shorter time scales. The effect of additional infrastructure is particularly seen with RDAM1 Storage1 and Tuinders Storage units, as they start being charged and discharged more frequently and during the heating, while are also

utilised during the summer.

Conversely, lower SOC variability is seen with DH Storage1, indicating its changed role to a long-term storage system. DH Storage1 is fed by two CHP and one gas boiler source in The Hague and with elevated production from electrified heat sources it utilisation rate drops. Hence, the changes in the TES utilisation patterns can be attributed to the location of these sources. Overall, storage units directly linked with electrified heat production systems experience more varied SOC levels, while fossil-fuel supplied heat storage systems see lower variability due to limited gas boiler and CHP use. Therefore, with electrified heat sources, the operational time scales of TES systems are lowered due to fast response and availability requirements. On the other hand, the use of heat storage units that are supplied by fossil-fuel driven systems is observable, but their role is limited to long-term storage of heat with seasonal to monthly variability.

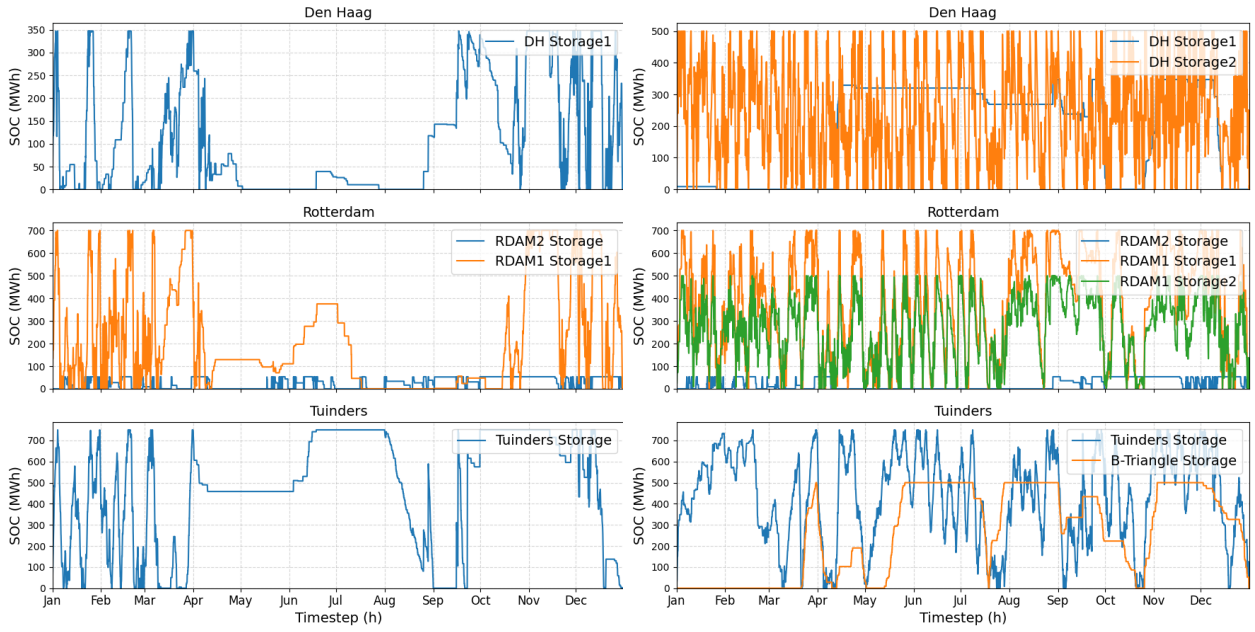

(a) Base network *(b) Full network*

Figure 4.11: TES state of charge in 2030 (low heat demand case)

4.3.2.5 DHN model output

Figure 4.12 presents the electricity demand of heat supply units and CHP production. In the base network expansion case, only a single geothermal source in The Hague draws power from the distribution network, resulting in electricity demand of 26.7 GWh. The opposite is true with respect to the fully expanded DHN, as in some cases the P2H and geothermal sources require close to 100 MW of electrical power, while the total electricity demand of all electrified heat sources is 187 GWh. In addition, electrical power generation occurs less in the full DHN expansion case, a result of the CHPs being less cost competitive due to the high carbon prices and the integration of electrified heat sources.

The structural changes caused by the implementation of additional heat production and thermal storage sources result in two distinct networks with vastly different operational dynamics and production profiles. The major change between the base and full network cases is observed in the utilisation of the WI plant, as the integration of additional geothermal and HP units with thermal storage results in halving the total annual heat production of the WI plant. IWH sources maintain identical levels of heat output in both scenarios. Furthermore, the electrification of the DHN results in the zero operation of six gas boilers (DH Gas1, DH Gas2, DH Gas3, RDAM Gas1, RDAM Gas2 and RDAM Gas3). Only RDAM Gas4 remains operational, continuing to serve as a peak load provider for Rotterdam and Tuinders regions in both scenarios. Similarly, the utilisation of CHP units declines sharply in the full network expansion case, as the total heat supply drops by close to 50%. At the

Tuinders demand node, the commissioning of the Tuinders Geo geothermal plant removes the biomass plant from its role as a base load unit to cover only peak heat demand periods, resulting in 105,354 MWh less heat output. The addition of HPs results in 144,536 MWh of annual heat supply, of which 91% is produced by the RDAM HP due to less competition with other heat sources in Rotterdam. The EB only produced 1,839 MWh of heat in 2030 due to competition with other electrified heat sources.

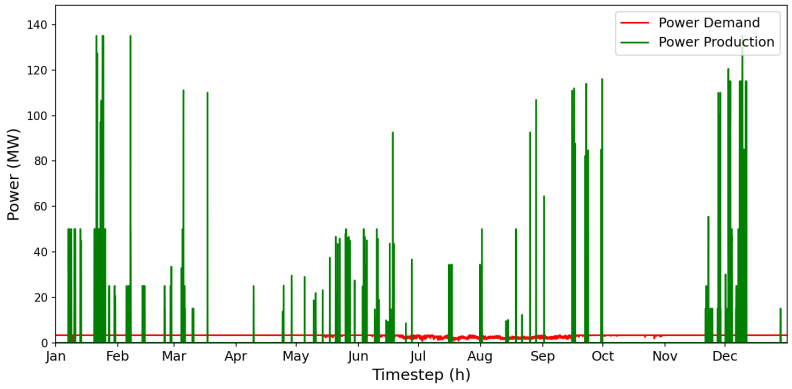

(a) Base network

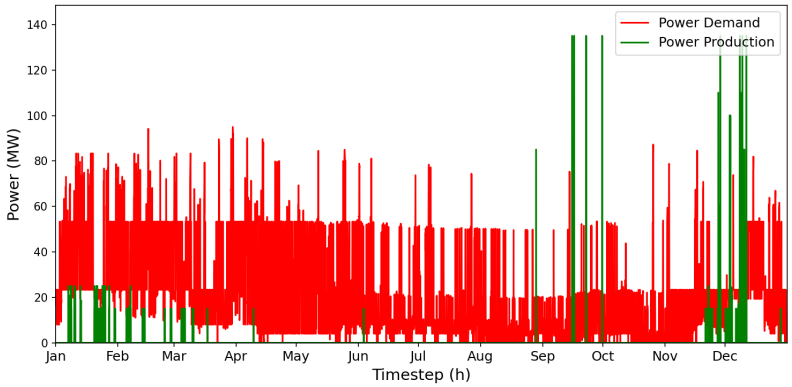

(b) Full network

Figure 4.12: Electricity demand and production in 2030 from heat supply units

The integration of three additional TES units significantly enhances the operational flexibility of electrified heat sources in the full DHN case. The heat supply of each storage unit in the 2030 scenario is summarised in Table 4.12. Among the additional units, DH Storage2 is especially critical, serving as the main heat storage hub for four geothermal units, one HP and one EB, resulting in DH Storage2 supplying more than 40% of all TES heat supply. Furthermore, the DH Storage1 and RDAM2 Storage units are supplied by CHP units and gas boilers, thus in the full network case the use of these units shifts towards long-term storage, with reduced utilisation levels. In contrast, the heat supply of the RDAM1 Storage1 and Tuinders Storage units increased by approximately 50%, reflecting their expanded role in supporting local geothermal and biomass production. Moreover, the use of the B-Triangle storage unit is limited due to heat transfer losses through the heat distribution pipeline for charging and discharging. However, while it is not exploited to its full potential, it still contributes as a flexibility inducing asset. In general, the inclusion of additional TES units is essential to enable a higher share of electrified heat production in the DHN. Storage assets allow flexible sources to operate optimally by shifting heat production to periods of low electricity prices; thus, heat supply is decoupled from instantaneous demand, which mitigates the variability introduced by dynamic market behaviour.

4.4 EDN Scenario results

This section describes the results of the South-Holland EDN operation. As in the previous DHN results section, at first, 2030 vs. 2050 with high heat demand case is discussed, followed by 2030 scenarios with two network expansion cases. The results comparing all cases of the EDN are summarised in Section 4.6. Moreover, the full results of all EDN cases case summarised in Appendix I.

4.4.1 EDN 2030 vs. 2050 with High heat demand

The comparison between transformer loading levels in 2030 and 2050 under high heat demand scenarios reveals a significant rise in loading levels across most MV substations and lines in the unenforced network. Figure 4.13 depicts the 2030, while Figure 4.14 the 2050 case with unenforced and enforced scenarios. In the 2050 case, the PFA model failed to convergence a total of 2,664 times, compared to the 660 in 2030, indicating an increase infrastructure overloading in the future EDN. In 2030, most network failures occurred during the winter period, while in 2050, transformer loading is distributed more evenly throughout the year. substations experience the highest loading levels during summer (for example, transformer C3 with 401.05% loading in July), primarily due to large increase in distributed energy generation. Table 26 in Appendix I lists the number of hours with negative demand (net power generation from loads). On average, the number of hours with negative demand is projected to increase by 48%, increasing from 1,741 hours in 2030 to 2,587 in 2050. This indicates that at the MV network level, the reverse power flows will significantly increase. As a result, this trend will lead to overloading of local transformers and lines, requiring reinforcements to maintain network stability and avoid curtailment of renewable generation.

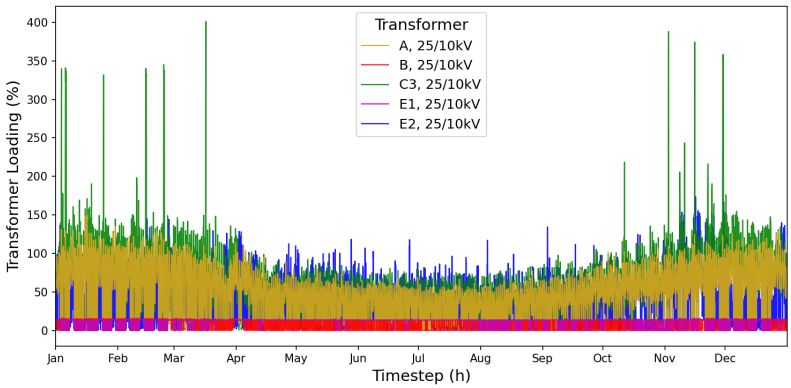

(a) Unenforced network

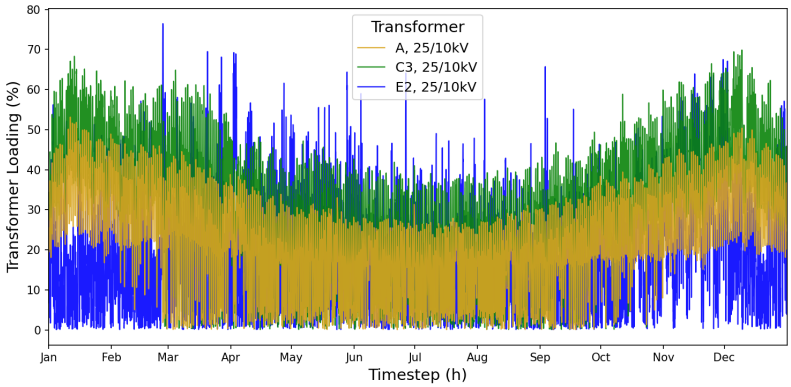

(b) Reinforced network

Figure 4.13: 25/10 kV transformer loading in 2030 (high heat demand)

In both cases, reinforcement measures were shown to be effective in keeping the network operation within safe margins. The exact number of reinforcements applied in 2030 and 2050 cases is listed in Tables 4.15 and

4.16 in section 4.7. Note that for, low and high heat demand cases the same number of reinforcement were found to be necessary. Although more electrical power throughout the year is required, the peak electricity load times remain unchanged due to the same Stedin load profiles used in both scenarios. Looking at the average transformer loading in Table 4.8, it can be reflected that on average the transformer loading does increase. Nevertheless, with maximum loading at the MV level remaining unchanged, no additional network reinforcements are required for the higher heat demand case. This experiment comparison suggests that the EDN has a large operational flexibility if reinforcements are implemented and the change in the DHN heat demand has only marginal effects on the EDN.

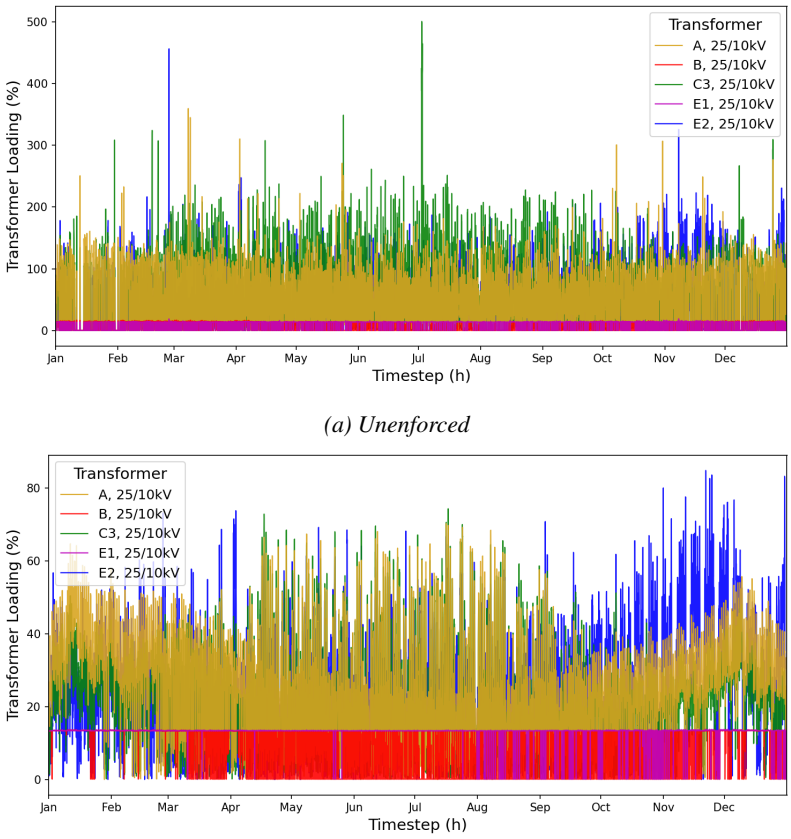

(a) Unenforced

(b) Reinforced

Figure 4.14: 25/10 kV transformer loading in 2050 (high heat demand)

With the removal of electrified heat sources, higher maximum transformer loading levels were achieved. In 2030, the addition of the Tuinders Geo source, results in a peak loading decrease of 1.26%. In 2050, the same is observed with the A transformer, which the maximum loading reduces by 1.61%. Determining the correlation between electrified heat sources and distributed RES generation from the maximum loading time steps is limited in showing the real impact. Only by looking at the Stedin load profiles and the two EDN simulation cases (enforced and "no P2H") side-by-side, the true repercussions can be seen. Looking at all time steps were the electrified heat source demand and distributed energy generation coincide, the removal of electrified heat sources always increases the substation loading. For example, in February 26th when the highest RES generation reaches -48.9 MW, E2 substation reaches 6.2% lower loading level (70.24% to 76.44%), as Tuinders Geo is demand 4 MW of power for heat supply.

	Type	2050 Low Full Avg (%)	2050 High Full Avg (%)
A	25/10 kV	26.43	26.96
B	25/10 kV	5.48	7.65
C1	25/23 kV	18.10	18.38
C2	23/10 kV	2.19	3.02
C3	25/10 kV	21.96	22.25
E1	25/10 kV	9.35	12.96
E2	25/10 kV	23.06	23.38

Table 4.8: Average transformer loading in 2050 with low and high demand, (%)

Tables 4.9 and 4.10 summarise the maximum loading levels of transformers and lines in each scenario with high heat demand.

	2030			**2040**			**2050**		
	Unenforced	**Enforced**	**No P2H**	**Unenforced**	**Enforced**	**No P2H**	**Unenforced**	**Enforced**	**No P2H**
Transformer Transformer	Max (%)	Max (%)	Max (%)	Max (%)	Max (%)	Max (%)	Max (%)	Max (%)	
Waterningen	148.41	67.08	65.27	173.09	64.91	63.39	168.58	71.05	69.85
Krimpen	62.90	59.50	56.85	76.06	93.70	86.10	78.25	49.54	45.46
Rijswijk	261.52	78.01	76.60	350.99	88.84	87.72	370.13	80.84	79.97
s'Gravenhage	160.97	75.61	63.61	190.93	96.74	85.81	192.90	66.04	61.50
Voorburg	352.67	79.91	78.01	428.34	82.68	80.65	347.94	72.95	73.68
Ommoord	209.91	65.61	62.94	254.51	89.46	86.59	257.76	95.08	92.31
Zuidwijk	101.77	53.65	39.77	125.17	83.65	69.34	126.94	87.70	73.63
A	149.38	60.45	53.11	360.24	88.89	81.25	359.37	70.21	71.82
B	16.07	13.82	0.20	16.72	13.92	0.20	16.80	13.75	0.20
C1	87.27	30.56	25.74	63.65	54.89	84.89	92.59	86.20	86.20
C2	38.16	5.54	0.07	14.15	5.57	0.07	13.32	5.46	0.07
C3	401.05	69.57	63.48	509.48	63.62	59.10	500.36	74.26	75.60
E1	15.47	13.71	0.20	18.92	14.02	0.20	18.93	13.88	0.20
E2	173.66	75.19	76.45	382.16	82.45	76.49	456.12	84.74	79.96
Number of failures[1]	**660**	**0**	**0**	**1867**	**0**	**0**	**2664**	**0**	**0**

[1] Number of PFA snapshots that did not converge

Table 4.9: Transformer loading with full network expansion in 2030, 2040 and 2050 (high heat demand case)

	2030			**2040**			**2050**		
	Unenforced	**Enforced**	**No P2H**	**Unenforced**	**Enforced**	**No P2H**	**Unenforced**	**Enforced**	**No P2H**
Transformer	Max (%)	Max (%)	Max (%)	Max (%)	Max (%)	Max (%)	Max (%)	Max (%)	
25kV_Substation_A_Trafo_A(1)	31.29	25.33	22.25	75.47	37.24	34.04	75.28	43.99	45.01
25kV_Substation_A_Trafo_A(2&3)	32.59	26.37	23.17	78.58	38.78	35.45	78.39	45.81	46.86
25kV_Substation_A_Trafo_A(4)	32.90	26.63	23.40	79.35	39.16	35.79	79.16	46.26	47.32
25kV_DH_CHP_Cables	35.04	32.75	32.75	33.78	32.87	32.87	33.46	32.81	32.81
25kV_Substation_C_Trafo_C1	100.77	35.29	29.58	73.37	63.23	62.23	106.81	49.69	49.69
25kV_Substation_C_Trafo_C3(1)	170.72	59.23	54.04	216.87	81.25	75.48	212.98	63.05	64.19
25kV_Substation_C_Trafo_C3(2)	176.59	61.27	55.90	224.87	84.05	78.07	220.31	65.21	66.40
25kV_Substation_E_Trafo_E2(1&2)	75.20	65.11	66.02	165.48	71.40	66.24	197.47	73.39	69.24
25kV_Substation_E_Substation_D(1&2)	71.98	70.04	70.07	72.69	70.78	70.58	70.73	70.65	70.35
25kV_Substation_B_DH_HP	102.94	90.51	0.04	108.32	91.03	0.04	111.89	44.27	0.04
25kV_Substation_B_DH_EB	63.70	58.23	0.00	66.66	58.15	0.00	65.81	57.50	0.00
23kV_Substation_F_RDAM_HP	99.18	47.54	0.05	100.56	48.39	0.05	100.97	47.80	0.05
10kV_Trafo_A_DH_Geo3	57.78	40.92	0.02	689.75	41.68	0.02	360.03	41.36	0.02
10kV_Trafo_B_DH_Geo2	45.92	39.32	0.00	47.81	39.63	0.00	48.03	39.11	0.00
10kV_Trafo_C2_DH_Geo4	293.54	42.15	0.03	108.67	42.40	0.03	102.32	41.51	0.03
10kV_Trafo_C3_DH_Geo1	671.68	34.99	0.02	450.86	35.61	0.02	315.87	34.52	0.02
10kV_Trafo_E2_Tuinders_Geo	52.23	42.69	0.02	500.69	44.31	0.02	124.60	43.93	0.02
10kV_Trafo_E1_RDAM_Geo	44.14	38.99	0.01	54.20	39.91	0.01	54.23	39.51	0.01

Table 4.10: Line loading with full network expansion in 2030, 2040 and 2050 (high heat demand case)

4.4.2 EDN 2030 Base vs. Full network expansion

4.4.2.1 MV transformers in base network expansion

Figure 4.15 indicates the loading percentages of the 25/10 kV transformers in the base network expansion scenario for both the unenforced and enforced cases. In the unenforced case, the PFA simulation failed to converge in 596 time steps, clearly indicating the need for network reinforcement. The non-convergence of the PFA is represented by zero values in the output of the transformer, line loading and bus voltages, thus the exact amount of complete network failures can be identified. In 2030 cases, all non-convergence occurred during winter when electricity demand reaches its peaks and the network lacks sufficient strength. In other extreme instances, the network remained operational but exhibited severe overloading. This is evident in sub-figure 4.15a, where the C3 transformer experienced a maximum loading level of 351.97% (for summarised values, refer to Table 22). Similarly, transformers A and E2 reached loadings of 123.74% and 158.17%, respectively. Significant overloading also occurred in the HV network. For example, the 380/150 kV Waterningen and 150/25 kV Voorburg transformers reached peak loading of 146.15% and 345.54%, accordingly.

These loading conditions greatly exceed the standard operating limits. Sustained overloading causes transformer overheating, which accelerates equipment degradation, reduces service life and increases risk of equipment failure. To address this, the base network was reinforced with the additional three MV transformers, one at each of the affected locations. Furthermore, to maintain stable operation under peak conditions, HV network reinforcement was also required, which led to the need for an additional 380/150 kV transformer in Waterningen and multiple 150/25 kV transformers (refer to Table 4.15 in Section 4.7). Sub-figure 4.15b indicates the operation of the MV transformers in reinforced configuration, where the maximum transformer loading levels were significantly reduced to 53.13% at transformer A, 69.85% at transformer C3 and 76.45% at transformer E2.

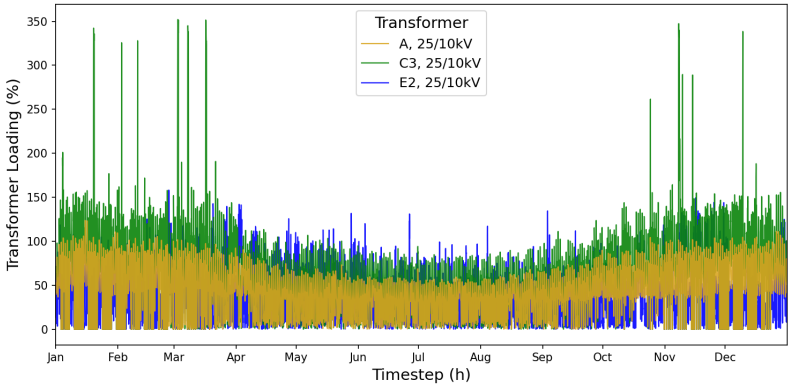

(a) Unenforced network

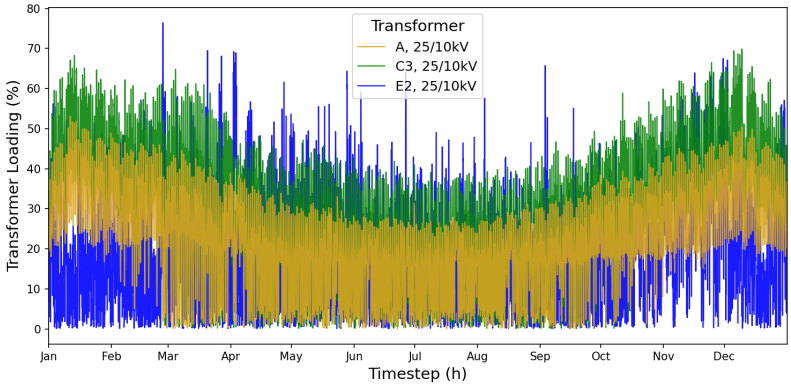

(b) Reinforced network

Figure 4.15: 25/10 kV transformer loading in 2030 with base network

Although the A and C3 substations share similar load profiles, the C3 25/10 kV substation is connected to the DH Geo1 heat source, resulting in an additional annual average power consumption of 3.05 MW. With the DH Geo1 in operation, the maximum loading level of the C3 transformer occurred at time step 8225 with a loading level of 69.85%. Conversely, without the electrified heat source, the maximum loading level of 63.48% was reached at the same time step, indicating a marginal reduction of 6.37%. Overall, the base network expansion scenario in 2030 demonstrates that even in the absence of multiple electrified heat sources the reinforcement of both MV and HV infrastructure is required to mitigate overload risks in response to increased electricity demand.

4.4.2.2 MV transformers in full network expansion

Figure 4.16 presents the loading level of the 25/10 kV transformers in the full network expansion case for both unenforced and enforced case. Compared to the base network expansion case, this scenario incorporates eight additional electrified heat sources, necessitating the integration of two new MV substation (transformers B and E1) and the installation of eight new MV lines for connection. In the unenforced configuration, the integration of additional heat sources is noticeable, with the PFA simulation failing to converge at 647 time steps, an increase of 51 additional failures from the base network configuration.

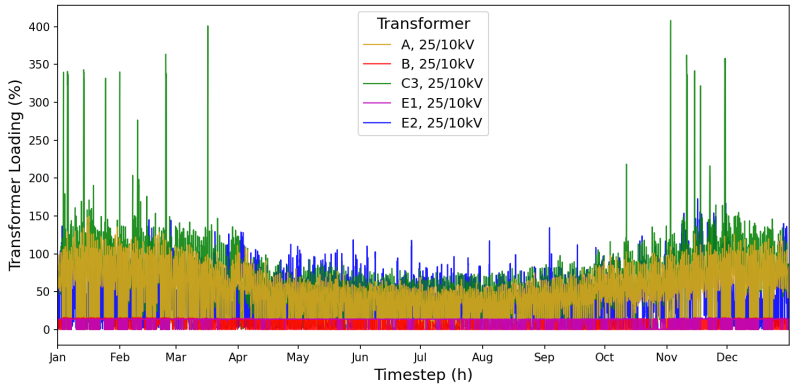

(a) Unenforced

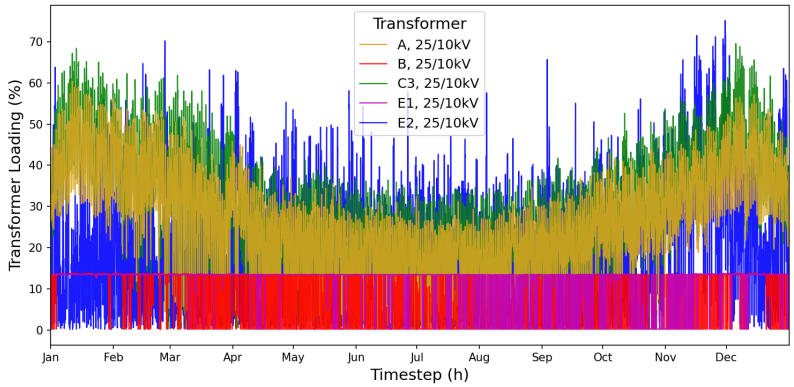

(b) Reinforced

Figure 4.16: 25/10 kV transformer loading in 2030 with full network

Moreover, the maximum observed loading levels of the MV substations reached 149.38% at transformer A, 408.13% at transformer C3 and 172.72% at transformer E2. The newly added substations, exhibit much lower maximum loading levels of 15.96% transformer B and 15.46% at transformer E1 (see sub-fig. 4.16a and Table 22). The lack of overloading is expected, as both substations are exclusively dedicated to geothermal integration and provide power to one electrified heat source each (DH Geo2 for transformer B and RDAM Geo for transformer E1). In contrast, transformers A, C3 and E2 serve the geothermal heat sources together with the aggregated demand profiles from Stedin, leading to significantly higher loading. To alleviate the overloading of the substations, both MV and HV reinforcements were implemented, resulting in the addition of a second

transformer at each overloaded MV substation.

Sub-figure 4.16b depicts the impact of these reinforcements, where the maximum loading levels drop to 60.45% at transformer A, 69.57% at transformer C3 and 71.56% at transformer E2. The loading percentages for transformers B and E1 remained relatively unchanged due to the absence of local demand, although benefits are seen from upstream HV reinforcements. Compared to the base network configuration, the reinforcements were similar, with the exception of adding an additional 150/23 kV transformer at Zuidwijk substation and a 23 kV line for RDAM HP connection reinforcement. Next, with the completion of the "no P2H" case, the reduction in the loading levels is evident across most substations due to the removed electrified heat sources. An exception to this trend is observed at the 25/10 kV E2 transformer, which supplies Tuinders Geo geothermal unit and is also connected to an aggregated load profile from Stedin. When this heat source is removed, the maximum loading of the E2 substation increases by 4.89%, from 71.56% to 76.45%, respectively (refer to Table 22).

The highest recorded loading without the geothermal source occurs at February 26th at noon, which coincides with -48.9 MW electricity demand due to local electricity export to the MV grid, likely from solar PV generation. In the aggregated profile of the E2 substation there are 4,427 time steps (half of the total time steps in the year) where the aggregated demand is negative, indicating power generation by the prosumers. If the Tuinders Geo is removed, at each of the time steps when power is fed into the distribution network the E2 substation is subjected to higher loading as the power must be transferred upstream. This indicates that in the future South-Holland EDN, in which the distributed generation amount will increase due to more solar PV and possibly battery storage (due to negative demand occurring at night hours), the integration of electrified heat sources can help mitigate substation loading by consuming the locally produced power. As a result, the electrified heat sources can contribute not only to decarbonise the DHN but also to stabilise the operation of the EDN.

4.4.2.3 Other MV transformers in base and full network expansion

The base EDN configuration includes an additional 25/23 kV transformer at the C1 substation. In the base network case, this transformer is only connected to the aggregated load profile provided by Stedin. As depicted by sub-figure 4.17a, the loading levels in the unenforced base case are within nominal limits, thus no additional transformer capacity was deemed necessary.

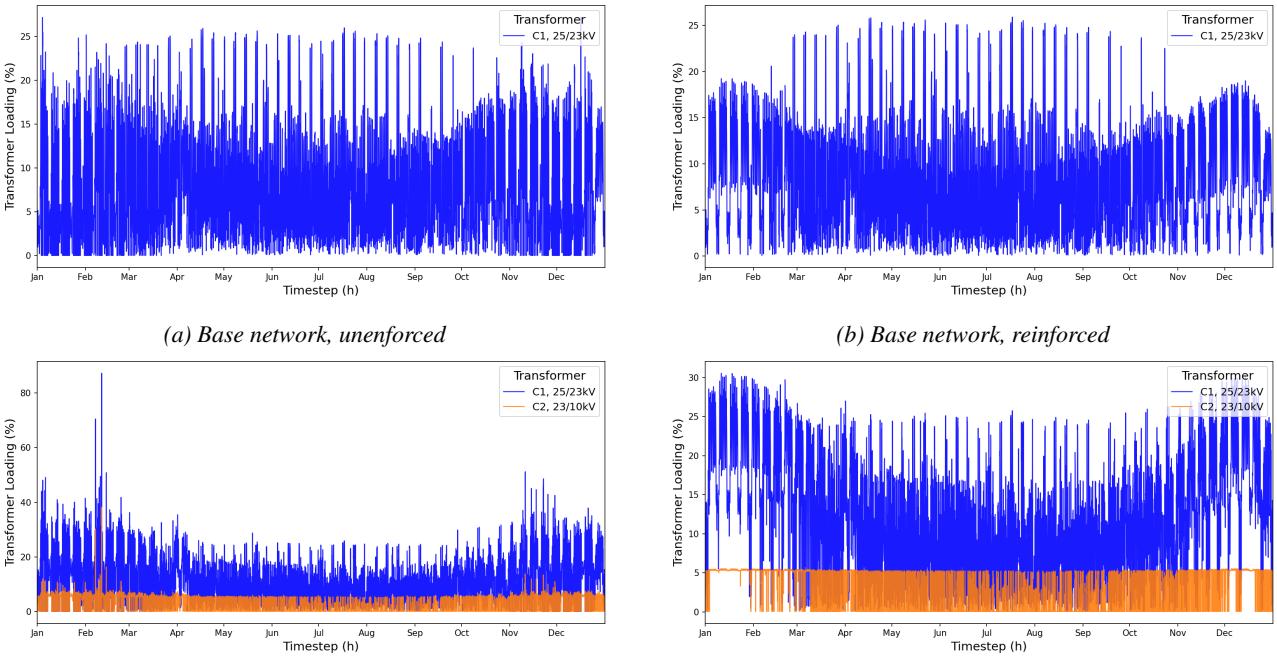

(a) Base network, unenforced

(b) Base network, reinforced

(c) Full network, unenforced

(d) Full network, reinforced

Figure 4.17: 25/23 kV and 23/10 kV transformer loading in 2030

However, with reinforcement of the surrounding network, the loading profile excludes zero values resulting from complete network failures, thus the profile is less saturated at the winter months (see sub-fig. 4.17b). In the full network scenario, and additional 23/10 kV C2 transformer is integrated to connect the DH Geo4 geothermal source to the distribution network. As in the base case, the C1 and C2 branch operates within nominal limits (sub-fig. 4.17c), with an exception of a single instance of increased loading observed in February. However, no reinforcement was implemented in both C1 and C2 substations, due to the introduction of an upstream HV transformer effectively reduced loading levels across the branch, as illustrated in the sub-figure 4.17d.

4.4.2.4 MV lines with base and full network expansion

Table 24 in Appendix I summarises the maximum loading levels of MV lines under both network configurations and their respective cases in 2030. In the base network scenario, the reinforcement of the substations resulted in a reduction in the 10 kV line loading, which connects the DH Geo1 source to the C3 transformer (from 693.33% to 34.92% in the enforced case, accordingly). The substantial reduction can be attributed to the increased capability of the reinforced substations to serve local demand, thus decreasing the need for power flow from the upstream external grid through the transmission and distribution lines. Moreover, reinforced substations have lower electrical impedance, hence local power exchange with the network is facilitated, lowering the stress on the distribution lines. With removal of the geothermal source, the 10 kV line is not utilised and the highest loading of 0.02% is observed. This minimal residual line loading is the result of minor reactive power flows, inherent to the operation of the EDN.

In the full network scenario, a similar operation trend is observed to that of the base network, as the reinforcements of the substations causes reduced line loading levels. However, additional reinforcement was needed for the 25 kV line that connects substation to the DH HP unit. With an additional line, the maximum observed line loading dropped to 90.46%. Despite the improvement, the operational warning threshold is reached, but the implementation of a third line was deemed unnecessary due to the operational characteristics of the DH HP unit, which does not run continuously due to price competition with four other geothermal sources and one EB in The Hague. Moreover, in the scenario where the electrified heat sources are removed, the utilisation of 25 kV, 23 kV and 10 kV lines that connect the heat sources to the EDN drop nearly to zero. The minimal observed loading under this case is primarily attributed to reactive power flows within the network, rather than active power transmission.

4.5 Summary of DHN results

4.5.1 Heat distribution pipes

The PyPSA package offers the functionality to optimise both the operation and optimal size of the DHN components. In the South-Holland DHN, a total of fifteen heat distribution pipes are operational, of which only two are bidirectional (Pipe10 and Pipe11), meaning that the South-Holland DHN is directional. The fixed capacities of only eight pipes were known prior to simulation, leaving seven other pipes with undefined capacities. Within the DHN optimisation model, pipes with unknown capacities were defined extendable, which means that the PyPSA optimisation model optimally sizes these heat distribution pipes based on the required heat flows in the network. Figure 4.18 presents the increase in the optimal pipe capacities in network expansion and heat demand comparison scenarios.

Regarding the sub-figure 4.18a, Pipe1 in The Hague is used for intracity heat transfer, while Pipe2 connects The Hague with IWH1 and W1 heat sources. The optimal capacity of Pipe1 in the base network was 94 MW, while in the full network configuration the optimal sizing increased to 108 MW. Moreover, Pipe2 capacity decreased significantly, from 72 MW to 43 MW. The changes in optimal pipe capacities reflect the increased independence of the heat network in The Hague, which requires more distribution capacity for intracity heat transfer via Pipe1 and less intercity capacity for heat imports from Rotterdam via Pipe2. Furthermore, in both

network expansion scenarios the optimal capacity of Pipe6 was determined to be 160 MW. This corresponds to the maximum production level of the WI unit and with the fixed capacity of Pipe7, also with 160 MW size, which is connected to Pipe6 and supplies heat to Rotterdam. Thus, a larger capacity of Pipe6 is unreasonable.

Moreover, Pipe10 shows a reduced capacity by 20 MW, from 263 MW to 243 MW, respectively. This can be attributed to the integration of the Tuinders Geo geothermal unit, which lowers the requirement for the distribution of heat through the network to meet the demand in Tuinders. This implies that with the addition of a geothermal source heat is produced and consumed locally, minimising the need of heat transfer from other production units. Additionally, in the base scenario, Pipe11 was not utilised due to the absence of the B-Triangle Storage unit, but in the full network configuration the inclusion of B-Triangle Storage results in Pipe11 being sized at an optimal capacity of 52 MW. Optimal size of 60 MW for Pipe12 was determined in both cases, corresponding to the fixed capacity of Pipe8 with 60 MW. Lastly, in the full network scenario, Pipe14 capacity is decreased by 12 MW, a direct consequence of the lower use of gas boiler and CHP plants due to the new geothermal and HP units in Rotterdam.

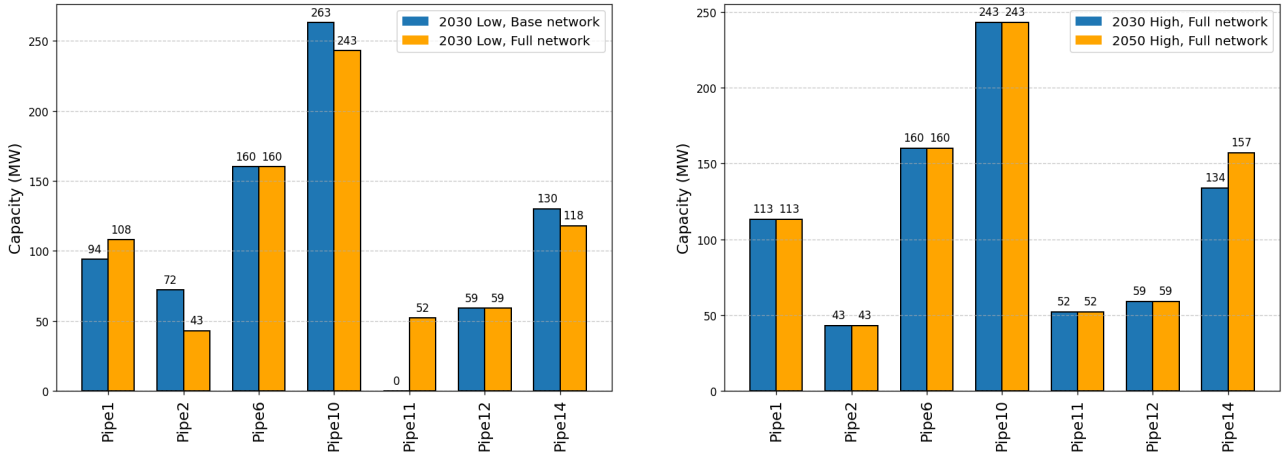

(a) 2030 with base and full network (low heat demand)

(b) 2030 and 2050 with full network (high heat demand)

Figure 4.18: Increase in pipe capacity under various scenarios

4.5.2 Summarised results

Tables 4.11 and 4.12 summarise the results of all the experiments performed with the future DHN of South-Holland. Moreover, Table 21 and Figure 4.20 depict the electricity demand of the P2H units and the electricity production of the CHP plants, the main output of the operational optimisation of the DHN. The key takeaway from all simulations of the DHN scenarios is that in the future DHN configuration with additional heat supply and storage source and with low or high heat demand, the primary heat production units are the geothermal energy plants, which on average supply 34.6% of heat demand in all full network expansion scenarios. Moreover, the amount of heat produced by the IWH units remains the same in all scenarios. With decreasing heat demand, the use of CHP units declines sharply, while with increasing heat demand the increase is marginal, showing that with the applied DHN model setup CHP units are being slowly phased out. With the reduction in heat demand the utilisation of HPs drops, while with a higher heat demand the production levels increase, which is a result of the change in heat demand in Rotterdam and Tuinders area. In addition, with increasing heat demand, the RDAM Gas4 gas boiler capacity factor increases to cover the peak heat demand period in the Rotterdam RoCa demand bus.

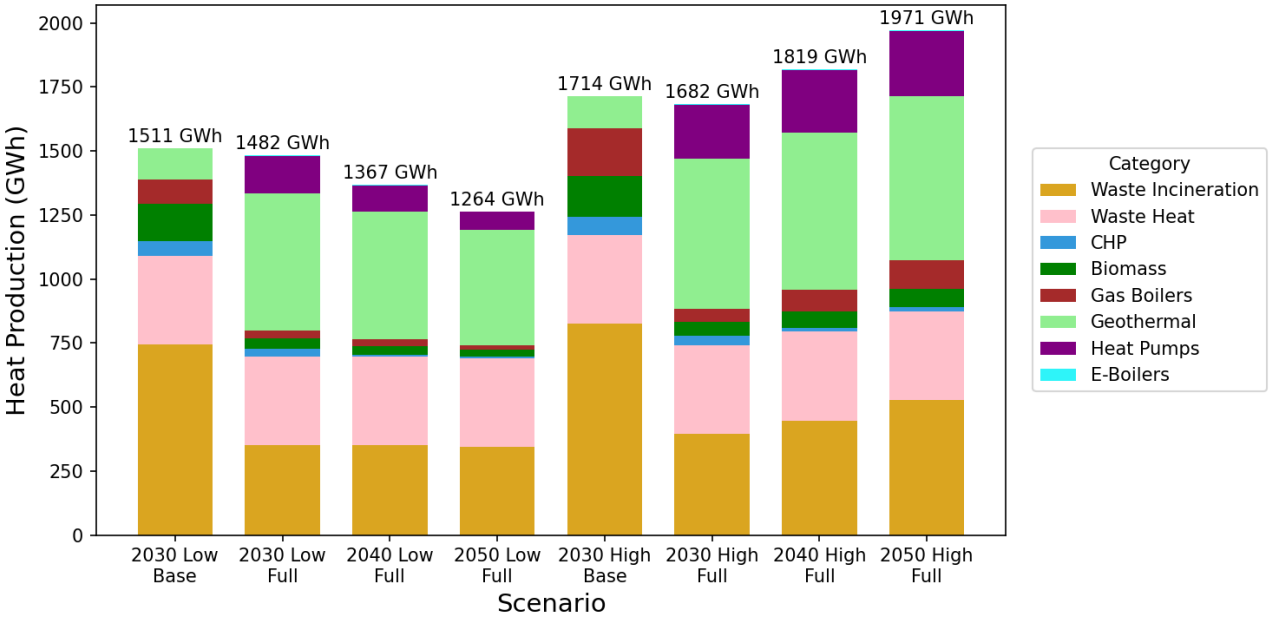

Figure 4.19: Total production per category by scenario, GWh

	2030 Low		2040 Low	2050 Low	2030 High		2040 High	2050 High
	Base	Full	Full	Full	Base	Full	Full	Full
WI	744,175	352,110	350,610	344,381	825,696	394,894	448,152	528,889
IWH	346,033	346,033	346,033	346,027	346,033	346,033	346,033	346,033
CHP	57,897	31,302	7,821	7,025	71,374	38,128	14,978	15,418
Biomass	145,505	40,151	34,017	26,578	158,439	54,212	63,957	72,913
Gas boilers	94,151	30,994	28,243	19,071	185,595	51,311	84,552	111,374
Geothermal	123,188	534,981	497,561	448,475	126,944	583,650	613,341	637,640
Heat pumps	-	144,536	101,330	71,088	-	211,885	246,019	256,799
E-Boiler	-	1,839	1,838	1,837	-	1,854	1,881	1,924
Total	1,510,949	1,481,946	1,367,453	1,264,482	1,714,081	1,681,967	1,818,914	1,970,990

Table 4.11: Total production per category of supply, MWh.

	2030 Low		2040 Low	2050 Low	2030 High		2040 High	2050 High
	Base	Full	Full	Full	Base	Full	Full	Full
DH Storage1	9,580	1,061	890	1,387	7,958	892	942	2,681
DH Storage2	-	83,172	83,087	81,274	-	86,389	90,367	91,293
RDAM1 Storage1	22,257	41,616	37,778	34,087	17,037	46,448	57,906	56,668
RDAM1 Storage2	-	40,178	36,279	28,417	-	43,633	43,625	40,178
RDAM2 Storage	3,660	2,447	904	773	3,406	2,721	971	38,925
Tuinders Storage	12,906	26,248	25,377	26,157	12,485	27,576	27,210	28,847
B-Triangle Storage	-	2,318	2,151	2,479	-	1,765	2,167	2,658
Total	48,404	197,041	186,466	174,574	40,888	209,424	223,188	261,250

Table 4.12: Total storage supply, MWh.

Figure 4.20 indicates the total electricity demand and production of the heat supply units. As seen in the figure, with decreasing heat demand, the electricity demand from electrified heat sources decreases, while the opposite is seen with the increase in heat demand, showing that the electrified heat sources in the DHN can be utilised at a larger rate when heat demand rises. Moreover, whether the heat demand increases or rises the production of CHP units decreases, which is a result of rising carbon prices, making their use financially unfeasible.

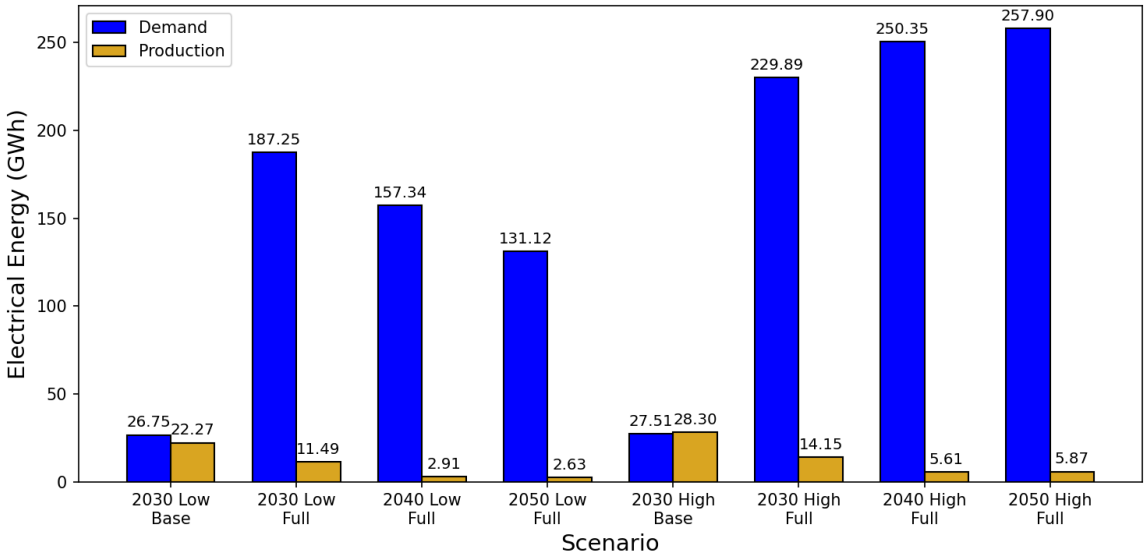

Figure 4.20: Total electricity demand and production from heat supply units, GWh

4.6 Summary of EDN results

Figure 4.21 presents the number of non-converged snapshots across unenforced EDN cases. In general, with each scenario the EDN experiences increasing loading levels due to the evolving aggregated Stedin load profiles. Moreover, the rising heat demand for the DHN translates into a higher annual electricity demand from electrified heat sources, which contributes to more frequent occurrences of elevated loading in the EDN. Deliberate and strategic reinforcement of the EDN can significantly reduce the overloading of components, resulting in nominal loading levels. In some cases, reinforcements can even enable additional network connections, especially in substations dedicated to supplying a single geothermal heat source.

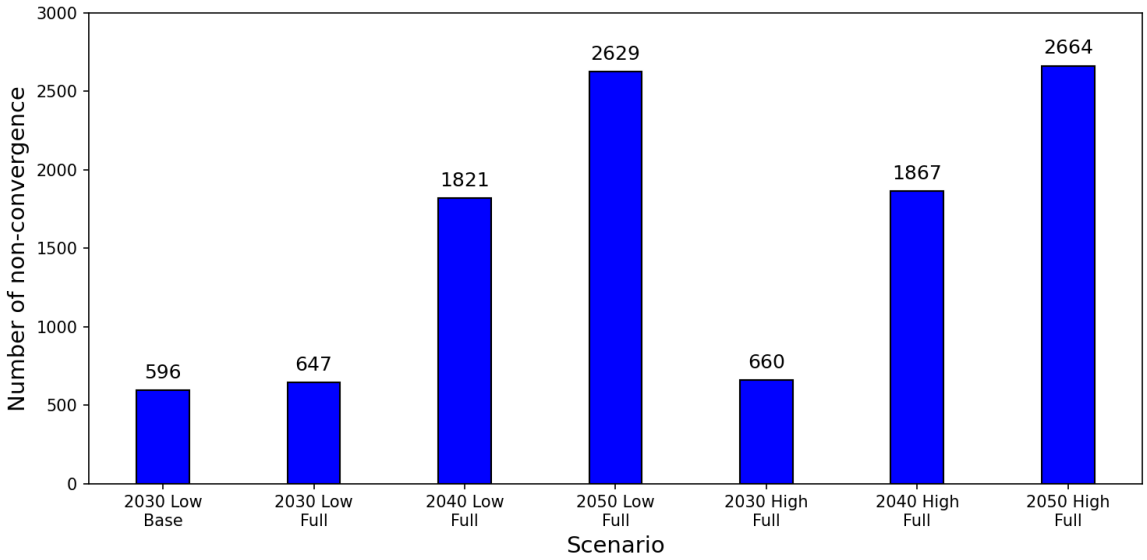

Figure 4.21: Number of snapshots for which the PFA did not converge in each scenario

Figure 4.22 illustrates all scenarios in which the removal of the electrified heat sources ("no P2H") results in a higher maximum transformer loading. As identified previously, during time steps with net negative demand (surplus electricity from distributed energy sources), electrified heat sources can consume electricity locally, without the need to transfer the electrical power upstream through MV and HV networks to the external grid. However, this figure only reflects the change in maximum loading, which may occur during a single time

step. For example, in the 2030 scenario with full network expansion and low DHN heat demand, the E2 substation transfers power upstream in roughly half the time steps. With the addition of the electrified heat source (Tuinders Geo), power is consumed on-site, effectively reducing transformer stress if the Tuinders Geo is operational.

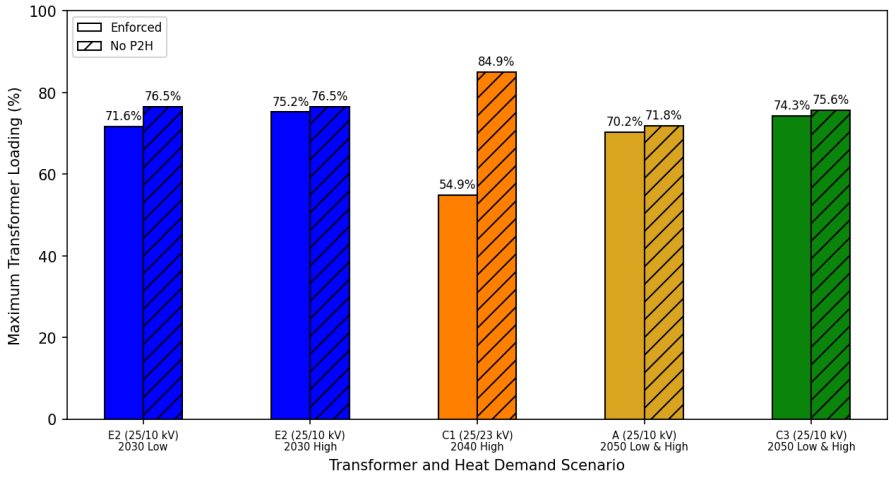

Figure 4.22: All cases showing higher maximum loading levels with "no P2H" case

Figure 4.23 shows transformer loading in the unenforced cases across all scenarios with high heat demand. As mentioned before, the number of non-convergent calculation rises from 660 in 2030, to 1867 in 2040 and 2664 in 2050. In 2030, the winter period is saturated as most failures occur during that time indicated by values going to zero. By 2050, the whole load profile is saturated with 0 values, indicating that transformer loading will not only be limited to peak heat and electricity demand time steps in the winter.

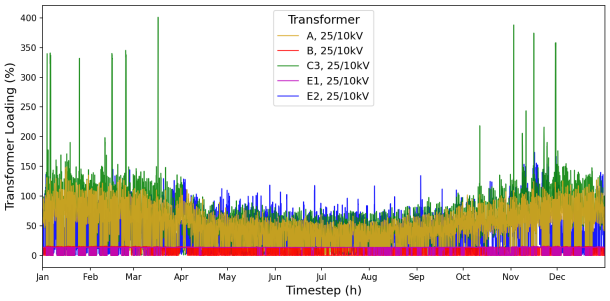

(a) Unenforced case in 2030

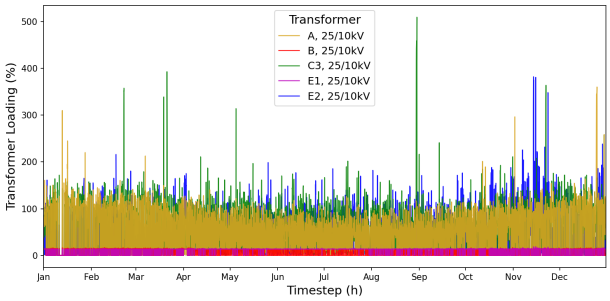

(b) Unenforced case in 2040

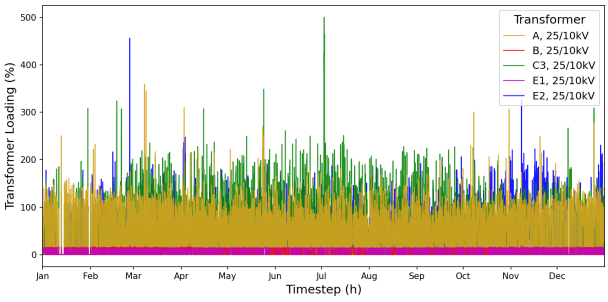

(c) Unenforced case in 2050

Figure 4.23: 25/10 kV transformer loading with full network expansion with high heat demand, unenforced

4.7 Investments in reinforcements

This section provides a financial analysis of the network reinforcements required in all EDN scenarios. The capital investment costs of the additional transformer and line units under different scenarios are evaluated. The analysis highlights the capital investment amount for the MV and HV components of the distribution and transmission network. The rough costs of the transformers (€/MVA) and lines (€/km) are expressed in Tables 8 and 9 in Appendix .1, which were confirmed by Stedin.

4.7.1 Connection infrastructure costs

Not all reinforcement costs in EDN scenarios are the result of transformer or line overloading. In the full network expansion scenario, the integration of new electrified heat sources requires new critical infrastructure to ensure a reliable power supply. These infrastructure additions represent the induced costs, which arise not from the additional load on the network, but from the necessity to connect and operate the new heat production units. The associated capital investment includes both new substations with transformers and line connections. Table 4.13 presents the costs related to the installation of new transformers, while Table 4.14 outlines the new distribution line costs in the MV network. The combined costs of this new critical infrastructure amount to a capital investment of €4,704,500.

Name	No.	Cost (€)
Trafo_B	1	750,000
Trafo_C2	1	2,000,000
Trafo_E1	1	750,000
Total		**€3,500,000**

Table 4.13: Cost of additional transformers for connection

Name	Length (km)	No.	Cost (€)
25kV_Substation_B_DH_HP	2.4	1	300,000
25kV_Substation_B_DH_EB	0.1	1	12,500
23kV_Substation_F_RDAM_HP	3	1	360,000
10kV_Trafo_A_DH_Geo3	1.5	1	142,500
10kV_Trafo_B_DH_Geo2	0.1	1	9,500
10kV_Trafo_C2_DH_Geo4	2	1	190,000
10kV_Trafo_E1_RDAM_Geo	0.5	1	47,500
10kV_Trafo_E2_Tuinders_Geo	1.5	1	142,500
Total			**€1,204,500**

Table 4.14: Cost of additional lines for connection

4.7.2 EDN in 2030

The results of EDN reinforcement for the 2030 scenario are presented in Table 4.15, where the optimal number of transformers and lines for both base and full network configurations are presented. In total, the base network requires €43.9 million capital investment, while with the full network expansion scenario €51.7 million would be needed. Based on the results provided in Appendix I, the transformer and line loading levels with low and high demand remain within the nominal limits; hence, for the full network with low and high heat demand, the same reinforcements were applied. The three scenarios are separated by an additional investment of €7,814,500. The difference is a result of the requirement to build a new infrastructure to connect electrified heat sources. Moreover, the full network expansion case requires an additional 150/23 kV transformer in Zuidwijk substation and an additional 23 kV line for the RDAM HP power supply. In general, even with the base network expansion scenario that only has one electrified heat source, a substantial investment is required.

		Base network 2030 Low			Full network 2030 Low & High		
Name	**Type (kV)**	**Initial No.**	**Final No.**	**Cost (€)**	**Initial No.**	**Final No.**	**Cost (€)**
Waterningen	380/150	1	2	17,500,000	1	2	17,500,000
Krimpen	150/25	1	1	0	1	1	0
Rijswijk	150/25	1	3	6,900,000	1	3	6,900,000
s'Gravenhage	150/25	1	2	3,450,000	1	2	3,450,000
Voorburg	150/25	1	3	6,900,000	1	3	6,900,000
Ommoord	150/25	1	3	6,900,000	1	3	6,900,000
Zuidwijk	150/23	1	1	0	1	2	2,750,000
A	25/10	1	2	750,000	1	2	750,000
B	25/10	-	-	-	1	1	0
C1	25/23	1	1	0	1	1	0
C2	23/10	-	-	-	1	1	0
C3	25/10	1	2	750,000	1	2	750,000
E1	25/10	-	-	-	1	1	0
E2	25/10	1	2	750,000	1	2	750,000
23kV_Substation_F_RDAM_HP	23	-	-	-	1	2	360,000
Total				**€43,900,000**			**€51,714,500**[1]

[1] plus connection infrastructure costs

Table 4.15: Additional reinforcement costs in 2030

4.7.3 EDN in 2040 & 2050

In the 2040 scenario, it is assumed that the critical infrastructure and network reinforcements built in 2030 are operational. Likewise, in the 2050 scenario, the network reinforcements added in 2040 are carried over. Therefore, the total capital investment for 2040 network reinforcement does not include the costs of the 2030 scenario, while the same is true for the 2050 scenario. Table 4.16 presents the optimal number of components for reinforcement in both future scenarios. For both cases of heat demand, the necessary reinforcement capacity was proved to be equal. In 2040, the main investment costs come from the need to strengthen the HV network, resulting in only 8.72% of total capital costs going to direct reinforcement of the EDN (€2.5 million in total). Moreover, in 2050, EDN investments represent a slightly large sum of €3,098,750, representing 9.4% of the total investment.

		Full network 2040 Low & High			Full network 2050 Low & High		
Name	**Type (kV)**	**Initial No.**	**Final No.**	**Cost (€)**	**Initial No.**	**Final No.**	**Cost (€)**
Waterningen	380/150	2	3	17,500,000	3	3	0
Krimpen	150/25	1	1	0	1	2	17,500,000
Rijswijk	150/25	3	4	3,450,000	4	5	3,450,000
s'Gravenhage	150/25	2	2	0	2	3	3,450,000
Voorburg	150/25	3	4	3,450,000	4	5	3,450,000
Ommoord	150/25	3	3	0	3	3	0
Zuidwijk	150/23	2	2	0	2	2	0
A	25/10	2	2	0	2	3	750,000
B	25/10	1	1	0	1	1	0
C1	25/23	1	1	0	1	1	0
C2	23/10	1	1	0	1	1	0
C3	25/10	2	3	750,000	3	4	750,000
E2	25/10	2	3	750,000	3	3	0
E1	25/10	1	1	0	1	1	0
150kV_Waterningen_Rijskwijk(1&2)	150	2	3	1,202,400	3	4	1,202,400
150kV_sGravenhage_Rijskwijk	150	1	2	540,000	2	2	0
23kV_Substation_F_RDAM_HP	23	2	2	0	2	2	0
25kV_Substation_B_DH_HP	25	1	1	0	1	2	300,000
25kV_Substation_C_Trafo_C3(1)	25	1	1	0	1	2	563,750
25kV_Substation_C_Trafo_C3(2)	25	1	1	0	1	2	545,000
25kV_Substation_C_Trafo_C1	25	1	1	0	1	2	865,000
25kV_Substation_E_Trafo_E2(1&2)	25	2	3	1,000,000	3	3	0
Total				**€28,642,400**			**€32,826,150**

Table 4.16: Additional reinforcement costs in 2040 and 2050 (low and high demand scenarios)

4.7.4 Financial investment summary

The overall accumulated investment costs of the in the full network expansion case in 2040 are €80.3 million, while by 2050 the total accumulated costs result in €113.18 million. Of the latter amount, 4.16% is required for the new substations and lines to supply power to the additional electrified heat sources, 7.85% of the total accumulated investment is reserved for the reinforcement of the EDN and the remaining 87.99% goes toward the reinforcement of the HV transmission network. Figure 4.24 shows the cost accumulation, while Table 4.17 presents the exact costs required for reinforcement by 2050.

The final costs provide a rough estimate of the required investments. Actual costs may be higher following a detailed market analysis of equipment suppliers and contractors. In general, the comparison between enforced and "no P2H" cases shows that in some cases the electrified heat sources can reduce transformer loading by enabling local consumption of electricity. In other instances, the addition of these sources results in a marginal increase in the maximum loading levels of the critical network infrastructure. This indicates that reinforcements are primarily driven by the future load demand profiles provided by Stedin. Nevertheless, total accumulated capital investment costs are largely influenced by the overloading at the MV distribution level. This highlights the importance of coordinated planning across all voltage levels of the network, as their interdependence is critical to ensuring stable and efficient network operation.

Scope	**Accumulated costs**
MV connection infrastructure	€4,704,500
MV network reinforcement (EDN)	€8,883,750
HV network reinforcement	€99,594,800
Total costs	**€113,183,050**

Table 4.17: Total accumulated investment costs by 2050 (low and high demand scenarios)

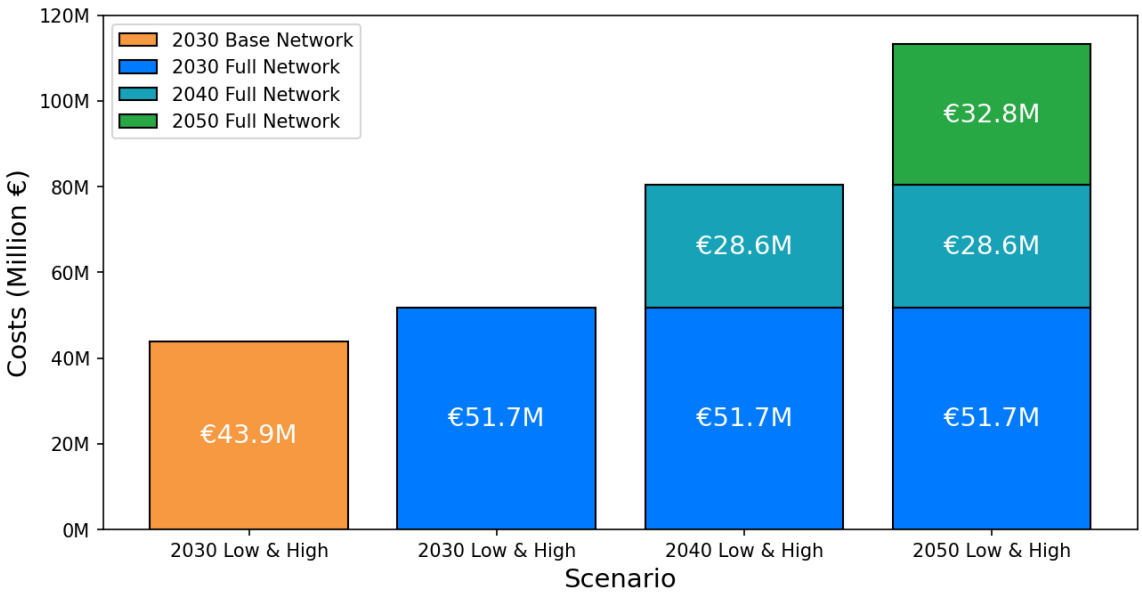

Figure 4.24: Total accumulated investment costs in each scenario

5 | Discussion

This chapter provides an interpretation of the case study results, while also answers the research questions that were raised in the beginning of the thesis. Moreover, a general observation and evaluation of the thesis methodology is presented and discussed.

5.1 Interpretation of case study results

5.1.1 DHN in 2030

The results of the 2030 scenarios demonstrate the impact of the transition towards electrified heat source integration in the future DHN, revealing a clear shift from a more demand-driven to a flexible and market responsive network. The operation of the future DHN not only depends on heat demand, natural gas and CO_2 prices, but also on the weather conditions and largely electricity market conditions. Due to the decarbonisation of the DHN a near complete phase-out of gas boilers occurs if the low heat demand projections are true. On the other hand with high heat demand scenario the RDAM Gas4 operates to supply heat to one of the key heat demand nodes of Rotterdam RoCa. Moreover, the utilisation of CHP units declines sharply in both heat demand cases, operating only during the hours when revenue from electricity sales can be made. The operation of the CHP's are largely limited by the carbon prices, which are projected to increase in the upcoming decades. In the full network expansion cases the geothermal energy plants take the primary role as base load providers followed by significant heat dispatch by WI and IWH units, the latter two each serving around a quarter of heat demand in each scenario.

In addition, the implementation of geothermal sources shifts the role of the biomass plant from the base load supplier to a peak-shaving heat production unit in the Tuinders region. With increasing heat demand the utilisation rate of the HP units (primarily RDAM HP) increases significantly. Conversely, decreasing heat demand results is lower RDAM HP utilisation as its dispatch is limited by the heat distribution network capacity and price completenesses with the WI and IWH units. With more TES units the decoupling of heat supply from the instantaneous demand is achieved, mitigating the variability introduced by the new dynamic market behaviour. Furthermore, due to the specific directionality of the DHN, the placement of TES near the electrified heat production units vastly increases the utilisation of heat buffers, providing additional flexibility to the DHN. Otherwise, TES placed near fossil-fuel powered systems shows low usage rates with low operational variability. Lastly, in 2030, with the integration of electrified heat sources, close to 100 MW of electrical power at peak times is required from the EDN to meet the heat demand, thus the ability of the EDN support this power demand is critical.

5.1.2 DHN in 2040 and 2050

The 2040 and 2050 DHN scenarios maintain similar operational dynamics to the full DHN scenario in 2030. Although the underlying input profiles remain structurally consistent, changes in the economic parameters, heat demand and climate data introduce new operational patterns. With the increase in heat demand the proportions of heat dispatch by category remain largely similar to the low heat demand cases, except for the HP, WI and gas boilers, which all increase their heat output due to demand increase in the Rotterdam and Tuinders regions. Also, the biomass plant keeps its role as a stable heat source in both scenarios with high heat demand In the low heat demand case, the utilisation of the RDAM HP drops due to price and efficiency competition with the nearby sources in Rotterdam. Moreover, heat supply from certain TES systems (RDAM1 Storage1 and RDAM1 Storage2) drops slightly due to lower heat demand and lower electrified heat source production (mainly RDAM HP).

On the other hand, in the high demand case, the same reduction in heat supply happens for both mentioned TES units. Due to increased heat demand it become more efficient to meet the heat demand directly than to

have transmission, charge and storage of the storage combined. Further findings suggest that an expansion to a multidirectional heat network could allow a better utilisation of the distributed heat production sources and certain heat buffers (especially the ones connected to CHP and gas boiler system). Meaning that either multi-directionality of the DHN or the placement of storage systems near the electrified heat sources are the solutions that would allow better integration. In addition, the total heat output from the geothermal plants remains largely similar between 2040 and 2050 cases. Four out of six geothermal sources are placed in The Hague, which results in curtailment of the these units as heat cannot be transferred to the wider network (only The Hague can receive heat from Rotterdam via the WLQ connection). With the high heat demand case, the power demand at peak times remain around 100 MW, however, on average more power is required for the operation of the electrified heat sources.

5.1.3 EDN in 2030

The 2030 EDN scenario highlights how the addition of multiple electrified heat sources affect the MV distribution network infrastructure. With the base network topology applied in 2030 it was identified that a single geothermal source only marginally increases the substation loading. More importantly, it was discovered that even in the absence of multiple electrified heat sources reinforcing the HV and MV networks is still required. This suggests that future load profiles from Stedin have larger impact on the reinforcement selection, which will stay evident in other scenarios as well. Moreover, it was shown that with the taken reinforcement measures a successful reduction in transformer and line loading can be achieved.

The maximum loading levels indicate that in cases of large local electricity production the electrified heat sources can reduce the substation overloading. This highlights the role of electrified heat sources as not only electricity consumers that create higher loading, but in some instances as systems that consume the electrical power locally, reducing the loading on the upstream components and balancing the network. Overall, whether with base or full network expansion scenarios, the 2030 case underlines the importance early investments in the network expansion ahead of widespread electrification. Even with low number of electrified heat production units, reinforcements are required, which highlights that the broader network planning must accommodate not just the DHN expansion, but also the general electrification trends in the South-Holland region.

5.1.4 EDN in 2040

By 2040, the EDN becomes increasingly more vulnerable to failures if no reinforcements are done in 2030. Although 2040 could be considered as a transitional year to 2050, a threefold increase in the number of non-convergent PFA calculations in the unenforced cases shows the anticipated increase in the future electrical power consumption and distributed generation. The pressure on the continues to increase with the growth in electrification and distributed electrical energy generation. In terms of network reinforcement, on top of the reinforcements that are assumed to be implemented in 2030, the reinforcement of two MV transformers and one line is required. Nevertheless, the majority of the capital investments result from the need to upgrade the upstream HV network. On the other hand, the 10 kV lines dedicated to geothermal integration show stable loading patterns during the year, revealing that geothermal energy sources require stable supply power. Overall, in the 2040 scenarios the importance of strategic network infrastructure planning is highlighted.

5.1.5 EDN in 2050

In the 2050 EDN scenario, the new complexity introduced by the increased penetration of distributed energy generation changes the seasonal loading patterns. This results in shifted peak load times, with a notable increase in peak loading in the summer due to large distributed energy generation, which results in more critical network failures if not reinforcements are implemented. Moreover, reinforcement of MV voltage lines connecting the 150/25 kV and 25/10 KV substations as well as two MV transformer was identified as a necessity to achieve nominal component loading. Similar to the EDN in 2040, the majority of the capital investments come from the need to reinforce the HV network. The continuation of the reinforcements in the 25 kV level, highlight that

distribution infrastructure remains one of the key constraints in achieving nominal network operation. Again, the 10 kV lines linked to geothermal sources required no reinforcement, reaffirming the reliability of local geothermal integration.

5.2 Sub-questions

5.2.1 SQ1

What modelling aspects must be considered when designing an integrated heat-electricity system to investigate the DHN interactions with the distribution grid?

The design of integrated heat-electricity networks inherently comes with a plethora of modelling factors that must be considered, including both institutional and technical modelling aspects. As highlighted in Chapter 2, a key starting point is the establishment of a collaborative frameworks between network operators where data is strategically shared and aligned to plan the operation and execution of network investments in a coordinated manner. The modeller is thus tasked to act as a mediator and translator between the professional knowledge of the network operators and the mathematical models required to simulate the integrated networks. This study, as part of the DEMOSES project, has shown the multiple stages of development of the integrated heat and electricity network models of the South-Holland region that aim to act as a decision support tools in helping the transition towards decarbonised networks. The construction of such models is a multi-step process that begins with definition of network boundaries, relevant input data and infrastructure constraints, all of which are critical to model real-world networks as realistically as possible. Moreover, choosing the right software tools that can be specifically applied to model interconnected multi-carrier energy networks is pivotal.

With the achieved institutional and conceptual alignment, the technical modelling aspects can be addressed. In this study, the DHN model was built using the PyPSA library, while the EDN model utilises pandapower framework, which both allow for detailed simulation of integrated energy systems. To provide a realistic and functional representation of the integrated heat and electricity networks, multiple modelling elements must be taken into account. At first, the temporal resolution of the input data must be considered. In this study, hourly resolution was chosen to capture the seasonal and intra-day variations in prices, temperatures and demands (heat and electricity), critical for the operation of both networks. Next, the behaviour of each component must be considered to achieve greater realism of the model. For example, HPs and geothermal sources must have variable COP values that reflect seasonal and daily temperature variations. Moreover, the operational time-frames of certain heat production units must be taken into account, such as seasonal operation of WI and CHP plants. Given the lack of PyPSA heat dumping functionality a custom modelling approach was considered to account for components with a minimum production limits. Furthermore, carefully defining the objective function is crucial, as it determines how the DHN balances the economic and technical variables. With regard to the EDN model, the accurate spatial mapping of the electrified heat sources is required to determine the exact connection points to the EDN. This enables a more accurate assessment of their impact on transformer and line loading, enabling accurate operation under future scenarios. Ultimately, the usefulness of such integrated models depends not only on the technical refinement, but also on how well they support the real-world network operation and reinforcement strategies.

5.2.2 SQ2

What are the different technology options for decarbonising heat demand (i.e. HP, EB, etc.), when combined into a DHN and what is the optimal mix from the perspective of the DHN?

To decarbonise heat demand, multiple technology options exist, particularly as electricity and other alternative low-carbon options are more widely applied in DHNs, offering unique operational characteristics. The key technologies in future DHN of South-Holland include the electrified heat sources like geothermal energy and HPs, as well as other low-carbon systems, such as WI, biomass and IWH systems and fossil-fuel powered gas

boilers. In addition, the CHPs and EBs were considered. In this thesis, HPs, EBs and geothermal energy represented electrified heat production technologies that facilitate the integration of the heat and electricity sectors. In the South-Holland case study, the optimal mix for future scenarios is derived from cost-based optimisation modelling in PyPSA, where heat production units are selected based on dynamic energy prices, emission costs and operational flexibility.

The results indicate that overtime the optimal energy mix for the South-Holland DHN shifts toward greater reliance on geothermal energy sources, supplying one third of the heat demand. On the other hand, HPs supply around one tenth of the heat demand in the future scenarios, while EB contribution to the final heat output was found to be marginal. HPs and EBs are primarily utilised during periods of low electricity prices, indicating their potential role in electricity network balancing. WI and biomass act as low-carbon heat supply units, with WI unit supplying the majority of heat to Rotterdam. With decreasing heat demand, the biomass unit shifts to a peak-shaving production, while increased heat demand allows the unit to operate steadily. Furthermore, in the future scenarios of the DHN it was discovered that the gas boilers remain a key production unit, which indicates a need for more electrified heat sources or a multi-directionality of the DHN. The evolution of the optimal energy mix demonstrates that in the future the most cost-optimal units will also be the low-emission ones. Future scenarios show that the South-Holland DHN will prioritise electrification, while the base load will be supported by low-carbon technologies and flexible heat storage units to balance seasonal and daily variability.

5.2.3 SQ3

How can operators of heat and electricity networks understand the impact of electrification of heat supply on their systems?

The South-Holland case study demonstrated that heat and electricity network operators can understand and quantify the impact of electrified heat technologies through integrated network modelling and scenario-based simulations. By applying an operational optimisation dispatch model in PyPSA the study depicted the operation of the future DHN. Crucially, the operation of the electrified heat technologies was modelled, namely HPs, EBs and geothermal energy systems, that interact with both heat and electricity networks. The results show that increased direct electrification of heat supply units raises the dependence on low-voltage electricity networks, especially during peak heat demand periods. The situation creates a dual challenge, where the supply of heat to end-consumers now requires the management of two integrated networks simultaneously. The integrated models suggest that geothermal energy and HP units are becoming dominant heat suppliers under the future scenarios, contributing to a significantly increased electricity demand. To address this, the study evaluated the electricity network reinforcement needs, mainly line and transformer number upgrades, enabling Stedin to plan future operation and reinforcement investments accordingly. Meanwhile, Eneco can use the insights of the model to align their network operation targets. Overall, with a flexible network modelling framework both parties can understanding the integrated operation and the critical infrastructure needs of both networks.

5.3 Main research question

How does the decarbonisation of the DHN of South-Holland, facilitated by the electrification of the heat supply, affect the electricity distribution network?

The decarbonisation of the South-Holland DHN, primarily driven by direct electrification of heat supply units, alters future electricity load profiles by introducing new peak demand periods and increasing overall electricity demand. While this results in additional stress on the EDN components, during periods of high distributed generation levels these sources were shown to reduce transformer loading by locally consuming excess electricity. As such, the real impact of the electrification of the DHN is mixed. With the operational optimisation model of the South-Holland DHN it was shown that around 40% of total heat demand will be met by electrified

heat supply units, primarily by geothermal energy and HPs, which produce around 30% and 10% of the total heat demand, respectively. Electrification of the heat supply units transforms the operation of the DHN, as heat production units become closely tied to electricity market prices or weather patterns; thus, introducing new operational variability, which is not dominant in the current heat network. Depending on the heat demand scenario, the total electrical power demand from the DHN ranges from 131 to 257 GWh annually.

This increased and variable demand adds further complexity to the balancing and load forecasting for the electricity distribution network operator, requiring Stedin to reevaluate their projected substation electricity demand profiles to prevent congestion and maintain supply security. The integration of electrified heat technologies essentially shifts the role of EDN with respect to the DHN i.e., from a passive (ensuring power supply to heat production plants as to regular customers) to a more active role that must adapt to a dynamic electricity demand. As was shown in the South-Holland case study, no distribution network reinforcement will result in an increasing number of critical network failures (non-convergence) every decade, from around 600 to over 2600. Moreover, the instances of when such critical failures occur is becoming more increasing in the summer and shoulder months due to increased distributed energy generation levels. As mentioned before, the network loading resulting from high distributed RES generation can be reduced by electrified heat supply units consuming the power locally. Moreover, with applied network reinforcements it was shown that the distribution network can operate within safe limits. By 2050, a total of €113 million of investments will be required to effectively integrate the electrified heat sources and meet the projected electricity demand of the local loads. Overall, with the anticipation of both networks becoming more tightly integrated, the impact of heat source electrification will not only be felt on the network scale, but also on the company scale, requiring more specialists working together to transform the DHN and EDN according to the heat transition and electricity network expansion goals.

5.4 Evaluation of Methodology & Limitations

5.4.1 DHN model

The new South-Holland DHN model represents a significant step forward in modelling its operation. The model effectively utilizes the open-source PyPSA library, allowing the user to define the variables, constraints, the objective function and scenario assumptions more intuitively, without the need to hard-code the optimisation model extensively. The performed case-study focused on addressing the operational side of the network, however the research conducted with the model could be extended to address network planning, assessment of future investments or sensitivity analysis. This inherent flexibility with PyPSA makes the model a valuable tool for the heat network operators that seek to investigate various decarbonisation pathways.

Nevertheless, the DHN model remains subdued to several limitations that affect its operational dynamics and lower its ability to achieve real-world operation conditions. Firstly, coherent input data regarding the attributes of heat production, storage and distribution pipelines is missing, leading to many simplifications. For example, only the CHP units have fixed start-up costs, making them the only unit-committable components. It results in all other heat generation units operating purely on marginal cost dispatch without cycling constraints. This reduces the operational realism of heat supply technologies that are typically not flexible, such as WI, biomass and gas boiler plants. Moreover, PyPSA introduces the ability to include many other attributes, such as stand-by costs, ramp-up and ramp-down times, shut-down costs and many others, without which the variability of heat dispatch is exaggerated in heat supply and storage units.

Moreover, some components have operational constraints, which greatly simplifies their behaviour or affects the network-wide operation. For instance, only a single heat distribution pipe connecting the Rotterdam WI plant to The Hague has assigned seasonal marginal costs of heat transfer. This results in the vast majority heat produced by the WI plant (99% of it) to be dispatched to Rotterdam, as heat transfer to The Hague is not optimal by cost. All other heat distribution pipes have zero marginal cost of heat transfer, which likely results in over-utilisation of certain heat pipes. In addition, the WI and biomass heat production units do not

have a defined CO_2factor, which does not associate them with the carbon price market. Moreover, the IWH1 unit operates with a fixed maximum annual heat production limit in each scenario, resulting in curtailment of heat production. With regard to IWH units, an alternative approach could have been selected to model them as electrified heat source units (same as HP or geothermal units) with a variable COP value, allowing the IWH to be dispatched based on price and efficiency competition with other electrified units. This was not done, assuming that IWH units have a waste heat source with a stable temperature. In terms of storage, only TTES type is considered, while long-term storage options are not specifically model.

5.4.2 EDN model

The introduction of the corresponding EDN in South-Holland is also a significant step in analysing the integrated operation of heat and electricity networks. Nevertheless, the model also hold a few limiting factors that lower the realistic representation and operation of the network. At first, the EDN model cannot be validated, as no equivalent model of the EDN exists. Moreover, the 380 kV external grid component is the only voltage regulating source, modelled as a slack bus, and no other voltage regulation is applied in the downstream network, which in some simulations results in bus voltages that exceed the safety margins. The external grid supplies power to the two main branches: one in The Hague and one in Rotterdam. In The Hague, the 150/25 kV transformers form a loop, which accurately reflects the real-world topology. In Rotterdam, the substations supplying electrified heat sources are more dispersed. Moreover, there are multiple substations and lines that located The Hague and Rotterdam, that connect the two areas and are not included in the model, for example, in Delft or Rotterdam West. This simplification limits the full representation of the South-Holland DHN and only takes the parts of it that connects to the electrified heat sources. Therefore, the model represents a conceptual network structure that approximates the real network topology. Overall, the simplified voltage control, network spatial generalisation are the factors that should be considered when interpreting the results.

5.4.3 Scenarios

The future scenarios were structured based on price, temperature, heat and electricity demand projection for 2030, 2040 and 2050. The future scenarios are of deterministic nature, rely on fixed assumptions and do not include uncertainty or stochastic variation in the simulations. Only heat demand is simulated with low and high assumptions, meaning that the results from integrated models reflect only a narrow range of possible conditions. Moreover, all time-dependant price data was scaled from the historic data of 2020 scenario, while heat demand was scaled based on 2022, which was a relatively mild year. As a result, scaling the 2022 data to represent high or low demand scenarios can underestimating potential peak load conditions in colder years. Still, with the use of low and high demand scenarios, the operational tendencies are covered in detailed.

With regard to the network expansion of the DHN, it is yet unclear whether all proposed additional heat production sources and storage units will be implemented in the future. Even if these units are eventually implemented, the infrastructure build-up timeline remains unclear. This study leans heavily on the fact that the electrified heat production units will become operational at once, as the primary goal was to determine their interactions with the EDN. However, this assumption brings uncertainty with regard to the real-world network development plans and their projected timing. If the integration of these units experience delays, are scaled down or are not implemented at all, the necessity of EDN infrastructure expansion and reinforcements to accompany the DHN demand may be significantly reduced or postponed.

6 | Conclusion

This Chapter provides the final conclusions of the research. In addition, the recommendations for further research are provided.

6.1 Conclusion

This master thesis studied the decarbonisation of the South-Holland DHN through direct electrification and evaluated its impact on the EDN. This goal was achieved by developing integrated heat and electricity models: an operational optimisation model of Eneco South-Holland DHN and a PFA model of Stedin EDN. To improve the accuracy and the usability of the DHN model, it was implemented with an open-source energy systems modelling tool PyPSA, while also included new attributes, such as seasonal heating schedules and coefficient of performance (COP) calculations for heat pumps (HPs) and geothermal systems. The corresponding EDN model was constructed with the pandapower library to represent a realistic distribution network, which is capable of supplying power to the electrified heat generation units and local loads. In the South-Holland case study, it was shown how these models can be applied to determine the operation of the future networks for the years 2030, 2040 and 2050, and to measure the impact of heat supply electrification on both heat and electricity networks. The constructed case study explored future scenarios by incorporating variable hourly data projections, including electricity, natural gas and CO_2 prices, air and ground temperatures, as well as projected heat and electricity demand.

Future scenarios demonstrated that electrified heat sources have the potential to produce a major part of the total heat supply, but that will also require high amounts of electrical energy to be supplied by EDN. The inclusion of TES sources alongside electrified heat supply units was identified as essential helping to lower the impact of electricity market variability and enabling higher utilisation of electrified heat sources. In addition, the case study demonstrated how the future EDN will face increased electricity demand and operational complexity, which will require strategically planned grid reinforcements to maintain reliable supply and to accommodate electrified heat production units and future increase in distributed energy generation. Overall, the creation of the integrated heat and electricity models in this study enables network operators to evaluate both networks in an integrated manner. The joint operational and infrastructure planning with shared and established technical priorities is highlighted. The results of this research can provide valuable insights to the decision makers at Eneco and Stedin, helping to coordinate operational strategy and formulate investment plans, as both networks are bound to pass through the energy transition and decarbonisation efforts.

6.2 Recommendations

- The future research should apply the capabilities introduced by PyPSA and pandapower, which allow to include extensive details with regard to network component operation attributes and fixed parameters. As mentioned before, only the CHPs have assigned start-up costs in the DHN model, while other units should also have this data included. Therefore, with the help of the professional from Eneco and Stedin, the current input data of network component parameters should be improved to achieve a more realistic representation of network operation.
- It this study, the unidirectional structure of the South-Holland DHN was found to constrain the heat dispatch and the utilisation rate of certain heat production and storage units. Future studies should investigate the feasibility and benefits of expanding the South-Holland DHN to a multi-directional network. Moreover, the comparison could be made between the relocation of the planned heat production and storage assets of the future to improve their operational flexibility and utilization rates.

- In the DHN model of South-Holland, the integration of large-scale electrified heating sources was the main focus. However, the impact of decentralised and smaller-scale heating and cooling units could be investigated in the future research. How would the integration of large number of electrified heat and cooling sources on a building level affect the flexibility and robustness of the distribution network should be further analysed.
- With regard to the EDN, the current model is limited by the geographical scope and voltage control functionality. The future model could be expanded to include more substations in the region (for example, Delft, Rotterdam West) to simulate the interconnections between Rotterdam and The Hague, which will increase model complexity, but could yield more accurate results that represent the real-world operation of the network. Moreover, implementing more realistic voltage control mechanisms in the EDN model, such as tap changers or local voltage regulators, would greatly enhance the model.
- In this study, a manual reinforcement methodology of the EDN was used. This approach could be improved through automating this approach, instead of relying on a step-wise approach, which is prone to human error. Maximum transformer and line loading levels could be identified to add reinforcements for the next simulation. Moreover, the validation of the EDN model remains an important step, which was not achieved in this thesis. Collaborating with network operators to acquire real-world operational data for comparison would enhance the credibility of the model and make it a more reliable tool for decision makers.
- The future DHN and EDN of South-Holland model development could benefit from incorporating other integrated energy systems beyond heat and electricity. Rotterdam Port is emerging as a key hub of the hydrogen economy. The integration of hydrogen production facilities and waste heat recovery systems could be investigated, as electrolysers will demand large amounts of electrical power supply from the EDN, while waste heat could be collected and distributed in the DHN. This would contribute to a more holistic view of the network operation and planning of the South-Holland region.
- With regard to the uncertainty introduced by deterministic scenarios, future research could utilise stochastic modelling approaches, which account for variability in weather, prices (natural gas, CO_2 and electricity) and future energy demand data. With this approach the robustness of the two network models could be investigated in more detail, which could improve the operational and investment strategies of the future networks.

Bibliography

[1] K. Kavvadias, N. J. P. Jimenez, and G. Thomassen, *Decarbonising the EU heating sector: Integration of the power and heating sector*, ISBN: 9789276083863 9789276083870 9789276141570 ISSN: 1831-9424, 1018-5593, 2019. DOI: 10.2760/943257. [Online]. Available: https://publications.jrc.ec.europa.eu/repository/handle/JRC114758.

[2] *The Netherlands 2020 – Analysis*, Sep. 2020. [Online]. Available: https://www.iea.org/reports/the-netherlands-2020.

[3] *StatLine - Homes; main heating installations, region*. [Online]. Available: https://opendata.cbs.nl/statline/#/CBS/nl/dataset/84948NED/table?dl=5E88B.

[4] M. v. B. Z. e. Koninkrijksrelaties, *Warmtewet*, wet, Last Modified: 2024-12-03. [Online]. Available: https://wetten.overheid.nl/BWBR0033729/2024-01-01#Hoofdstuk2.

[5] Directorate-General for Energy (European Commission), Fraunhofer ISI, Institute for Resource Efficiency and Energy Strategies GmbH, *et al.*, *District heating and cooling in the European Union: overview of markets and regulatory frameworks under the revised Renewable Energy Directive*, eng. Publications Office of the European Union, 2022, ISBN: 978-92-76-52343-7. [Online]. Available: https://data.europa.eu/doi/10.2833/962525.

[6] X. Malcher and M. Gonzalez-Salazar, "Strategies for decarbonizing European district heating: Evaluation of their effectiveness in Sweden, France, Germany, and Poland," *Energy*, vol. 306, p. 132 457, Oct. 2024, ISSN: 0360-5442. DOI: 10.1016/j.energy.2024.132457. [Online]. Available: https://www.sciencedirect.com/science/article/pii/S036054422402231X.

[7] P. Sorknæs, "Hybrid energy networks and electrification of district heating under different energy system conditions," *Energy Reports*, The 17th International Symposium on District Heating and Cooling, vol. 7, pp. 222–236, Oct. 2021, ISSN: 2352-4847. DOI: 10.1016/j.egyr.2021.08.152. [Online]. Available: https://www.sciencedirect.com/science/article/pii/S2352484721007563.

[8] *Net Zero by 2050 – Analysis*, May 2021. [Online]. Available: https://www.iea.org/reports/net-zero-by-2050.

[9] W. Liu, F. Best, and W. Crijns-Graus, "Exploring the pathways towards a sustainable heating system – A case study of Utrecht in the Netherlands," *Journal of Cleaner Production*, vol. 280, p. 125 036, Jan. 2021, ISSN: 0959-6526. DOI: 10.1016/j.jclepro.2020.125036. [Online]. Available: https://www.sciencedirect.com/science/article/pii/S0959652620350800.

[10] M. v. E. Z. e. Klimaat, *Probleemanalyse Congestie in het laagspanningsnet - Rapport - Rijksoverheid.nl*, rapport, Last Modified: 2024-01-22T10:35 Publisher: Ministerie van Algemene Zaken, Jan. 2024. [Online]. Available: https://www.rijksoverheid.nl/documenten/rapporten/2024/01/22/bijlage-2-probleemanalyse-congestie-in-het-laagspanningsnet.

[11] *DEMOSES*. [Online]. Available: https://www.tudelft.nl/ewi/over-de-faculteit/afdelingen/electrical-sustainable-energy/intelligent-electrical-power-grids-iepg-group/projects/current-projects/demoses.

[12] *The natural gas phase-out in the Netherlands*. [Online]. Available: https://cedelft.eu/publications/the-natural-gas-phase-out-in-the-netherlands/.

[13] M. v. E. Z. e. Klimaat, *National Climate Agreement - The Netherlands - Publicatie - Klimaatakkoord*, publicatie, Last Modified: 2019-08-28T10:42 Publisher: Ministerie van Economische Zaken en Klimaat, Jun. 2019. [Online]. Available: https://www.klimaatakkoord.nl/documenten/publicaties/2019/06/28/national-climate-agreement-the-netherlands.

[14] H. Ng, *From third to fourth generation district heating in Leeuwarden : An exploration of feasibility and risks*, info:eu-repo/semantics/masterThesis, Publisher: University of Twente, Aug. 2019. [Online]. Available: https://essay.utwente.nl/79496/?utm_source=chatgpt.com.

[15] H. Lund, S. Werner, R. Wiltshire, *et al.*, "4th Generation District Heating (4GDH): Integrating smart thermal grids into future sustainable energy systems," *Energy*, vol. 68, pp. 1–11, Apr. 2014, ISSN: 0360-5442. DOI: 10.1016/j.energy.2014.02.089. [Online]. Available: https://www.sciencedirect.com/science/article/pii/S0360544214002369.

[16] H. Böhm, S. Moser, S. Puschnigg, and A. Zauner, "Power-to-hydrogen & district heating: Technology-based and infrastructure-oriented analysis of (future) sector coupling potentials," *International Journal of Hydrogen Energy*, vol. 46, no. 63, pp. 31 938–31 951, Sep. 2021, ISSN: 0360-3199. DOI: 10.1016/j.ijhydene.2021.06.233. [Online]. Available: https://www.sciencedirect.com/science/article/pii/S0360319921025477.

[17] S. S. Harmsen, "Optimal Distribution Network Planning in an Integrated Energy System," 2021. [Online]. Available: https://repository.tudelft.nl/record/uuid:9528878a-40d0-4782-b0cb-4868dcc8d06c.

[18] L. a. H. Vergroesen, "Optimisation of an integrated energy system consisting of a power grid and carbon neutral heat grid," 2024. [Online]. Available: https://repository.tudelft.nl/record/uuid:bf4b18d8-6dbd-433b-9bc4-78b603cdb353.

[19] *No extra space on electricity grid in large part of Noord-Holland next decade*. [Online]. Available: https://www.tennet.eu/news/no-extra-space-electricity-grid-large-part-noord-holland-next-decade.

[20] *Alliander: 'Nog zeker tien jaar file op stroomnet, duizenden technici uit buitenland nodig' | Financieel | Telegraaf.nl*, Mar. 2024. [Online]. Available: https://www.telegraaf.nl/financieel/939560999/alliander-nog-zeker-tien-jaar-file-op-stroomnet-duizenden-technici-uit-buitenland-nodig.

[21] *Capaciteitskaart invoeding elektriciteitsnet*. [Online]. Available: https://capaciteitskaart.netbeheernederland.nl.

[22] E. de Winkel, Z. Lukszo, M. Neerincx, and R. Dobbe, "Adapting to limited grid capacity: Perceptions of injustice emerging from grid congestion in the Netherlands," *Energy Research & Social Science*, vol. 122, p. 103 962, Apr. 2025, ISSN: 2214-6296. DOI: 10.1016/j.erss.2025.103962. [Online]. Available: https://www.sciencedirect.com/science/article/pii/S221462962500043X.

[23] G. Alva, Y. Lin, and G. Fang, "An overview of thermal energy storage systems," *Energy*, vol. 144, pp. 341–378, Feb. 2018, ISSN: 0360-5442. DOI: 10.1016/j.energy.2017.12.037. [Online]. Available: https://www.sciencedirect.com/science/article/pii/S036054421732056X.

[24] J. Mitali, S. Dhinakaran, and A. A. Mohamad, "Energy storage systems: A review," *Energy Storage and Saving*, vol. 1, no. 3, pp. 166–216, Sep. 2022, ISSN: 2772-6835. DOI: 10.1016/j.enss.2022.07.002. [Online]. Available: https://www.sciencedirect.com/science/article/pii/S277268352200022X.

[25] E. Guelpa and V. Verda, "Thermal energy storage in district heating and cooling systems: A review," *Applied Energy*, vol. 252, p. 113 474, Oct. 2019, ISSN: 0306-2619. DOI: 10.1016/j.apenergy.2019.113474. [Online]. Available: https://www.sciencedirect.com/science/article/pii/S0306261919311481.

[26] D. W. van Helden, *Large Thermal Energy Storages for District Heating*. [Online]. Available: https://iea-es.org/task-39/.

[27] *Home batteries drive Dutch energy storage installations*, Oct. 2024. [Online]. Available: https://innovationorigins.com/en/home-batteries-drive-dutch-energy-storage-installations/.

[28] C. K. Das, O. Bass, G. Kothapalli, T. S. Mahmoud, and D. Habibi, "Overview of energy storage systems in distribution networks: Placement, sizing, operation, and power quality," *Renewable and Sustainable Energy Reviews*, vol. 91, pp. 1205–1230, Aug. 2018, ISSN: 1364-0321. DOI: 10.1016/j.rser.2018.03.068. [Online]. Available: https://www.sciencedirect.com/science/article/pii/S1364032118301606.

[29] *Services to Support Distribution Infrastructure*, Aug. 2021. [Online]. Available: https://www.energystoragenl.nl/wp-content/uploads/2025/01/Diensten-ter-ondersteuning-distributie-infrastructuur.pdf.

[30] *Solar and storage synergies for a sustainable future Dutch PV and energy storage technology*, Apr. 2024. [Online]. Available: https://www.rvo.nl/sites/default/files/2024-07/Solar%20Energy%20Storage%20Guide%202024_0.pdf.

[31] R. Jing, Y. Zhou, and J. Wu, "Integrated energy system," in *Encyclopedia of Electrical and Electronic Power Engineering*, J. García, Ed., Oxford: Elsevier, Jan. 2023, pp. 165–176, ISBN: 978-0-12-823211-8. DOI: 10.1016/B978-0-12-821204-2.00138-0. [Online]. Available: https://www.sciencedirect.com/science/article/pii/B9780128212042001380.

[32] M. Abeyseker, J. Wu, and N. Jenkins, "Integrated energy systems: An overview of benefits, analysis, research gaps and opportunities," Hubnet Position Paper Series, 2016.

[33] E. Guelpa, A. Bischi, V. Verda, M. Chertkov, and H. Lund, "Towards future infrastructures for sustainable multi-energy systems: A review," *Energy*, Shaping research in gas-, heat- and electric- energy infrastructures, vol. 184, pp. 2–21, Oct. 2019, ISSN: 0360-5442. DOI: 10.1016/j.energy.2019.05.057. [Online]. Available: https://www.sciencedirect.com/science/article/pii/S0360544219309260.

[34] J. Ramsebner, R. Haas, A. Ajanovic, and M. Wietschel, "The sector coupling concept: A critical review," *WIREs Energy and Environment*, vol. 10, no. 4, 2021, ISSN: 2041-840X. DOI: 10.1002/wene.396.

[35] *Energy Systems Integration | Research Subjects | Department TFE*. [Online]. Available: https://www.utwente.nl/en/et/tfe/research-chairs/te/research/research/Energy_Systems_Integration/.

[36] Q. Wu, J. Tan, X. Jin, M. Zhang, and A. Turk, "Chapter 1 - Introduction of integrated energy systems," in *Optimal Operation of Integrated Multi-Energy Systems Under Uncertainty*, Q. Wu, J. Tan, X. Jin, M. Zhang, and A. Turk, Eds., Elsevier, Jan. 2022, pp. 1–16, ISBN: 978-0-12-824114-1. DOI: 10.1016/B978-0-12-824114-1.00006-8. [Online]. Available: https://www.sciencedirect.com/science/article/pii/B9780128241141000068.

[37] R. Geyer, D. Hangartner, M. Lindahl, and S. V. Pedersen, *Heat Pumps in District Heating and Cooling Systems*, Apr. 2020. [Online]. Available: https://heatpumpingtechnologies.org/annex47/final-report-for-hpt-tcp-annex-47-heat-pumps-in-district-heating-and-cooling-systems/.

[38] Z. Pan, Q. Guo, and H. Sun, "Interactions of district electricity and heating systems considering time-scale characteristics based on quasi-steady multi-energy flow," *Applied Energy*, vol. 167, pp. 230–243, Apr. 2016, ISSN: 0306-2619. DOI: 10.1016/j.apenergy.2015.10.095. [Online]. Available: https://www.sciencedirect.com/science/article/pii/S0306261915013227.

[39] X. Liu, J. Wu, N. Jenkins, and A. Bagdanavicius, "Combined analysis of electricity and heat networks," *Applied Energy*, vol. 162, pp. 1238–1250, Jan. 2016, ISSN: 0306-2619. DOI: 10.1016/j.apenergy.2015.01.102. [Online]. Available: https://www.sciencedirect.com/science/article/pii/S0306261915001385.

[40] K. Kavvadias, G. Thomassen, M. Pavičević, and S. Quoilin, "Electrifying the heating sector in Europe: The impact on the power sector," *Proceedings of the 32nd International Conference on Efficiency, Cost, Optimization, Simulation and Environmental Impact of Energy Systems*, 2019.

[41] C. Magni, S. Quoilin, and A. Arteconi, "Evaluating the Potential Contribution of District Heating to the Flexibility of the Future Italian Power System," *Energies*, vol. 15, no. 2, p. 584, Jan. 2022, Number: 2 Publisher: Multidisciplinary Digital Publishing Institute, ISSN: 1996-1073. DOI: 10.3390/en15020584. [Online]. Available: https://www.mdpi.com/1996-1073/15/2/584.

[42] T. Brown, D. Schlachtberger, A. Kies, S. Schramm, and M. Greiner, "Synergies of sector coupling and transmission reinforcement in a cost-optimised, highly renewable European energy system," *Energy*, vol. 160, pp. 720–739, Oct. 2018, ISSN: 0360-5442. DOI: 10.1016/j.energy.2018.06.222. [Online]. Available: https://www.sciencedirect.com/science/article/pii/S036054421831288X.

[43] N. Javanshir, S. Syri, S. Tervo, and A. Rosin, "Operation of district heat network in electricity and balancing markets with the power-to-heat sector coupling," *Energy*, vol. 266, p. 126 423, Mar. 2023, ISSN: 0360-5442. DOI: 10.1016/j.energy.2022.126423. [Online]. Available: https://www.sciencedirect.com/science/article/pii/S0360544222033096.

[44] P. Friedrich, T. Huynh, and S. Niessen, "Optimizing district heating operations: Network modeling and its implications on system efficiency and operation," *Smart Energy*, vol. 18, p. 100 175, May 2025, ISSN: 2666-9552. DOI: 10.1016/j.segy.2025.100175. [Online]. Available: https://www.sciencedirect.com/science/article/pii/S2666955225000036.

[45] T. Brown, J. Hörsch, and D. Schlachtberger, "PyPSA: Python for Power System Analysis," *Journal of Open Research Software*, 2018. DOI: 10.5334/jors.188.

[46] T. Brown, J. Hoersch, F. Neumann, M. Victoria, and L. Zeyen, *PyPSA-Eur Documentation*, 2025. [Online]. Available: https://pypsa-eur.readthedocs.io/en/latest/supply_demand.html.

[47] L. Thurner, A. Scheidler, F. Schafer, *et al.*, "Pandapower—An Open-Source Python Tool for Convenient Modeling, Analysis, and Optimization of Electric Power Systems," *IEEE Transactions on Power Systems*, vol. 33, no. 6, pp. 6510–6521, Nov. 2018, ISSN: 0885-8950, 1558-0679. DOI: 10.1109/TPWRS.2018.2829021. [Online]. Available: https://ieeexplore.ieee.org/document/8344496/.

[48] E. M. Colussi, "An integrated modeling approach to provide flexibility and sustainability to the district heating system in South-Holland, the Netherlands," 2024. [Online]. Available: https://repository.tudelft.nl/record/uuid:d2edc481-9acd-41c3-877a-5ea0838d88c0.

[49] *Warmte voor de toekomst*, Mar. 2025. [Online]. Available: https://www.warmtelinq.nl/.

[50] *Warmtesysteem Noord Rotterdam*. [Online]. Available: https://warmtenetwerk.nl/warmteproject/warmtesysteem-noord-rotterdam/.

[51] *Industry hook-up for the Rotterdam heat grid*. [Online]. Available: https://cedelft.eu/publications/industry-hook-up-for-the-rotterdam-heat-grid/.

[52] *The Hague city plant | Uniper*. [Online]. Available: https://www.uniper.energy/netherlands/power-plants-in-the-netherlands/hague.

[53] A. A. Hagberg, D. A. Schult, and P. J. Swart, "Exploring Network Structure, Dynamics, and Function using NetworkX," Pasadena, California, Jun. 2008, pp. 11–15. DOI: 10.25080/TCWV9851. [Online]. Available: https://doi.curvenote.com/10.25080/TCWV9851.

[54] W. E. Hart, J.-P. Watson, and D. L. Woodruff, "Pyomo: Modeling and solving mathematical programs in Python," en, *Mathematical Programming Computation*, vol. 3, no. 3, pp. 219–260, Sep. 2011, ISSN: 1867-2949, 1867-2957. DOI: 10.1007/s12532-011-0026-8. [Online]. Available: http://link.springer.com/10.1007/s12532-011-0026-8.

[55] T. Brown, J. Hörsch, F. Hofmann, *et al.*, *PyPSA: Python for Power System Analysis*, Apr. 2025. DOI: 10.5281/ZENODO.3946412. [Online]. Available: https://zenodo.org/doi/10.5281/zenodo.3946412.

[56] *HoogspanningsNet Netkaart*. [Online]. Available: https://webkaart.hoogspanningsnet.com/index2.php#14/52.0619/4.3229.

[57] J. Grainger and W. D. Stevenson, *Power System Analysis*. McGraw-Hill Education, 1994, Google-Books-ID: NBIoAQAAMAAJ, ISBN: 978-0-07-061293-8.

[58] *What is the maximum load capacity of a transformer?* [Online]. Available: https://www.ztelecgroup.com/zt-technical-article/767.html.

[59] linkec.cn, *Ultimate 500 kva Transformer For Guide | Daelim Transformer*. [Online]. Available: https://www.daelimtransformer.com/500-kva-transformer.html.

[60] J. Hörsch, F. Hofmann, D. Schlachtberger, and T. Brown, "PyPSA-Eur: An open optimisation model of the European transmission system," *Energy Strategy Reviews*, vol. 22, pp. 207–215, Nov. 2018, ISSN: 2211-467X. DOI: 10.1016/j.esr.2018.08.012. [Online]. Available: https://www.sciencedirect.com/science/article/pii/S2211467X18300804.

[61] A. P. Jansen, "Forecasting the space heating demand of Dutch households," Sep. 2020. [Online]. Available: https://thesis.eur.nl/pub/52814.

[62] *Hour values of weather stations*. [Online]. Available: https://www.daggegevens.knmi.nl/klimatologie/uurgegevens.

[63] *Soil temperatures - temperatures at various depths at a 10 minute interval - KNMI Data Platform*. [Online]. Available: https://dataplatform.knmi.nl/dataset/bodemtemperaturen-1-0.

[64] Directorate-General for Climate Action (European Commission), Directorate-General for Energy (European Commission), Directorate-General for Mobility and Transport (European Commission), *et al.*, *EU reference scenario 2020: energy, transport and GHG emissions : trends to 2050*. Publications Office of the European Union, 2021, ISBN: 978-92-76-39356-6. [Online]. Available: https://data.europa.eu/doi/10.2833/35750.

[65] A. Schmitt, *EU Energy Outlook 2050: How will the European electricity market develop over the next 30 years?* Apr. 2022. [Online]. Available: https://blog.energybrainpool.com/en/eu-energy-outlook-2050-how-will-the-european-electricity-market-develop-over-the-next-30-years/.

[66] I. Sifnaios, D. M. Sneum, A. R. Jensen, J. Fan, and R. Bramstoft, "The impact of large-scale thermal energy storage in the energy system," *Applied Energy*, vol. 349, p. 121 663, Nov. 2023, ISSN: 0306-2619. DOI: 10.1016/j.apenergy.2023.121663. [Online]. Available: https://www.sciencedirect.com/science/article/pii/S0306261923010279.

[67] *International Biomass Exchange | BALTPOOL*, May 2022. [Online]. Available: https://www.baltpool.eu/en/home-page/.

[68] E. van der Roest, R. Bol, T. Fens, and A. van Wijk, "Utilisation of waste heat from PEM electrolysers – Unlocking local optimisation," *International Journal of Hydrogen Energy*, vol. 48, no. 72, pp. 27 872–27 891, Aug. 2023, ISSN: 0360-3199. DOI: 10.1016/j.ijhydene.2023.03.374. [Online]. Available: https://www.sciencedirect.com/science/article/pii/S0360319923015410.

[69] M. de Leeuw and R. Koelemeijer, "Decarbonisation options for the Dutch waste incineration industry," *Manufacturing Industry Decarbonisation Data Exchange Network*, Jul. 2022. [Online]. Available: https://www.pbl.nl/sites/default/files/downloads/pbl-2022-decarbonisation-options-for-the-dutch-waste-incineration-industry-4916.pdf.

[70] E. Comission, *Costs for Municipal Waste Management in the EU*. [Online]. Available: https://ec.europa.eu/environment/pdf/waste/studies/euwastemanagement_annexes.pdf.

[71] C. Bang, A. Vitina, Jay Sterling Gregg, and Hans Henrik Lindboe, "Analysis of biomass prices," *Ea Energy Analyses*, Jun. 2013. [Online]. Available: https://www.ea-energianalyse.dk/wp-content/uploads/2020/02/1280_analysis_of_biomass_prices.pdf.

[72] Market Research Future, *Waste Heat To Power Market Size, Growth, Trends Report 2032*. [Online]. Available: https://www.marketresearchfuture.com/reports/waste-heat-to-power-market-23001.

[73] C. Jongsma, J. Dehens, M. Nauta, and T. Scholten, *Power-to-Heat en warmteopslag in warmtenetten*, NL. [Online]. Available: https://ce.nl/publicaties/power-to-heat-en-warmteopslag-in-warmtenetten/.

[74] K. Calvin, D. Dasgupta, G. Krinner, *et al.*, "IPCC, 2023: Climate Change 2023: Synthesis Report. Contribution of Working Groups I, II and III to the Sixth Assessment Report of the Intergovernmental Panel on Climate Change [Core Writing Team, H. Lee and J. Romero (eds.)]. IPCC, Geneva, Switzerland.," Intergovernmental Panel on Climate Change (IPCC), Tech. Rep., Jul. 2023, Edition: First. DOI: 10.59327/IPCC/AR6-9789291691647. [Online]. Available: https://www.ipcc.ch/report/ar6/syr/.

Appendices

A Model configuration

Old model	New Model	Modelled as
AVR	W1	Link
WBR	IWH1	Generator
SNR	IWH2	Generator
GasDV	RDAM Gas1	Link
GasWSG	RDAM Gas2	Link
GasAC	RDAM Gas3	Link
RoCa-ketel	RDAM Gas4	Link
RoCa1	RDAM CHP1	Link
RoCa2	RDAM CHP2	Link
RoCa3	RDAM CHP3	Link
Heatpump RDAM	RDAM HP	Link
Geothermal RDAM	RDAM Geo	Link
Rotterdam	Rotterdam	Load
Rotterdam RoCa	Rotterdam RoCa	Load
STEG1	DH CHP1	Link
STEG2	DH CHP2	Link
GasBezuidenhout	DH Gas1	Link
GasAdh	DH Gas2	Link
Gas-CR	DH Gas3	Link
GeoHAL	DH Geo1	Link
Geothermal DH1	DH Geo2	Link
Geothermal DH2	DH Geo3	Link
Geothermal DH3	DH Geo4	Link
Heatpump DH	DH HP	Link
E-boiler DH	DH EB	Link
Den Haag	Den Haag	Load
TBM	Biomass	Generator
Geothermal B3hoek	Tuinders Geo	Link
Tuinders	Tuinders	Load

Table 1: DHN model heat supply units

Old model	New Model	Modelled as
Rotterdam-buffer	RDAM1 Storage1	Storage unit
Storage RDAM	RDAM1 Storage2	Storage unit
RoCa-buffer	RDAM2 Storage	Storage unit
CR-buffer	DH Storage1	Storage unit
Storage DH	DH Storage2	Storage unit
Tuinders-buffer	Tuinders Storage	Storage unit
Storage B3hoek	B-Triangle Storage	Storage unit

Table 2: DHN model heat storage units

Name	From bus	To bus	P_{nom}, MW	Efficiency	Bidirectional
Pipe 1	Bus_CR_plein	Bus_DenHaag	EXT	0.98	No
Pipe 2	Bus_WLQ	Bus_CR_plein	EXT	0.947	No
Pipe 3	Bus_Point_V	Bus_WLQ	75	0.947	No
Pipe 4	Bus_W1_DH	Bus_Point_V	100	0.98	No
Pipe 5	Bus_Point_V	Bus_LoN	160	0.975	No
Pipe 6	Bus_W1_RDAM	Bus_LoN	EXT	0.98	No
Pipe 7	Bus_LoN	Bus_Rotterdam1	160	0.975	No
Pipe 8	Bus_Rotterdam1	Bus_Boszoom	60	0.98	No
Pipe 9	Bus_Boszoom	Bus_To_Tuinders	25	0.98	No
Pipe 10	Bus_To_Tuinders	Bus_Tuinders	EXT	0.97	Yes
Pipe 11	Bus_To_Tuinders	Bus_B_Triangle	EXT	0.98	Yes
Pipe 12	Bus_Boszoom	Bus_Rotterdam2	EXT	0.98	No
Pipe 13	Bus_RoCa	Bus_To_Tuinders	250	0.97	No
Pipe 14	Bus_RoCa	Bus_Rotterdam2	EXT	0.98	No
Pipe 15	Bus_RoCa	Bus_Rotterdam1	25	0.98	No

Table 3: DHN model heat transfer pipelines, modelled as links

Name	**Purpose**	**Modelled as**
ExternalGrid	Feeds power to links (geothermal, EB and HPs)	Generator
Waste_supply	Acts as waste fuel source for waste incineration plant	Store
Gas_supply	Acts as waste fuel source for links (CHPs and gas boilers)	Store
RDAM_CHP1_heat_sink	Heat sink[1]	Store
RDAM_CHP2_heat_sink	Heat sink[1]	Store
RDAM_CHP3_heat_sink	Heat sink[1]	Store
IWH2_heat_sink	Heat sink[2]	Store
W1_heat_sink	Heat sink[2]	Store
Electricity_sink	Acts as external grid where power is fed to	Store
LinkBus_RDAM_CHP1	Heat sink bus	Bus
LinkBus_RDAM_CHP2	Heat sink bus	Bus
LinkBus_RDAM_CHP3	Heat sink bus	Bus
LinkBus_IWH2	Heat sink bus	Bus
LinkBus_W1	Heat sink bus	Bus
RDAM_CHP1_output	Heat supply controller[3]	Link
RDAM_CHP2_output	Heat supply controller[3]	Link
RDAM_CHP3_output	Heat supply controller[3]	Link
IWH2_output	Heat supply controller[3]	Link
W1_RDAM_output	Heat supply controller[4]	Link
W1_DH_output	Heat supply controller[4]	Link

[1] used when electricity can be produced due to low prices, but heat demand is very low
[2] used for generated heat when heat demand is very low
[3] used to supply the fraction of heat that does not go into the heat sink
[4] used to control the maximum allowable heat supply to Den Haag and Rotterdam

Table 4: DHN model auxiliary components

Name	CO_2 factor (t/MW)
DH Gas1	0.2300
DH Gas2	0.2280
DH Gas3	0.2267
DH CHP1	0.4725
DH CHP2	0.4725
RDAM Gas1	0.2325
RDAM Gas2	0.2280
RDAM Gas3	0.2347
RDAM Gas4	0.2329
RDAM CHP1	0.2265
RDAM CHP2	0.2265
RDAM CHP3	0.4500

Table 5: CO_2 factor of gas-consuming heat supply sources

Name	Standard Type	Length (km)
150kV_Waterningen_Rijskwijk(1&2)	150kV CS 500mm2	3.34
150kV_sGravenhage_Rijskwijk	150kV CS 500mm2	1.5
150kV_sGravenhage_Voorburg	150kV CS 500mm2	5.96
150kV_Voorburg_Waterningen	150kV CS 500mm2	11.56
150kV_Krimpen_Ommoord(1)	150kV CS 500mm2	11.9
150kV_Krimpen_Ommoord(2)	150kV CS 500mm2	11.61
150kV_Krimpen_Zuidwijk	150kV CS 500mm2	11.33
25kV_Substation_A_Trafo_A(1)	25kV CS 240mm2	4.29
25kV_Substation_A_Trafo_A(2&3)	25kV CS 240mm2	4.12
25kV_Substation_A_Trafo_A(4)	25kV CS 240mm2	4.08
25kV_DH_CHP_Cables	25kV CS 630mm2	0.1
25kV_Substation_B_DH_HP	25kV CS 240mm2	2.4
25kV_Substation_B_DH_EB	25kV CS 240mm2	0.1
25kV_Substation_C_Trafo_C1	25kV CS 240mm2	6.92
25kV_Substation_C_Trafo_C3(1)	25kV CS 240mm2	4.51
25kV_Substation_C_Trafo_C3(2)	25kV CS 240mm2	4.36
25kV_Substation_E_Trafo_E2(1&2)	25kV CS 240mm2	8.0
25kV_Substation_E_Substation_D(1&2)	25kV CS 240mm2	2.77
23kV_Substation_F_RDAM_HP	23kV CS 240mm2	3.0
10kV_Trafo_A_DH_Geo3	10kV CS 150mm2	1.5
10kV_Trafo_B_DH_Geo2	10kV CS 150mm2	0.1
10kV_Trafo_C2_DH_Geo4	10kV CS 150mm2	2.0
10kV_Trafo_C3_DH_Geo1	10kV CS 150mm2	1.5
10kV_Trafo_E1_RDAM_Geo	10kV CS 150mm2	0.5
10kV_Trafo_E2_Tuinders_Geo	10kV CS 150mm2	1.5

Table 6: Full EDN model line components

Name	Standard Type	Rated apparent power (MVA)
Waterningen	380/150 kV	500
Krimpen	380/150 kV	500
Rijswijk	150/25 kV	115
s'Gravenhage	150/25 kV	115
Voorburg	150/25 kV	115
Ommoord	150/25 kV	115
Zuidwijk	150/23 kV	110
Trafo_C1	25/23 kV	40
Trafo_E2	25/10 kV	30
Trafo_C3	25/10 kV	30
Trafo_A	25/10 kV	30
Trafo_B	25/10 kV	30
Trafo_E1	25/10 kV	30
Trafo_C2	23/10 kV	80

Table 7: Full EDN model transformer components

Standard Type	*Rough Cost (€/MVA)
380/150 kV	35,000
150/25 kV	30,000
150/23 kV	25,000
25/23 kV	30,000
25/10 kV	25,000
23/10 kV	25,000

**Confirmed by Stedin*

Table 8: Transformer CAPEX costs

Standard Type	*Rough Cost (€/km)
150kV CS 500mm2	360,000
25kV CS 240mm2	125,000
25kV CS 630mm2	170,000
23kV CS 240mm2	120,000
10kV CS 150mm2	95,000

**Confirmed by Stedin*

Table 9: Line CAPEX costs

B Line & Transformer Standard Types

Name	c (nF/km)	r (/km)	x (/km)	max_i (kA)	type	q area (mm²)	alpha	Voltage Rating
150kV CS 500mm2	13	0.05	0.3	1.2	cs	500	0.004	HV
25kV CS 630mm2	40	0.1	0.08	1	cs	630	0.004	MV
25kV CS 240mm2	30	0.2	0.15	0.8	cs	240	0.004	MV
23kV CS 240mm2	30	0.2	0.15	0.8	cs	240	0.004	MV
10kV CS 150mm2	45	0.4	0.12	0.6	cs	150	0.004	LV

Table 10: Line parameters

Name	i0 (%)	pfe (kW)	vkr (%)	P_{rated} (MVA)	vk (%)	Vector group	Shift degree
380/150 kV	0.035	180	0.4	500	11	Yy0	0
150/25 kV	0.03	120	0.35	115	19.2	YNd5	150
150/23 kV	0.03	120	0.35	110	10	YNd5	150
25/23 kV	0.02	50	0.22	40	4.5	YNyn0	0
25/10 kV	0.025	60	0.25	30	12.4	YNd11	330
23/10 kV	0.025	55	0.25	80	7.5	Dyn5	150

Table 11: Transformer parameters

C DHN model validation

Production unit	Heat. Eff.	El. Eff.	Min. prod. (MW)	Max. prod. (MW)	Gas con. (MW)	CO_2 factor (ton/MW)	El. prod. (MW)	SU cost (€)	Variable cost (€)
Rotterdam									
WI	1	-	60	160	-	0	-	0	0
IWH1	1	-	0	39.17	-	0	-	0	0
IWH2	1	-	4	20	-	0	-	0	0
RDAM Gas1	0.789	-	0	120	152	0.233	-	0	0
RDAM Gas2	0.801	-	0	25	31.2	0.228	-	0	0
RDAM Gas3	0.788	-	0	43.89	55.7	0.235	-	0	0
RDAM Gas4	0.791	-	0	140	177	0.233	-	0	0
RDAM CHP1	0.487	0.214	34.17	56.94	117	0.227	25	1652	101
RDAM CHP2	0.487	0.214	34.17	56.94	117	0.227	25	1652	101
RDAM CHP3	0.4	0.38	90	200	500	0.46	190	13500	413
Biomass	1	-	-	21.67	-	0	-	0	0
Den Haag									
DH CHP1	0.389	0.414	0	40	102.7	0.4725	42.5	5000	110
DH CHP2	0.389	0.414	0	40	102.7	0.4725	42.5	5000	110
DH Gas1	0.797	-	0	110	138	0.2300	-	0	0
DH Gas2	0.791	-	0	25	31.6	0.2280	-	0	0
DH Gas3	0.808	-	0	45	55.7	0.2267	-	0	0
DH Geo1	1	-	3.33	3.33	-	0	-	0	0

Table 12: Base model generation sources and their parameters.

Storage	Buffer Capacity (MWh)	Rated Capacity (MWh)	Max SOC (Hours)	Eff.
DH Storage1	347	40	8.675	1
RDAM1 Storage1	700	700	1	1
RDAM2 Storage	53.3	53.3	1	1
Tuinders Storage	750	750	1	1

Table 13: Base model TES and their parameters used for model validation.

Heat source	Real-life data (MWh)	PyPSA model (MWh)	Change in share of total production (%)
Waste Incineration	787,512	739,457	0.1
Waste heat	201,265	170,833	-1.1
CHP and DH Gas3	543,362	484,129	-1.6
Biomass	38,864	120,129	5.4
Gas boilers	60,769	2,504	-3.5
Geothermal	17,846	27,410	0.7
Total	1,649,618	1,554,461	-6.4

Table 14: Model validation: Total heat supply per category in 2022 (without WLQ connection and IWH2).

Heat source	Pyomo model (MWh)	PyPSA model (MWh)	Change in share of total production (%)
Waste Incineration	933,997	826,161	-0.6
Waste heat	312,435	309,156	1.9
CHP	337,185	265,656	-2.3
Biomass	112,616	124,443	1.5
Gas boilers	13,424	1,202	-0.7
Geothermal	27,490	27,410	0.2
Total	1,738,740	1,554,027	-10.54

Table 15: Model validation: Total heat supply per category in 2022.

Heat storage	**Pyomo model (MWh)**	**PyPSA model (MWh)**	**Change in share of total supply(%)**
DH Storage1	25,969	68,691	16.7
RDAM1 Storage1	76,648	89,202	-5.8
RDAM2 Storage	11,120	21,689	3.4
Tuinders Storage	42,070	26,012	-14.3
Total	155,806	205,594	31.95

Table 16: Model validation: Total supply by storage in 2022.

D DHN model verification

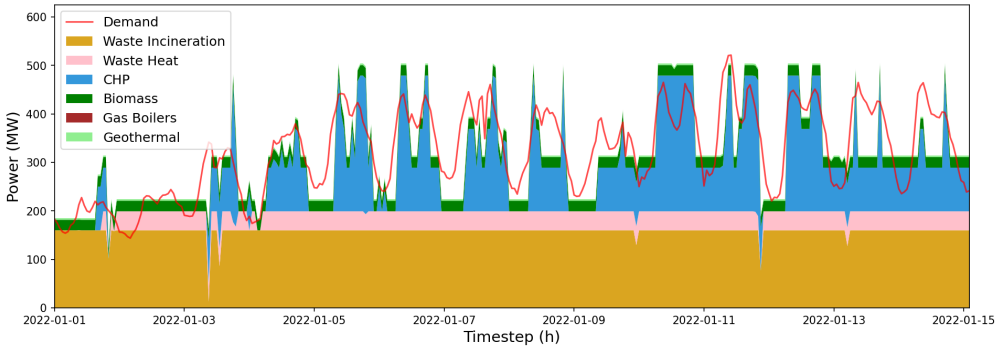

(a) Base model

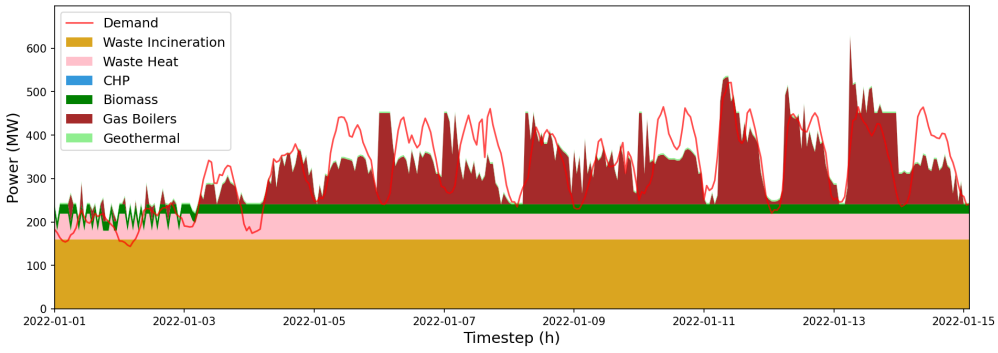

(b) No electricity revenue expression

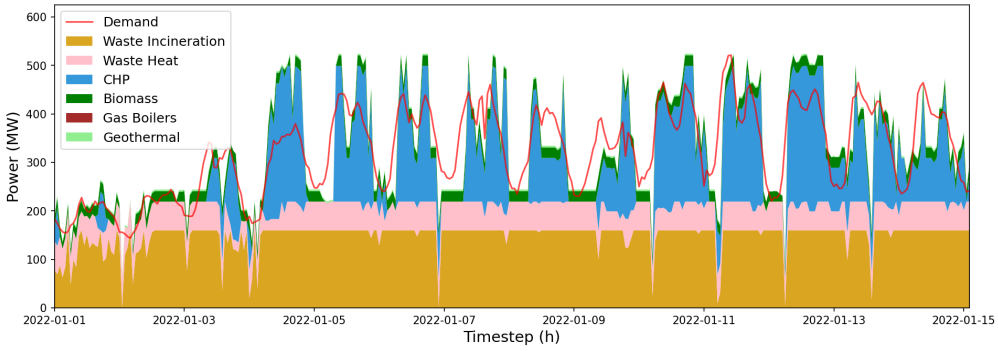

(c) No CO_2 costs

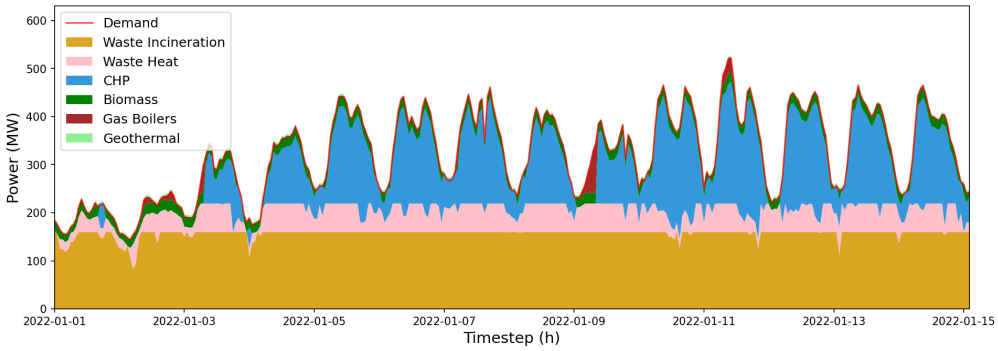

(d) No TES

Figure 1: Model verification. Total production per time step, 1st–15th of January 2022.

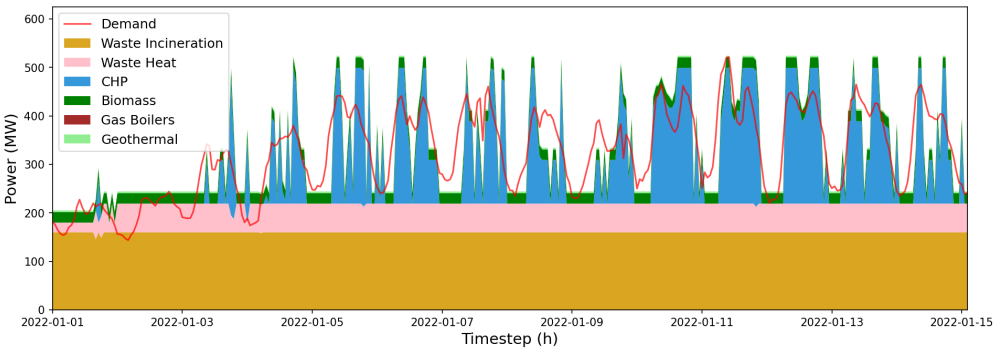

(e) No SU costs

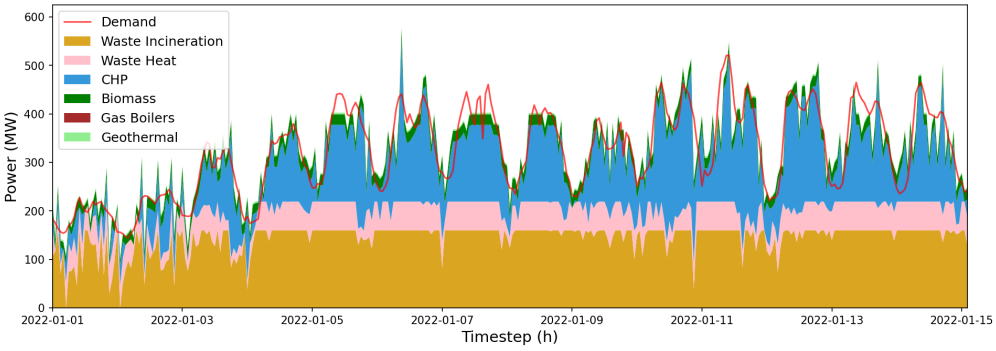

(f) No UC constraints

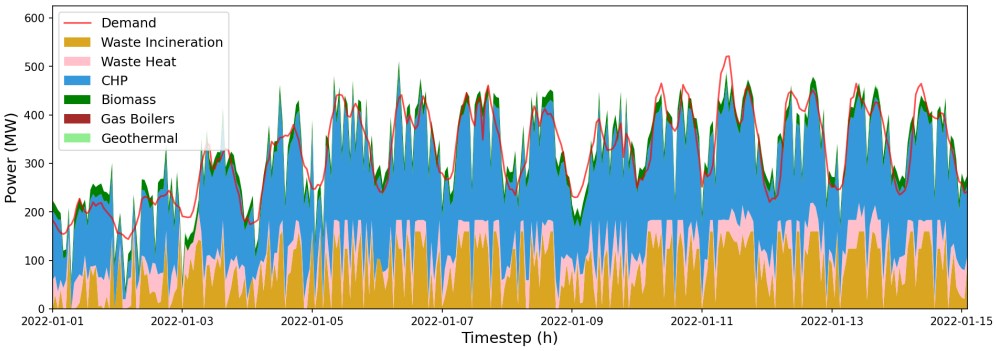

(g) No gas costs

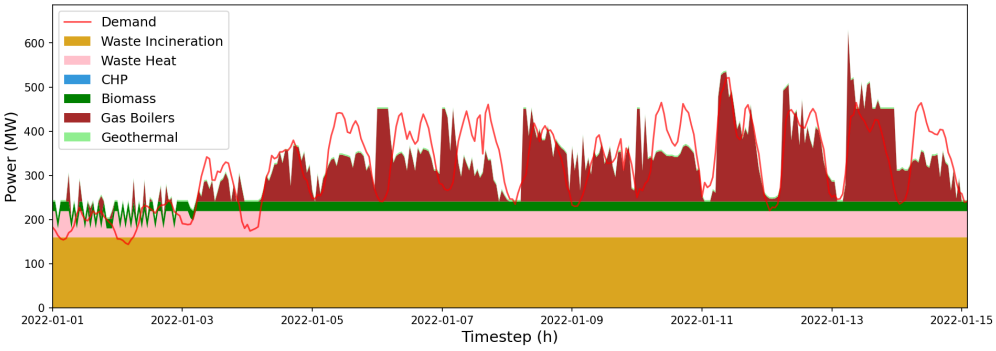

(h) Added variable costs

Figure 1: DHN model verification. Total production per time step, 1st–15th of January 2022.

	Base	No el. revenue	No CO_2 price	No TES	No CHP SU costs	No UC	No gas price	Added fixed CHP costs
WI	826,161	1,026,231	743,932	858,497	822,675	683,867	354,932	1,026,379
IWH	309,156	235,270	302,815	280,662	308,995	303,033	232,245	235,051
CHPs	265,656	0	364,270	281,711	267,925	415,494	826,318	6,755
Biomass	124,443	67,274	121,475	95,117	124,972	121,909	121,726	67,308
Gas boilers	1,202	200,737	604	12,314	1,201	0	0	191,624
Geothermal	27,410	29,167	16,122	26,606	27,410	27,410	582	29,164
Total	1,554,027	1,558,679	1,549,219	1,554,906	1,553,179	1,551,712	1,535,803	1,556,282

Table 17: DHN model verification. Total production per category in 2022, MWh.

	Base	No el. revenue	No CO_2 price	No TES	No CHP SU costs	No UC	No gas price	Added fixed CHP costs
DH Storage1	68,691	81,096	88,656	0	72,970	47,117	100,520	82,155
RDAM1 Storage1	89,202	217,654	81,559	0	86,830	60,982	58,727	213,963
RDAM2 Storage	21,689	10,651	25,516	0	25,838	29,099	4,366	10,534
Tuinders Storage	26,012	56,375	25,539	0	26,550	6,857	7,774	56,648
Total	205,594	365,777	221,271	0	212,188	144,056	171,387	363,301

Table 18: DHN model verification. Storage supply per unit in 2022, MWh.

E EDN model verification

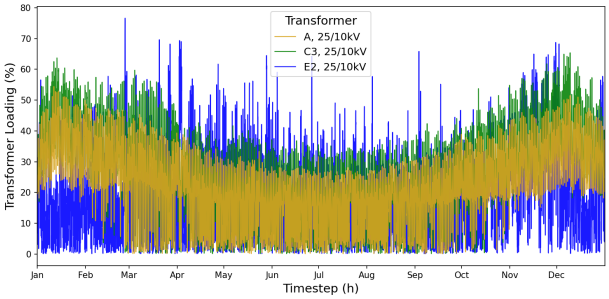

(a) Enforced, 25/10 kV

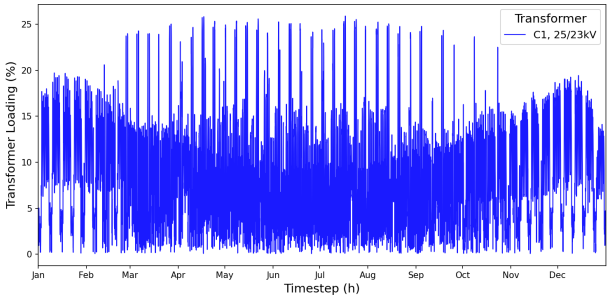

(b) Enforced, 25/23 kV

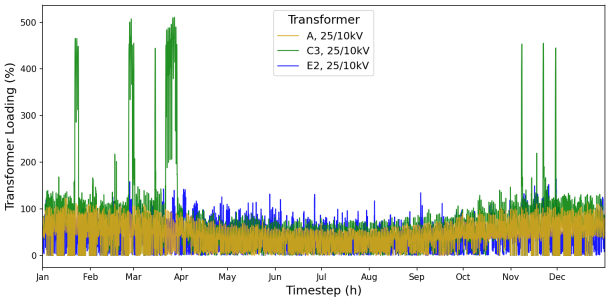

(c) Unenforced, 25/10 kV

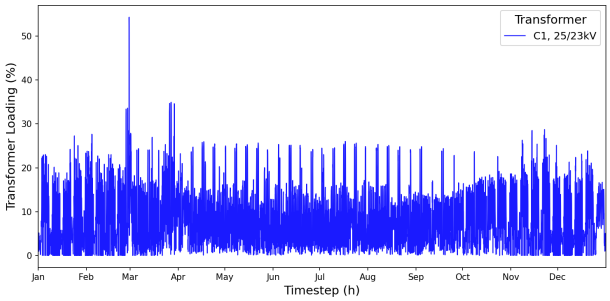

(d) Unenforced, 25/23 kV

Figure 2: Medium voltage transformer loading with enforced and unenforced base network in 2030, (experiment No. 3)

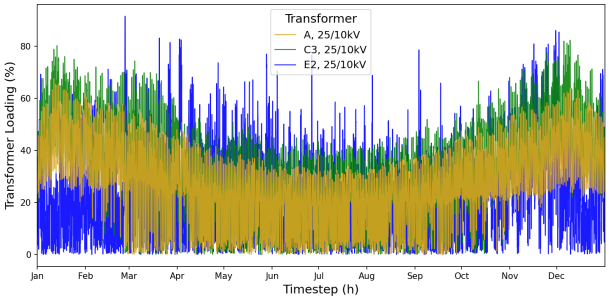

(a) Increased demand, 25/10 kV

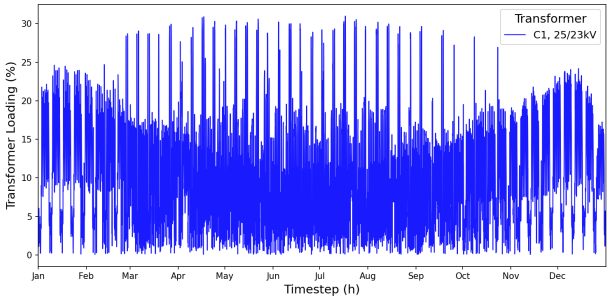

(b) Increased demand, 25/23 kV

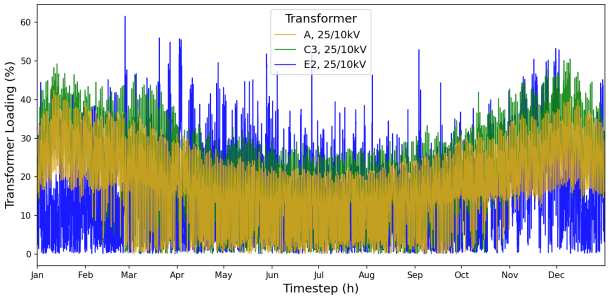

(c) Decreased demand, 25/10 kV

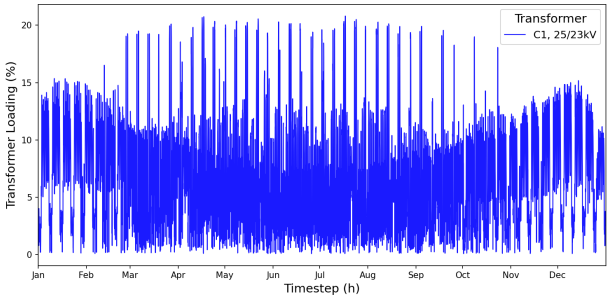

(d) Decreased demand, 25/23 kV

Figure 3: Medium voltage transformer loading with enforced base network in 2030, (experiment No. 4 & 5)

Name	Type	No. 2	No. 3		No. 4	No. 5
		No trafo (%)	Unenforced (%)	Enforced (%)	Demand increase (%)	Demand decrease (%)
		Max	Max	Max	Max	Max
Waterningen	380/150 kV	-	146.15	66.95	82.91	52.41
Krimpen	380/150 kV	63.32	60.89	57.82	70.59	45.66
Rijswijk	150/25 kV	-	255.71	117.65	145.77	92.05
s'Gravenhage	150/25 kV	-	133.94	63.94	78.07	50.50
Voorburg	150/25 kV	-	345.54	121.65	151.42	94.90
Ommoord_HV	150/25 kV	222.95	202.51	96.68	119.04	75.91
Zuidwijk	150/23 kV	80.70	74.41	80.24	96.98	63.82
A	25/10 kV	-	123.74	54.38	67.59	42.45
C1	25/23 kV	-	27.19	25.90	30.96	20.80
C3	25/10 kV	-	351.97	65.33	82.34	50.52
E2	25/10 kV	164.27	158.17	76.59	91.54	61.61

Table 19: Transformer loading with base EDN network in 2030, verification experiment results

Name	No. 2	No. 3		No. 4	No. 5
	No trafo (%)r	Unenforced (%)	Enforced (%)	Demand increase (%)	Demand decrease (%)
	Max	Max	Max	Max	Max
150kV_Waterningen_Rijskwijk(1&2)	-	78.97	73.96	93.29	59.05
150kV_sGravenhage_Rijskwijk	-	84.67	68.92	85.99	54.81
150kV_sGravenhage_Voorburg	-	49.04	31.16	38.86	26.49
150kV_Voorburg_Waterningen	-	81.79	64.08	81.14	51.07
150kV_Krimpen_Ommoord(1)	40.61	36.89	34.63	43.37	27.66
150kV_Krimpen_Ommoord(2)	41.62	37.81	35.49	44.45	28.35
150kV_Krimpen_Zuidwijk	28.47	26.25	28.26	34.22	22.52
25kV_Substation_A_Trafo_A(1)	-	25.92	22.26	28.32	17.79
25kV_Substation_A_Trafo_A(2&3)	-	26.99	23.18	29.49	18.52
25kV_Substation_A_Trafo_A(4)	-	27.26	23.41	29.78	18.70
25kV_DH_CHP_Cables	-	34.92	32.75	33.46	32.61
25kV_Substation_C_Trafo_C1	-	31.39	29.74	36.60	23.86
25kV_Substation_C_Trafo_C3(1)	-	149.83	59.47	70.11	43.02
25kV_Substation_C_Trafo_C3(2)	-	154.98	61.52	72.52	44.49
25kV_Substation_E_Trafo_E2(1&2)	71.13	68.40	66.02	79.09	53.17
25kV_Substation_E_Substation_D(1&2)	73.36	72.32	70.27	71.64	70.22
10kV_Trafo_C3_DH_Geo1	-	693.33	34.92	41.90	27.94

Table 20: Line loading with base EDN network in 2030, verification experiment results

F Validation DHN model structure

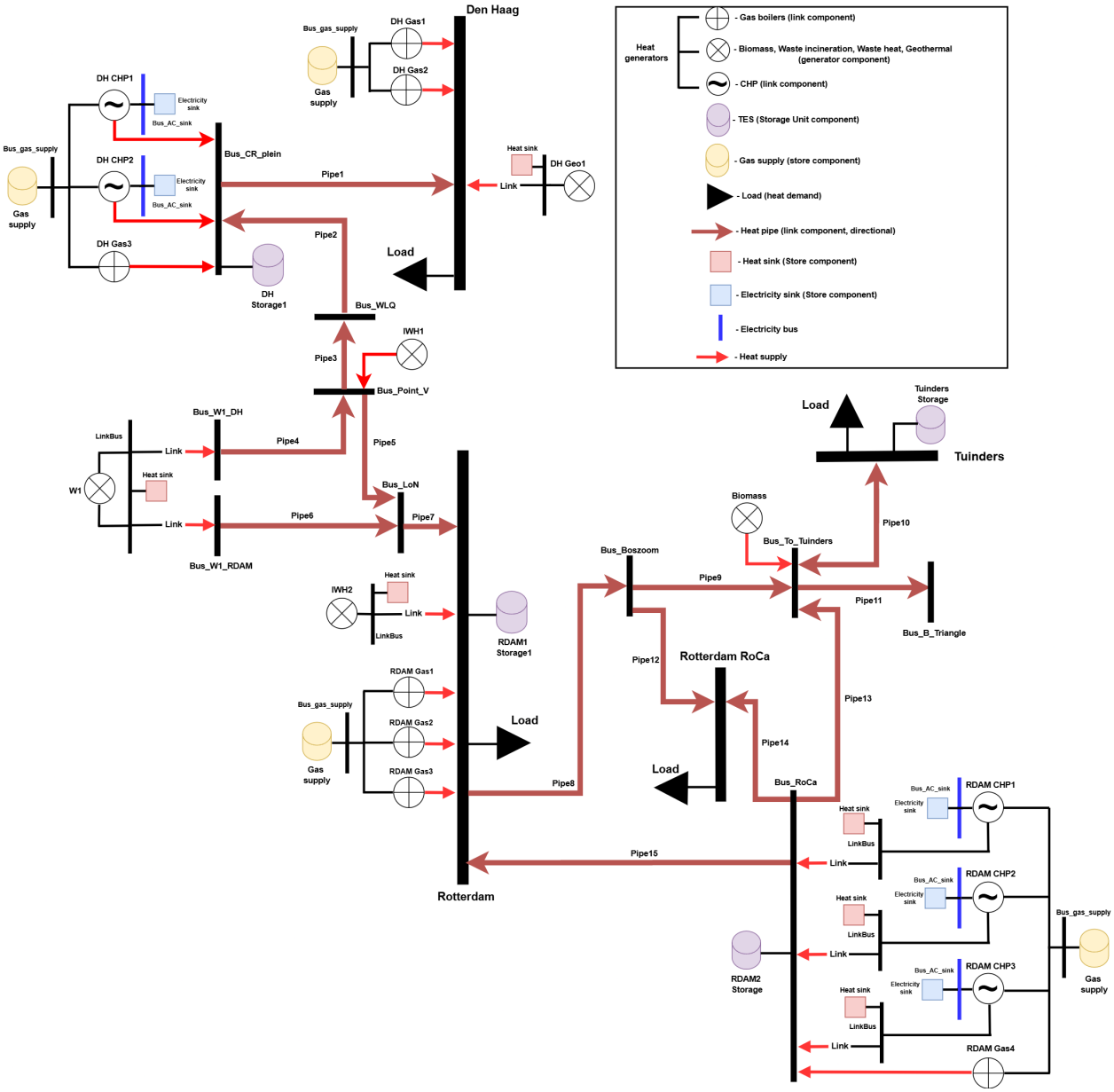

Figure 4: DHN of South-Holland used for model validation

G Final DHN model structure

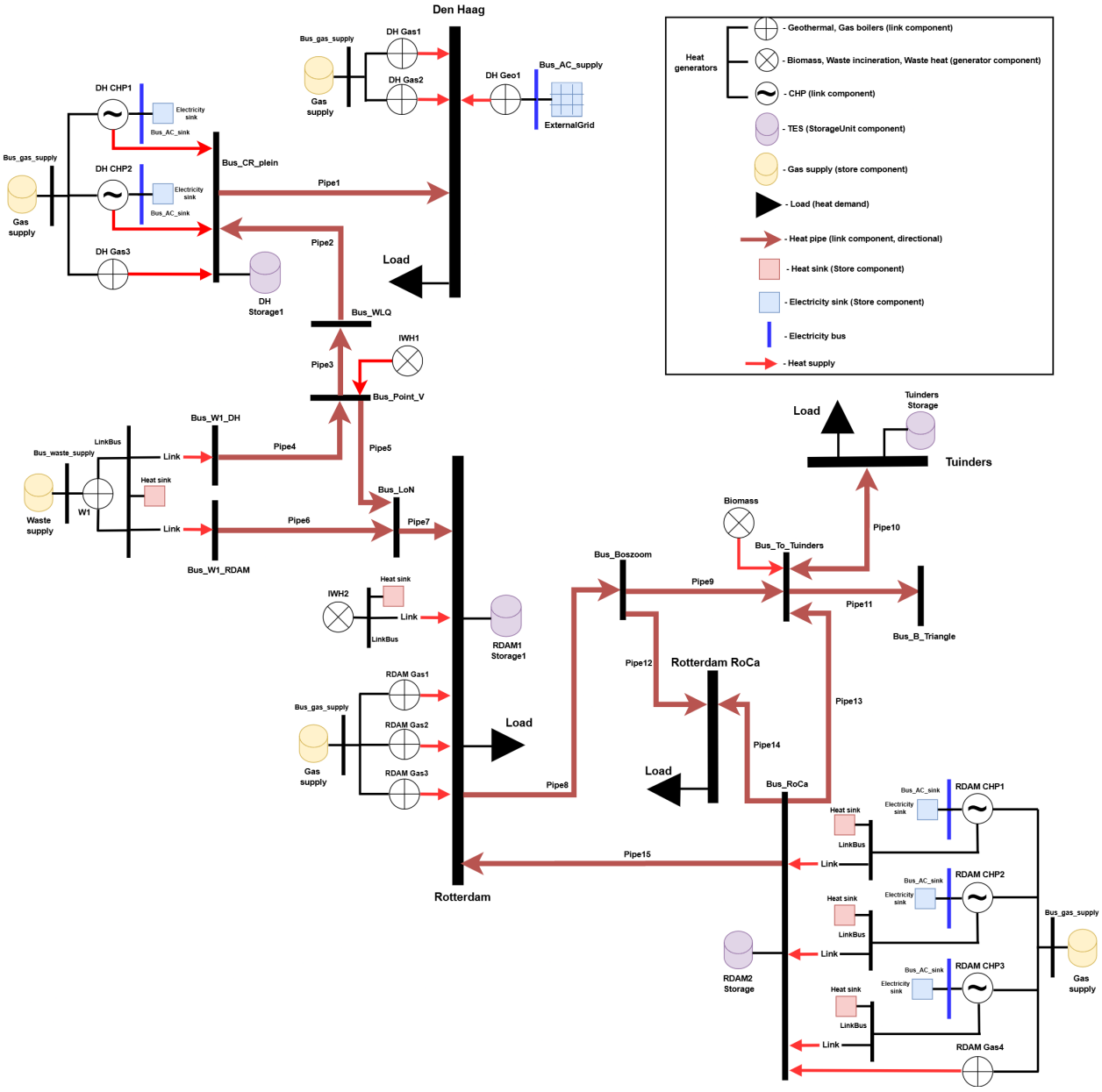

Figure 5: Base DHN of South-Holland

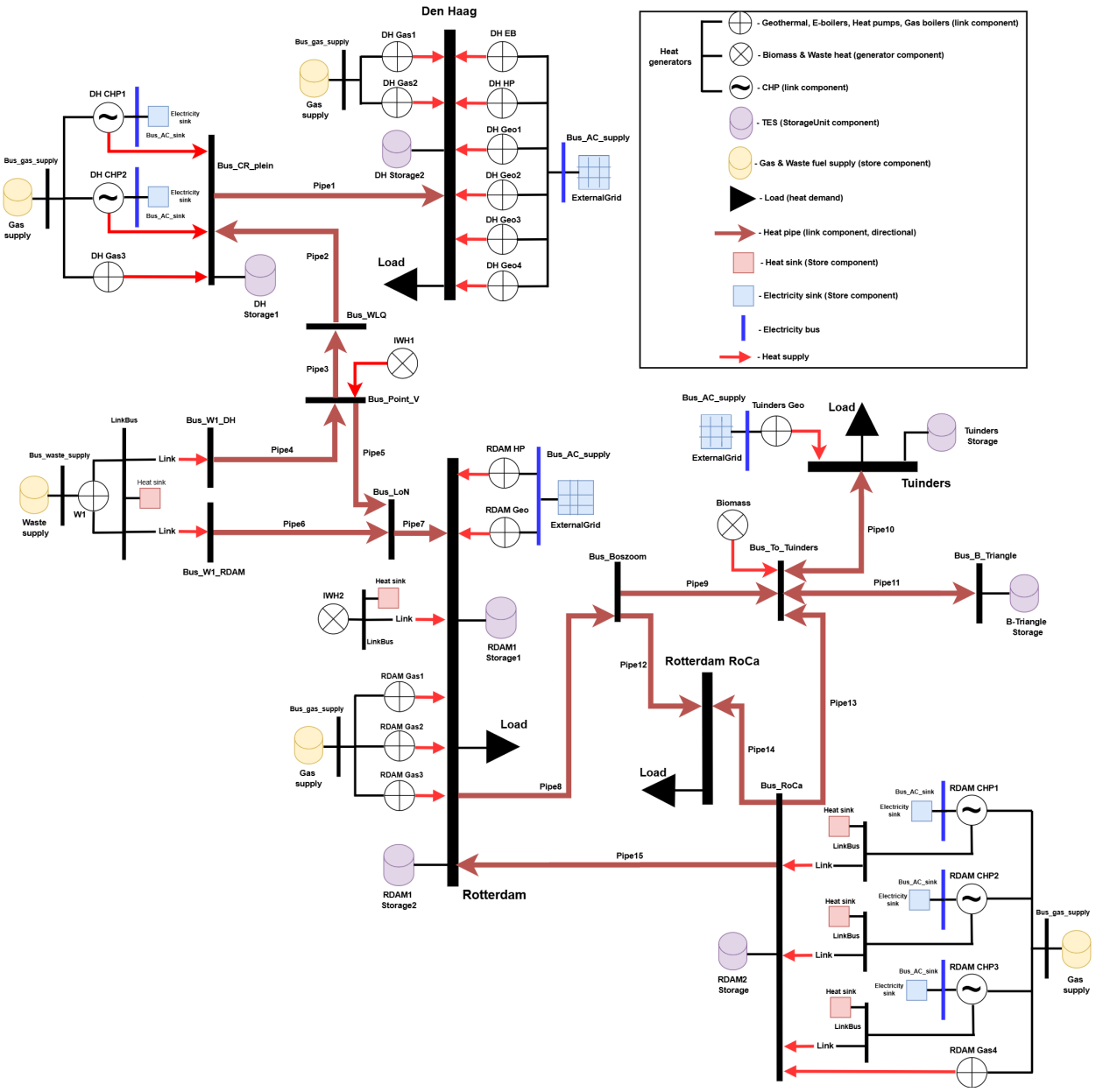

Figure 6: Full DHN of South-Holland

H Final EDN model structure

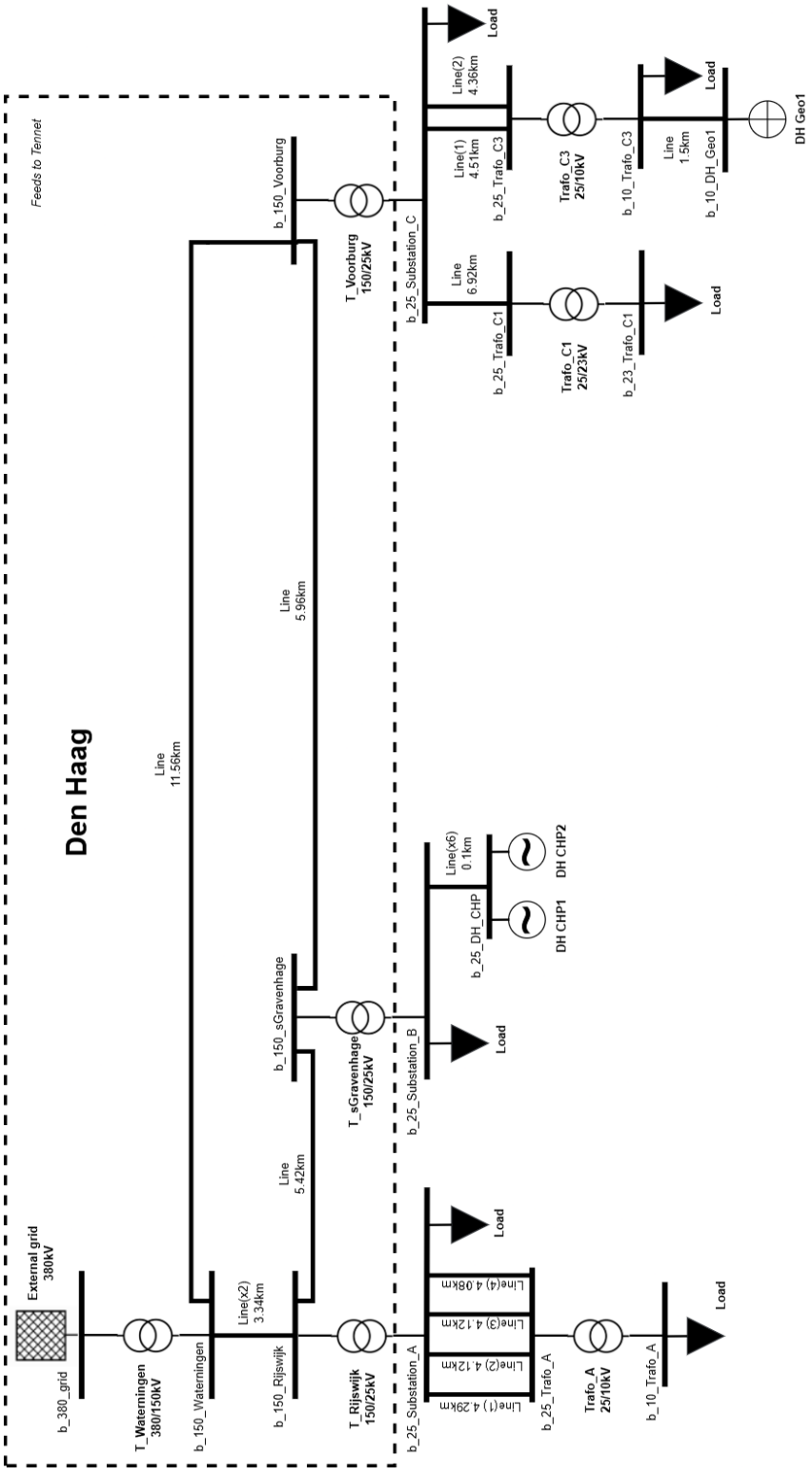

Figure 7: Base EDN, Den Haag branch

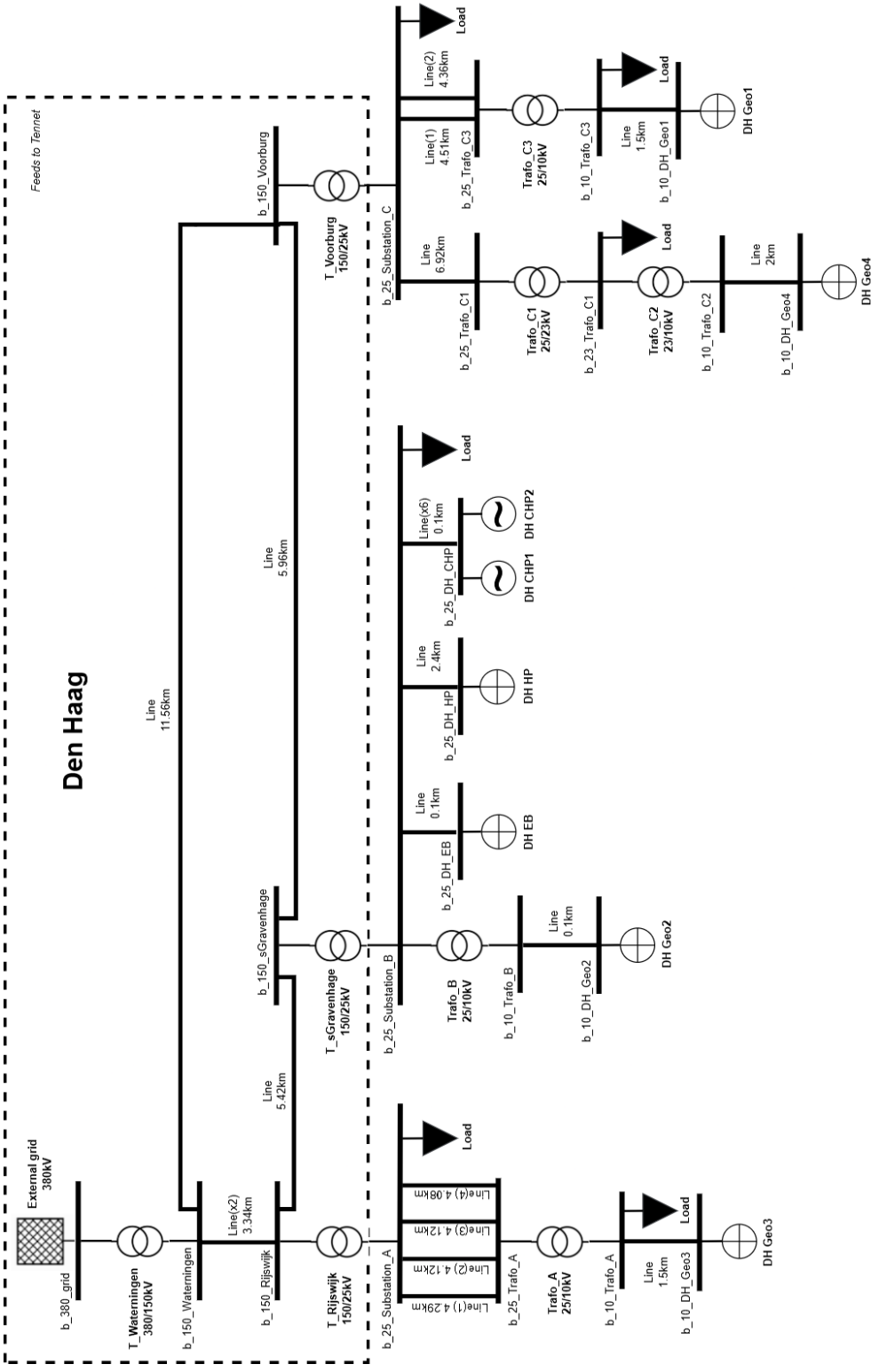

Figure 8: Full EDN, Den Haag branch

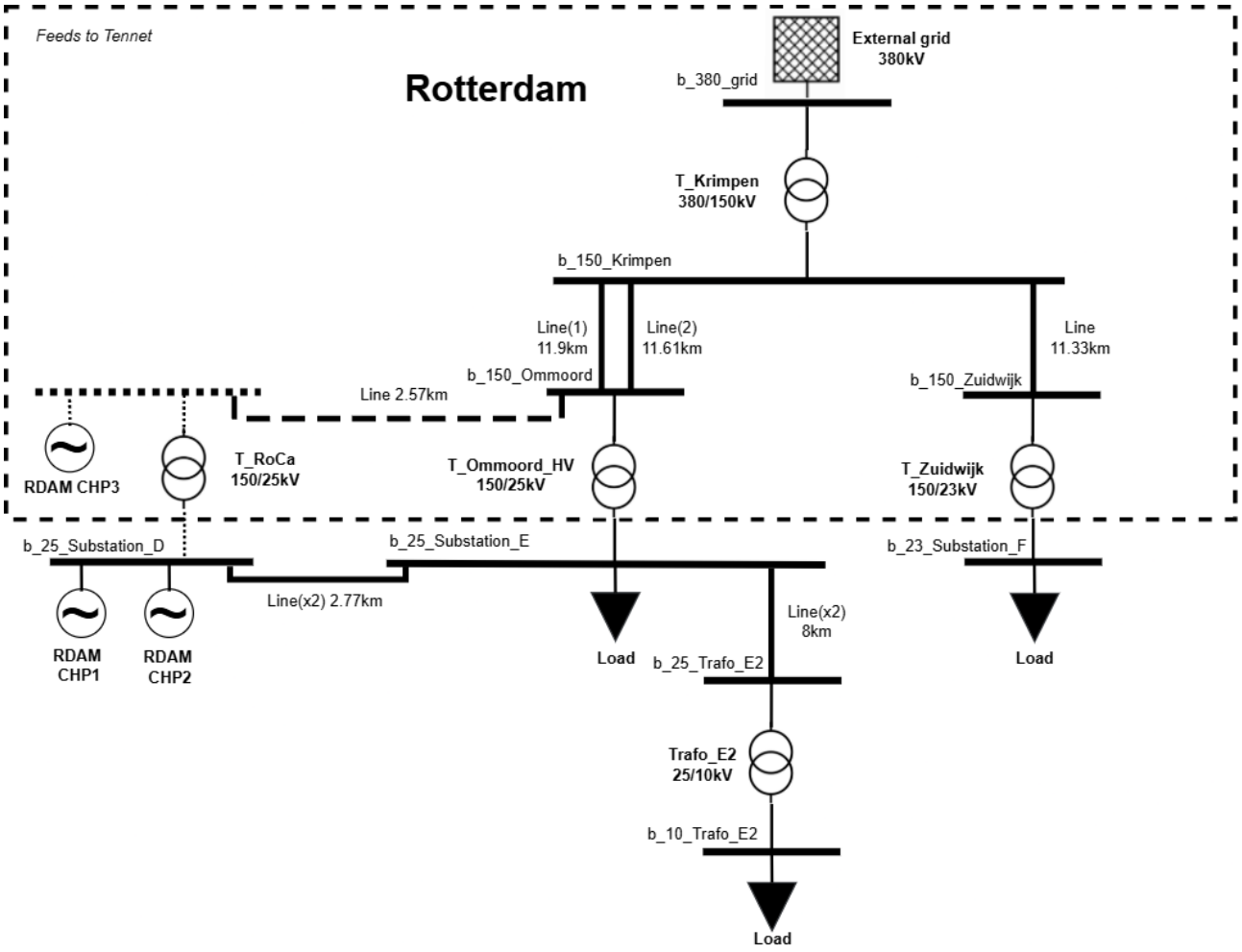

Figure 9: Base EDN, Rotterdam branch

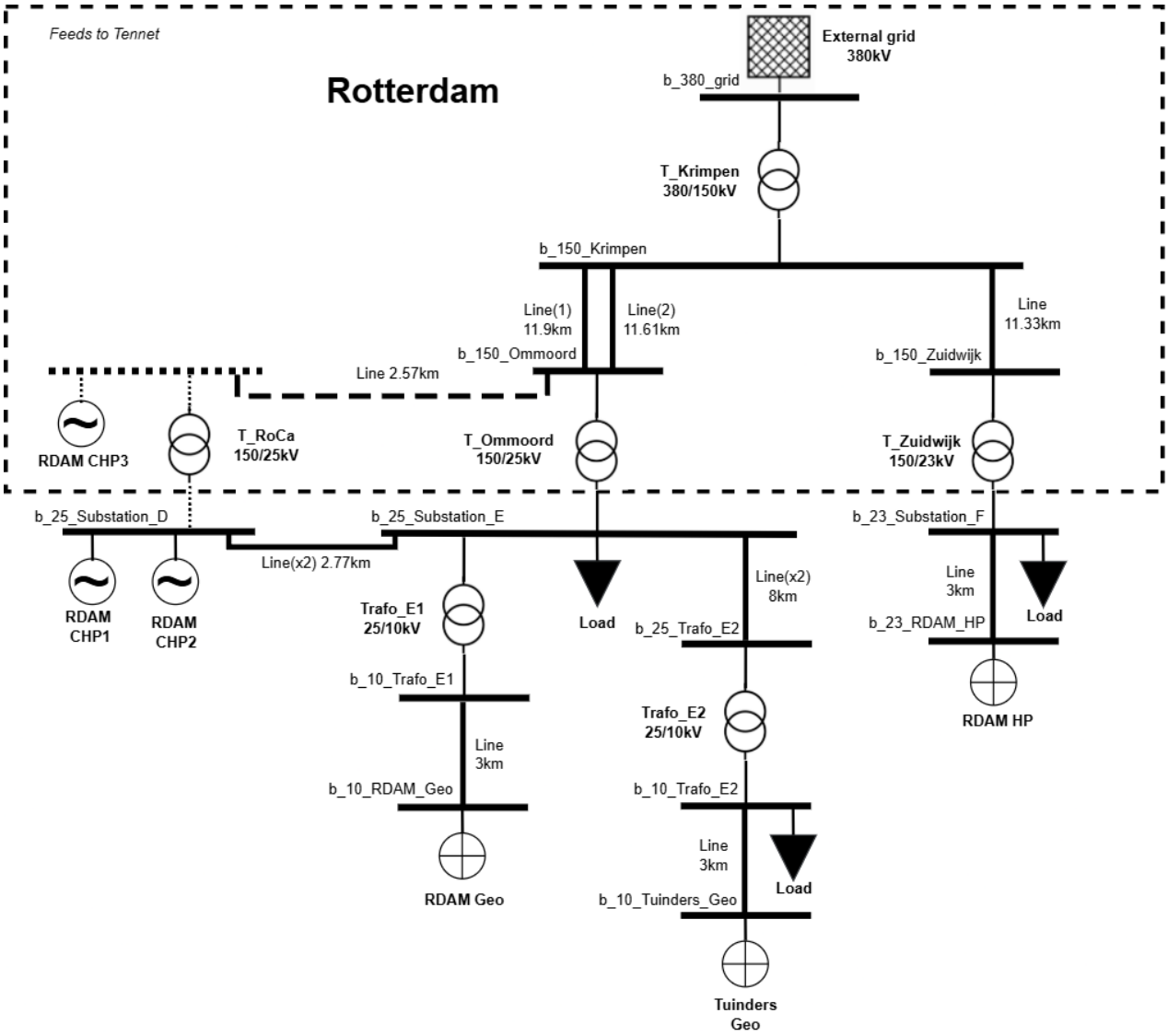

Figure 10: Full EDN, Rotterdam branch

I South-Holland case study results

Total production per category in DHN scenarios

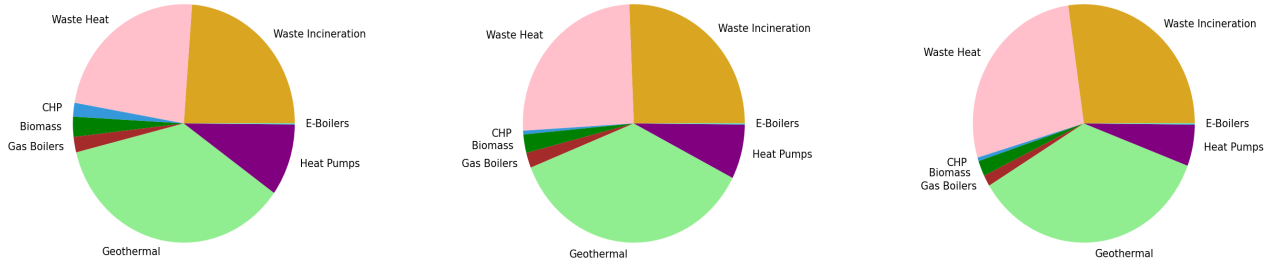

(a) 2030 Full network *(b) 2040 Full network* *(c) 2050 Full network*

Figure 11: Total heat supply per category in 2030, 2040 and 2050 (low heat demand case)

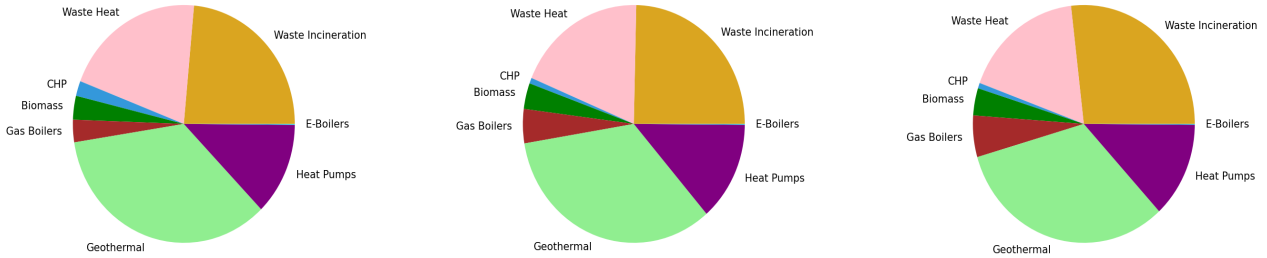

(a) 2030 Full network *(b) 2040 Full network* *(c) 2050 Full network*

Figure 12: Total heat supply per category in 2030, 2040 and 2050 (high heat demand case)

Main DHN model outputs

	2030 Low		2040 Low	2050 Low	2030 High		2040 High	2050 High
	Base	Full	Full	Full	Base	Full	Full	Full
Demand	26,754	187,254	157,343	131,116	27,506	229,890	250,348	257,902
Production*	22,273	11,491	2,914	2,633	28,296	14,154	5,611	5,871

* Without RDAM CHP3

Table 21: Total electricity demand and production from heat supply units, MWh.

Transformer and line loading with low heat demand

		Base network 2030			Full network 2030		
		Unenforced	**Enforced**	**No P2H**	**Unenforced**	**Enforced**	**No P2H**
Transformer	Type	Max (%)	Max (%)	Max (%)	Max (%)	Max (%)	Max (%)
Waterningen	380/150 kV	146.15	65.67	65.26	150.07	67.08	65.27
Krimpen	380/150 kV	60.89	57.22	57.22	62.75	57.69	56.85
Rijswijk	150/25 kV	255.71	76.62	76.60	261.52	78.01	76.60
s'Gravenhage	150/25 kV	133.94	63.61	63.58	154.63	75.61	63.61
Voorburg	150/25 kV	345.54	79.17	77.99	362.21	79.91	78.01
Ommoord	150/25 kV	202.51	63.37	63.37	209.63	64.16	62.94
Zuidwijk	150/23 kV	74.41	80.11	80.11	96.85	53.02	39.77
A	25/10 kV	123.74	53.13	53.11	149.38	60.45	53.11
B	25/10 kV	-	-	-	15.96	13.81	0.20
C1	25/23 kV	27.19	25.88	25.89	87.27	30.56	25.74
C2	23/10 kV	-	-	-	38.16	5.54	0.07
C3	25/10 kV	351.97	69.85	63.48	408.13	69.57	63.48
E1	25/10 kV	-	-	-	15.46	13.68	0.20
E2	25/10 kV	158.17	76.45	76.45	172.72	71.56	76.45
Number of failures[1]		**596**	**0**	**0**	**647**	**0**	**0**

[1] Number of PFA snapshots that did not converge

Table 22: Transformer loading with base and full network expansion in 2030 (low heat demand case)

		2040			**2050**		
		Unenforced	**Enforced**	**No P2H**	**Unenforced**	**Enforced**	**No P2H**
Transformer	Type	Max (%)	Max (%)	Max (%)	Max (%)	Max (%)	Max (%)
Waterningen	380/150 kV	175.90	64.55	63.29	172.13	71.05	69.85
Krimpen	380/150 kV	70.05	88.09	86.10	74.33	46.42	45.46
Rijswijk	150/25 kV	356.53	88.84	87.72	374.74	80.84	79.97
s'Gravenhage	150/25 kV	185.42	89.05	85.81	182.73	62.74	61.50
Voorburg	150/25 kV	405.36	82.68	80.65	409.42	72.95	73.68
Ommoord	150/25 kV	234.41	89.46	86.59	231.40	94.42	92.31
Zuidwijk	150/23 kV	112.11	81.46	69.34	112.28	73.76	73.63
A	25/10 kV	360.24	88.89	81.25	355.02	70.21	71.82
B	25/10 kV	16.91	13.85	0.20	16.70	13.75	0.20
C1	25/23 kV	63.65	54.89	54.89	91.10	86.20	86.20
C2	23/10 kV	15.69	5.57	0.07	12.06	5.46	0.07
C3	25/10 kV	509.44	63.62	59.10	509.26	74.26	75.60
E1	25/10 kV	16.59	14.02	0.20	18.67	13.88	0.20
E2	25/10 kV	238.40	82.45	76.49	456.00	84.74	79.96
Number of failures[1]		**1821**	**0**	**0**	**2629**	**0**	**0**

[1] Number of PFA snapshots that did not converge

Table 23: Transformer loading with full network expansion in 2040 and 2050 (low heat demand case)

	Base network 2030			Full network 2030		
	Unenforced	**Enforced**	**No P2H**	**Unenforced**	**Enforced**	**No P2H**
Transformer	Max (%)	Max (%)	Max (%)	Max (%)	Max (%)	Max (%)
25kV_Substation_A_Trafo_A(1)	25.92	22.26	22.25	31.29	23.33	22.25
25kV_Substation_A_Trafo_A(2&3)	26.99	23.18	23.17	32.59	26.37	23.17
25kV_Substation_A_Trafo_A(4)	27.26	23.41	23.40	32.90	26.63	23.40
25kV_DH_CHP_Cables	34.62	32.75	32.75	35.04	32.75	32.75
25kV_Substation_C_Trafo_C1	31.39	29.74	29.74	100.77	35.29	29.58
25kV_Substation_C_Trafo_C3(1)	149.83	59.47	54.08	173.74	59.23	54.04
25kV_Substation_C_Trafo_C3(2)	154.98	61.52	55.90	179.71	61.27	55.90
25kV_Substation_E_Trafo_E2(1&2)	68.40	66.02	66.02	74.79	65.11	66.02
25kV_Substation_E_Substation_D(1&2)	73.32	70.27	70.27	71.98	70.07	70.07
25kV_Substation_B_DH_HP	-	-	-	99.92	90.46	0.04
25kV_Substation_B_DH_EB	-	-	-	63.64	58.22	0.00
23kV_Substation_F_RDAM_HP	-	-	-	99.08	47.53	0.05
10kV_Trafo_A_DH_Geo3	-	-	-	57.78	40.92	0.02
10kV_Trafo_B_DH_Geo2	-	-	-	45.59	39.30	0.00
10kV_Trafo_C2_DH_Geo4	-	-	-	293.54	42.15	0.03
10kV_Trafo_C3_DH_Geo1	693.33	34.92	0.02	676.61	34.99	0.02
10kV_Trafo_E1_RDAM_Geo	-	-	-	44.12	38.99	0.01
10kV_Trafo_E2_Tuinders_Geo	-	-	-	51.92	42.69	0.02

Table 24: Line loading with base and full network expansion in 2030 (low heat demand case)

	2040			2050		
	Unenforced	**Enforced**	**No P2H**	**Unenforced**	**Enforced**	**No P2H**
Transformer	Max (%)	Max (%)	Max (%)	Max (%)	Max (%)	Max (%)
25kV_Substation_A_Trafo_A(1)	75.47	37.24	34.04	74.37	43.99	45.01
25kV_Substation_A_Trafo_A(2&3)	78.58	38.78	35.45	77.44	45.81	46.86
25kV_Substation_A_Trafo_A(4)	73.35	39.16	35.79	78.20	46.26	47.32
25kV_DH_CHP_Cables	33.78	32.87	32.87	33.46	32.81	32.81
25kV_Substation_C_Trafo_C1	73.37	63.23	63.23	105.08	49.69	49.69
25kV_Substation_C_Trafo_C3(1)	216.86	81.25	75.48	216.78	63.05	64.19
25kV_Substation_C_Trafo_C3(2)	224.31	84.05	78.07	224.23	65.21	66.40
25kV_Substation_E_Trafo_E2(1&2)	103.23	71.40	66.24	197.42	73.39	69.24
25kV_Substation_E_Substation_D(1&2)	43.10	70.58	70.58	21.95	70.35	70.35
25kV_Substation_B_DH_HP	102.76	89.49	0.04	98.64	43.75	0.04
25kV_Substation_B_DH_EB	66.13	58.10	0.00	65.33	57.46	0.00
23kV_Substation_F_RDAM_HP	99.06	48.18	0.05	98.85	47.58	0.05
10kV_Trafo_A_DH_Geo3	691.17	41.68	0.02	404.20	41.36	0.02
10kV_Trafo_B_DH_Geo2	48.34	39.42	0.00	47.76	39.11	0.00
10kV_Trafo_C2_DH_Geo4	120.54	42.40	0.03	92.60	41.51	0.03
10kV_Trafo_C3_DH_Geo1	117.31	35.61	0.02	503.14	34.52	0.02
10kV_Trafo_E2_Tuinders_Geo	63.43	44.31	0.02	165.35	43.93	0.02
10kV_Trafo_E1_RDAM_Geo	47.43	39.91	0.01	53.47	39.51	0.01

Table 25: Line loading with full network expansion in 2040 and 2050 (low heat demand case)

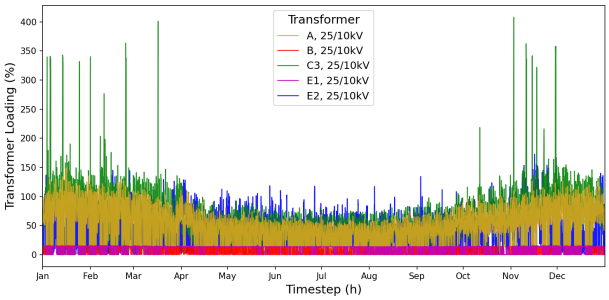

(a) Unenforced case in 2030

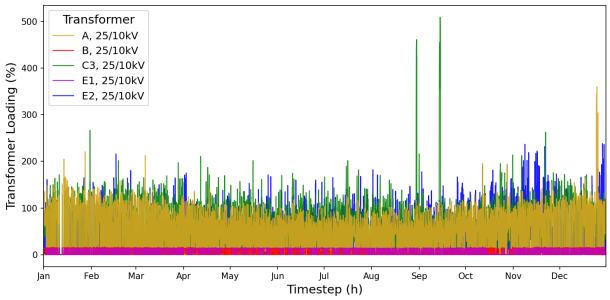

(b) Unenforced case in 2040

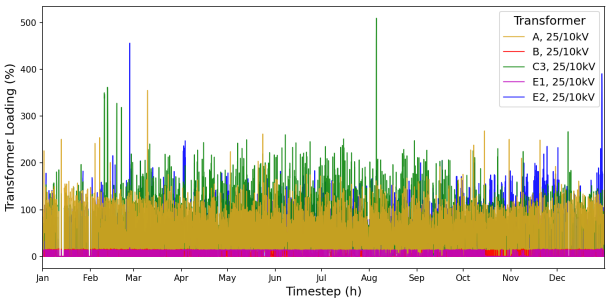

(c) Unenforced case in 2050

Figure 13: 25/10 kV transformer loading with full network expansion with high low demand, unenforced

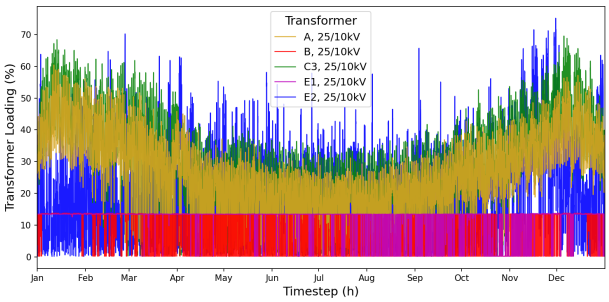

(a) Enforced case in 2030

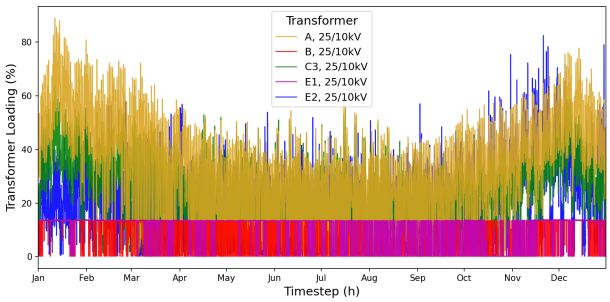

(b) Enforced case in 2040

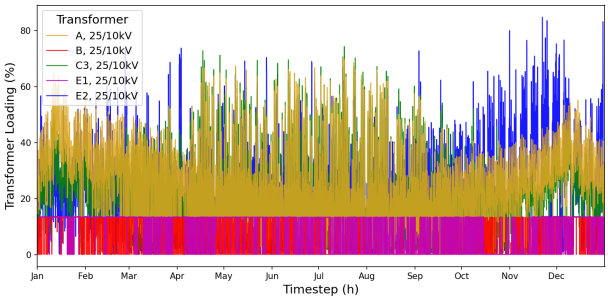

(c) Enforced case in 2050

Figure 14: 25/10 kV transformer loading with full network expansion with low heat demand, enforced

Transformer and line loading with high heat demand

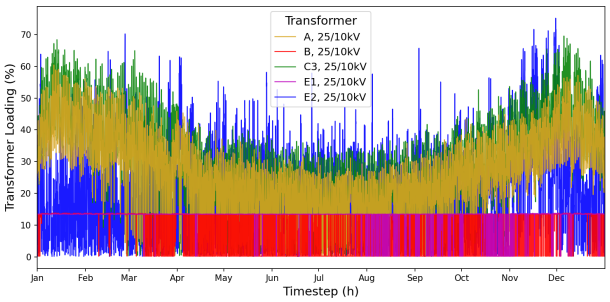

(a) Enforced case in 2030

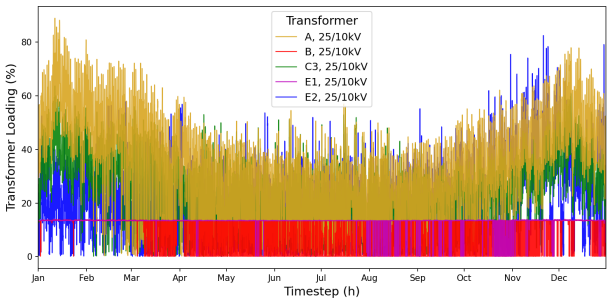

(b) Enforced case in 2040

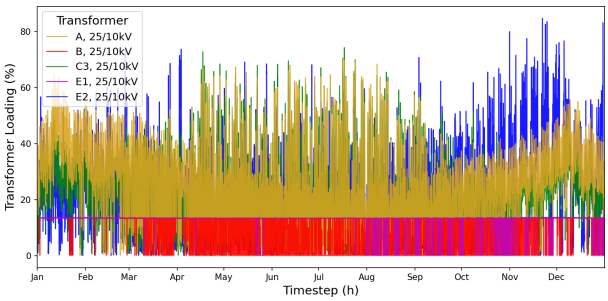

(c) Enforced case in 2050

Figure 15: 25/10 kV transformer loading with full network expansion with high heat demand, enforced

Negative electricity demand hours in each scenario

Substation	2030	2040	2050
A	994	1,484	1,965
B	0	173	531
C2	2,195	3,864	4,832
C3	1,091	1,783	2,277
E2	4,427	3,111	3,334
Average	**1,741**	**2,083**	**2,587**

Table 26: Total number of hours in a year with net generation from distributed energy sources at MV substations